An ***IPRF*** Research Report

Innovative Pavement Research Foundation

Airport Concrete Pavement Technology Program

Report IPRF-01-G-002-3

Innovative Rehabilitation of Pavement for Light Load Aircraft

Programs Management Office
1010 Massachusetts Avenue, N.W.
Suite 200
Washington, DC 2001

September 2004

This page intentionally left blank.

An ***IPRF*** Research Report

Innovative Pavement Research Foundation

Airport Concrete Pavement Technology Program

Report IPRF-01-G-002-3

Innovative Rehabilitation of Pavement for Light Load Aircraft

Principal Investigators

Dr. Jim W. Hall, Jr., P.E., Applied Research Associates, Inc.
Dr. Athar Saeed, P.E., Applied Research Associates, Inc.
A. Michel Alexander, Engineering Research and Development Center

Programs Management Office
1010 Massachusetts Avenue, N.W.
Suite 200
Washington, DC 2001

This report has been prepared by the Innovative Pavement Research Foundation under the Airport Concrete Pavement Technology Program. Funding is provided by the Federal Aviation Administration under Cooperative Agreement Number 01-G-002. Dr. Satish Agrawal is the Manager of the FAA Airport Technology R&D Branch and the Technical Manager of the Cooperative Agreement.

The Innovative Pavement Research Foundation and the Federal Aviation Administration thanks the Technical Panel that willingly gave of their expertise and time for the development of this report. They were responsible for the oversight and the technical direction. The names of those individuals on the Technical Panel follow.

Mr. Rodney Joel, P.E.	**Federal Aviation Administration**
Dr. James Cable, P.E.	**Iowa State University**
Mr. Randy Vogel, P.E.	**Crawford, Murphy and Tilly, Inc.**
Mr. Frank Kozeliski, P.E.	**Gallup Sand and Gravel Co.**
Mr. Archie F. Carter, P.E.	**Retired**
Dr. David Brill, P.E.	**FAA Technical Advisor**

TABLE OF CONTENTS

This page intentionally left blank.

LIST OF FIGURES

LIST OF TABLES

This page intentionally left blank.

ACKNOWLEDGEMENTS

Applied Research Associates (ARA), Inc., ERES Consultants Division (ERES), was awarded contract IPRF Project FAA-01-G-002-3 on November 23, 2001. ARA had overall responsibility for this study; the U.S. Army Engineer Research and Development Center (ERDC) provided laboratory facilities, and was responsible for the laboratory testing phase of the research.

The project principal investigator (PI) was Dr. Jim W. Hall, Jr., P.E. (ERES). Dr. Athar Saeed, P.E., (ERES) and Mr. Alton M. Alexander (ERDC) assisted Dr. Hall as Co-PIs. Mr. Alexander and Mr. Richard Haskins (ERDC) conducted the laboratory test program. Dr. Saeed, Messrs. Alexander and Haskins, and Dr. Hall prepared this report.

This page intentionally left blank.

ABSTRACT

This report presents findings of research conducted under IPRF Project FAA-01-G-002-3. The research was conducted in two parts – Track 1 was a field evaluation of existing ultra-thin-whitetopping (UTW) projects, and Track 2 was a laboratory evaluation of the UTW bond on specially prepared samples.

Track 1 encompassed field study of in-service (UTW) pavements. Three airfields with UTW pavements and five highway/parking lot UTW projects were visited to gain first-hand knowledge about UTW performance over the years. These projects ranged in age from almost new too fairly old. The oldest project, despite being 12 years old, was still performing well. Corner breaks, cracks, and shattered slabs were the predominant distresses at all the sites visited; there was no real evidence of loss of bond due to climate. Most of the distresses were in areas subjected to heavy traffic (fuel trucks and school buses generally weighing more than 30 kips).

Track 2 involved the laboratory evaluation of the UTW bond (when subjected to simulated environmental conditions) and included construction of a test section and laboratory testing of samples obtained from the field test section. The test section was constructed at ERDC on an old asphalt concrete (AC) test road. UTW samples, measuring 34 inches by 34 inches by 7 inches (864 mm by 864 mm by 178 mm), were extracted from the test section and subjected to laboratory freeze and thaw (F&T) and wet and dry (W&D) environmental exposure (in specially designed exposure stations). The hot/cold (H&C) tests that were initially planned were not conducted.

The laboratory results indicated that when a UTW pavement is constructed using field durable materials and the AC surface is properly milled and cleaned prior to placement of the Portland cement concrete (PCC), then the bond between the two materials is at least as durable as the AC or PCC. This essentially means that if a UTW pavement is constructed using proper construction techniques, bond failure due to environmental factors should not be a concern.

This page intentionally left blank.

EXECUTIVE SUMMARY

Conventional (PCC) overlays of aged (AC) pavements, at least 5 inches (125 mm) thick, have been used as a viable rehabilitation alternative. These overlays are designed assuming no bond between the original AC and the PCC overlay. During the last decade, thinner PCC overlays, less than 4 inches (100 mm) thick, have been successfully used. This rehabilitation technique is referred to as UTW, and it requires a bond between the PCC and the old AC surface to form a composite section.

A composite section comprised of PCC over AC with bond between the two is considered essential for UTW performance because it reduces load stresses at the bottom of the PCC that would otherwise lead to premature cracking. UTW research conducted so far has concentrated on traffic and fatigue-related aspects of UTW performance; there is a gap in knowledge about the durability of bond under exposure to environmental factors. It is the objective of this research project to determine if environmental factors cause degradation of bond between the AC and PCC to such an extent that this rehabilitation technique is unsuitable for use at light load airports (the Federal Aviation Administration classifies airports that service aircraft with gross loads of 30,000 lb or less as light load).

The research described is being conducted through two tracks. Track 1 encompasses field study of in-service UTW pavements, and Track 2 is comprised of laboratory tests to study PCC–AC bond degradation.

The following UTW projects were visited during Track 1:

- Savannah-Hardin County Airport, TN
- New Smyrna Beach Municipal Airport, FL
- Spirit of St. Louis Airport, MO
- Holiday Inn parking lot, Decatur, IL
- Iowa Highway 21, Iowa County, IA
- Williamstown Jr. & Sr. High School parking lot, KY
- State Road 119, Longmont, CO
- Life Bridge Christian Church parking lot, Longmont, CO

The purpose of the site visits was to observe and document the performance of selected UTW projects and to gather project-related information including construction data, mapping of PCC distresses, and a visual distress survey of UTW pavement surfaces. Corner breaks, cracks, and shattered slabs were the predominant distresses at all the sites visited. Most of these distresses were in areas subjected to heavy traffic, and there was no evidence of loss of bond due to climate.

The Track 2 research evaluated the bond deterioration between the PCC and AC by subjecting field-prepared samples to simulated laboratory extreme environmental conditions of F&T and W&D; H&C tests, though planned initially, could not be conducted. Full-size

UTW test specimens (34 inches by 34 inches by 7 inches) represented actual UTW pavements in terms of sample size, sample preparation, and material properties. A UTW field test section was constructed at ERDC to provide samples for a laboratory test program.

UTW specimens were subjected to environmental exposures in specially designed exposure stations. Material and bond deterioration was evaluated using an ultrasonic underwater measuring system (USUMS). Laboratory investigations indicated that when a UTW pavement is constructed using field durable materials and the AC surface is properly milled and cleaned prior to PCC placement, then the bond between the two materials is at least as durable as the less durable of the two materials. This essentially means that if a UTW pavement is constructed using proper construction techniques, bond failure due to environmental factors should not be a concern.

1. INTRODUCTION

1.1. BACKGROUND

PCC overlays placed over AC pavements, commonly called whitetopping, have been used during the last two decades as a viable alternative to increase the pavement's structural capacity, improve the operational surface, and extend performance life. The thickness of conventional PCC overlays is typically 5 inches (125 mm) or greater and these are generally designed assuming no bond between the original AC and the PCC overlay [1]. During the last 12 years, some agencies have used thinner PCC overlays, referred to as UTW, for deteriorated AC pavements that were structurally sound. These PCC overlays have generally had nominal thicknesses of 4 inches (100 mm) and bond with the old AC surface to form a composite section [2].

A composite section comprised of PCC over AC with bond between the two is considered essential for UTW performance because it reduces load stresses at the bottom of the PCC that would otherwise lead to pavement failure. Since September 1991, when the first UTW project was built in Louisville, Kentucky, over 150 UTW projects [3] have been built. Most of these were placed on old, weathered AC pavements in city streets; intersections, truck weigh stations, and low to medium volume roads [4]. UTW has been constructed at three airports – Spirit of St. Louis, Missouri; New Smyrna Beach, Florida; and Savannah, Tennessee. The latest was a runway rehabilitation project at the Savannah Hardin County Airport in Tennessee (SNH) [5,6,7].

1.2. PROJECT OBJECTIVE

UTW thickness design and performance has been validated using accelerated load testing [8,9,10] however, the long-term durability of the bond between the PCC and AC has not been evaluated. The objective of this project is to study the long-term durability of the bond between PCC and AC and to determine if degradation of this bond will result from exposure to simulated environmental factors of freeze/thaw, wet/dry, and hot/cool.

The objective of this research was to evaluate the durability of the bond between the PCC and AC layers of UTW pavement as a function of environmental (climate) factors.

1.3. RESEARCH APPROACH

The work reported herein was conducted through two tracks to meet research objectives. Track 1 encompassed field study of in-service UTW pavements, and Track 2 was comprised of laboratory tests to study PCC–AC bond degradation.

Track 1 research included the following activities:

- Compile a list of UTW projects in the U.S.

- Document and review UTW performance for selected airport and highway projects, including reviewing and verifying project construction information, mapping of PCC distresses, and a visual distress survey of UTW pavement surfaces.
- Make recommendations on the applicability of UTW-related highway research to airports.

Track 2 was the laboratory evaluation of the bond between AC and PCC (when subjected to simulated environmental conditions) and included construction of a test section and laboratory testing of samples obtained from the field test section. Track 2 began with a review of recommendations originating from Track 1 research and preparation of a work plan.

This report includes a discussion of findings from both Tracks and includes description of laboratory tests, test results, data analysis, and research conclusions.

2. FIELD STUDY OF IN-SERVICE UTW PAVEMENTS

2.1. HISTORY OF UTW IN THE U.S.

Both PCC and AC-surfaced pavements deteriorate and exhibit distresses over their life due to traffic and environment and eventually need to be rehabilitated when distressed beyond a certain threshold. The proper selection of the rehabilitation and the timing of its application within the pavement life cycle can significantly increase the service life of a pavement. Rehabilitation of distressed AC pavements using a PCC overlay, commonly called whitetopping, has been used in the U.S. extensively since the mid-1970's [2].

Conventional whitetopping has been used to increase the structural capacity of existing highways to accommodate increasing traffic loads and volumes. These are generally at least 5 inches (125 mm) thick and do not require bonding to the existing pavement surface; in fact, bonding of the PCC to existing pavement is sometimes considered detrimental to successful performance.

A whitetopping technique developed in the early 1990's utilizes the structural capacity of an existing AC pavement by bonding a thin PCC overlay to the existing AC surface. Due to the bond between the PCC and AC, these thin bonded overlays can be constructed significantly thinner than conventional whitetopping with typical thicknesses ranging from 2 to 4 inches (50 to 100 mm) of PCC. The bond between the PCC and the AC results primarily from milling of the AC surface. UTW, as opposed to conventional PCC overlays, utilizes the structural capacity of the existing AC pavement in a composite section to reduce the thickness of the PCC overlay.

The AC–PCC bond is considered essential for long-term UTW performance, as it allows the AC and PCC layers to act as a composite section. The existence of a good bond causes the PCC slab neutral axis (NA) to shift from the middle of the slab down towards the bottom of the slab. Shifting of the NA reduces the tensile stresses at the bottom of the PCC to an acceptable level. However, at the corners, the shifting down of the NA causes the surface stresses to increase because the corners are acting as a cantilever [1]. The critical location thus moves from the edge to the corner, depending upon material and layer properties if the NA shifts low enough.

The first experimental UTW section was constructed on the access road to a waste disposal facility in Louisville, Kentucky [11,12,13]. The Louisville UTW pavement experimented with two PCC thicknesses (2 to 3.5 inches [50 and 90 mm]) and two joint spacings (2 to 6 ft [0.61 and 1.83 m]). The Louisville experiment concluded that UTW pavements could carry the traffic typical of a low-volume road and a parking lot or a residential street. The shorter joint spacing of 2 ft (0.61 m) had considerably less cracking because it lowered the stresses due to curling, and load is carried in deflection rather than in bending.

The Tennessee and Georgia Departments of Transportation (DOTs) have constructed many UTW sections on urban highways, streets, and intersections starting in 1992 [1,14]. Pavement condition index (PCI) surveys conducted in 1995 and 1996 indicated that the majority of the projects were performing well and in excellent condition (PCI ≥ 90) [1]. Other researchers have reported highway UTW applications in many states, including North Carolina, Kansas [15], Iowa [16,17,18], Pennsylvania, New Jersey, Minnesota [10], Colorado [19,20], Missouri [20,21], Mississippi [13], Virginia, and Florida [4,22]. Most of these were placed on deteriorated AC pavements in city streets; intersections, truck weigh stations, and low to medium volume roads.

There are three known airfields with UTW pavements; these are:

- Savannah-Hardin County Airport, Tennessee (SNH)
- New Smyrna Beach Municipal Airport, Florida (NSB)
- Spirit of St. Louis Airport, Missouri (SUS)

The GA apron at the Spirit of St. Louis Airport in Chesterfield, Missouri, was built in 1995. The UTW at SUS has a thickness of 3.5 inches (89 mm) with a 50-inch (1270-mm) joint spacing [20,21]. The apron at the NSB GA airport in Florida was constructed in 1996 and experimented with several factors, including UTW thickness ranging from 2 to 3.5 inches (50 to 89 mm) [23]. The latest airport UTW project is runway rehabilitation at SNH in Tennessee constructed in 2000 [5,6]. According to the *Engineering News Record*, SNH is the first UTW runway rehabilitation project constructed at a GA airport in the U.S. SNH utilizes a UTW thickness of 4 inches (100 mm) with a 48-inch (1220-mm) joint spacing.

2.2. NEED OF FIELD STUDY

From the very beginning, practitioners have recognized the importance of the bond between PCC and AC to successful UTW performance. However, most of the research effort during the last decade has been devoted to developing algorithms for structural design of UTW and verifying and validating these procedures. Prominent among these studies are efforts conducted by the Portland Cement Association (PCA), American Concrete Pavement Association (ACPA), Federal Highway Administration (FHWA), and the Colorado, Florida, and Iowa DOTs, to name a few. Recently, researchers have started to investigate the best practices for replacing severely distressed UTW panels.

The PCC–AC bond is considered essential for UTW performance, and the primary purpose of this research is to broaden the knowledge about the long-term durability of this bond. A list maintained by the ACPA (all UTW pavements) was consulted to select eight projects for detailed site visits. The three airfields with UTW pavements were selected, as were five highway/parking lot projects. These are listed in Table 2.1.

Table 2.1. List of UTW projects selected for site visits.

Airport Projects	Highway/Parking Lot Projects
• Savannah-Hardin County Airport, TN • New Smyrna Beach Municipal Airport, FL • Spirit of St. Louis Airport, MO	• Holiday Inn Parking Lot, Decatur, IL • Iowa Highway 21, Iowa County, IA • Williamstown Jr. & Sr. High School, KY • State Road 119, Longmont, CO • Life Bridge Christian Church Parking Lot, Longmont, CO

2.3. FIELD PERFORMANCE OF UTW ON AIRPORTS

The purpose of the site visits was to observe and document the performance of selected UTW projects and to gather information including:

- PCC slab size and construction technique
- PCC mix design including the use of fibers
- PCC mix properties from on-site plant or ready mix production
- Condition and thickness of existing asphalt surface
- Thickness of all pavement layers
- AC surface preparation technique (milling, cleaning, etc.)
- Other construction-related information

Knowledge of pavement design and construction history is important to understand its performance during the design life. Besides original construction information, the design approach and method used, the construction procedure, design traffic, and other factors were reviewed during site visits.

Failures in UTW projects are typically noticed at slab corners. A survey was made at each field site of all slabs mapping all distress types (especially, crack types, pattern, and magnitude).

This visual distress survey of UTW pavement surface also provided data to calculate the PCI in accordance with the standardized procedure outlined in ASTM D5340. This was in addition to the distress mapping activity described earlier; PCI ratings were used to compare the relative UTW performance at different geographic locations. A PCI survey involves identifying distress types, severity level of distresses, and measuring the quantity of each distress. These data are used to calculate the PCI ratings (0 to 100).

Site visit details are provided in the following sections. Appendix A contains MicroPAVER PCI summary reports. PCI summaries are provided for comparison purposes only; PCI alone cannot be used to determine if UTW is a preferred rehabilitation alternative.

2.3.1. SAVANNAH-HARDIN COUNTY AIRPORT, TENNESSEE

Savannah-Hardin County Airport is located just off Tennessee Highway 69 to the east of the town of Savannah in Hardin County. A layout of the airfield pavements is shown in Figure 2.1. The airport has one runway, Runway 18-36, which is 100 ft (30.5 m) wide and 5000 ft (1524 m) long.

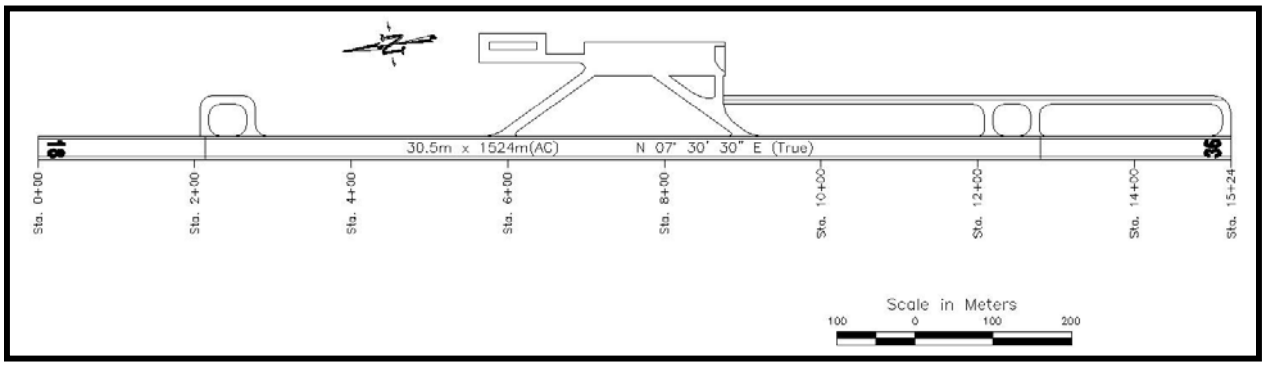

Figure 2.1. Layout of airfield pavements at Savannah-Hardin County Airport.

2.3.1.1. Runway 18-36 Construction History

Runway 18-36 was initially constructed in 1962 and was 3500 ft (1067 m) long and 75 ft (22.9 m) wide. The original construction had a total pavement thickness of 10 inches (255 mm) comprised of 6.5-inch (165-mm) crushed aggregate base and 3.5-inch (89-mm) AC surface. In 1975, the runway was rehabilitated using a 3-inch (75-mm) AC overlay. At that time, the runway was also extended by 700 ft (213 m) and 800 ft (244 m) on the north and south ends, respectively. The extensions are comprised of 10-inch (255-mm) crushed aggregate base with a 3-inch (75-mm) AC surface. The width was also increased to 100 ft (30.5 m) by adding 12.5-ft (3.8-m) wide sections on both sides. In 1989, cracks on the runway were sealed and repaired [5,6].

2.3.1.2. Pavement Condition Prior to UTW Construction

The existing AC surface at SNH was aged and exhibited significant fatigue and thermal cracking. Existing pavement condition was assessed using the PCI, and the structural capacity was estimated using the falling weight deflectometer (FWD) and the dynamic cone penetrometer (DCP). Originally, only the runway was to be rehabilitated, so no pre-construction testing was conducted at other parts of the airport. However, apron rehabilitation was added at a later date (without any pre-construction evaluation).

The SNH runway was divided into nine distinct pavement features with consistent characteristics to determine the PCI rating. The PCI for the center part of the runway ranged from 60 to 78; PCI ratings for all nine features are shown in Table 2.2.

Table 2.2. Pavement condition index ratings for SNH Runway 18-36.

Feature No.	Runway 18-36 Feature	Stations		PCI	Condition Category
		From	*To*		
1	Main Runway (south extension)	12+80	15+24	78	Very Good
2	Main Runway (original construction)	2+13	12+80	60	Good
3	Main Runway (north extension)	0+00	2+13	68	Good
4	Right Shoulder (south extension)	12+80	15+24	74	Very Good
5	Right Shoulder	2+13	12+80	71	Very Good
6	Right Shoulder (north extension)	0+00	2+13	84	Very Good
7	Left Shoulder (south extension)	12+80	15+24	82	Very Good
8	Left Shoulder	2+13	12+19	69	Good
9	Left Shoulder (north extension)	0+00	2+13	69	Good

The surface of Runway 18-36 was generally in fair to good condition. Figure 2.2 shows low- and medium-severity block cracking observed along the entire length of the runway; the inset shows a close-up of typical crack intersections. Low-severity longitudinal and transverse cracks were also noted (Figure 2.3).

Figure 2.2. Block cracking observed on both sides of the runway centerline at SNH.

Figure 2.3. Longitudinal and transverse cracking observed at SNH.

FWD and DCP tests were conducted along two lines each offset approximately 25 ft (7.5 m) from the centerline. Tests were spaced 500 ft (150 m) apart along each line to effectively provide a test every 250 ft (75 m) along the runway. Two-inch (50-mm) diameter cores were also taken near the points where FWD tests were conducted to determine the layer thickness at that point and to conduct DCP tests.

Impulse stiffness moduli (ISM) were calculated by dividing the FWD impulse load by corresponding deflections. The ISM provides a relative indication of the overall strength variation in pavement structure, as shown in Figure 2.4. The FWD data were entered into a software tool called MODULUS to backcalculate the layer moduli (see Table 2.3). AC layer thicknesses from extracted cores were used during backcalculation of moduli.

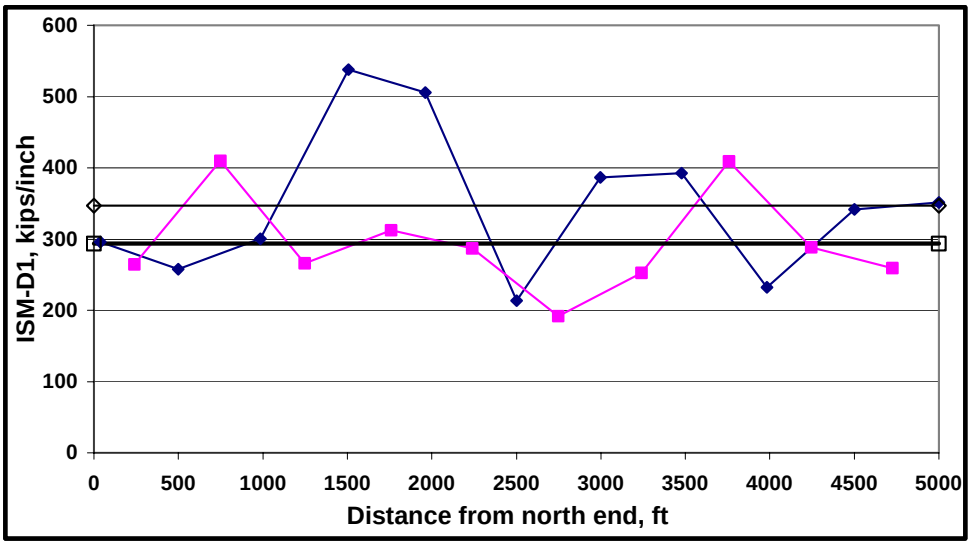

Figure 2.4. ISM of existing AC pavement.

Table 2.3. Results of NDT field tests at SNH using FWD and DCP.

Station	FWD Backcalculated Moduli, psi			DCP Estimated CBR		Thickness of AC, inch
	AC	Base	Subgrade	CBR Base	CBR SG	
0+12	168,969	24,656	8,267	40	20	3.0
0+73	177,961	23,061	7,252	40	9	3.0
1+52	177,961	61,061	3,046	40	14	2.9
2+28	55,985	40,611	13,489	42	20	5.6
3+01	50,038	115,450	3,771	30	20	5.3
3+81	57,000	74,839	2,466	40	15	5.0
4+59	98,045	149,969	6,817	35	15	5.0
5+36	59,030	19,870	19,870	40	11	5.8
5+98	121,977	43,656	12,183	35	20	4.7
6+82	50,038	79,916	4,061	40	12	5.0
7+62	57,000	16,824	5,656	30	17	4.6
8+38	50,038	41,191	1,885	40	12	5.0
9+14	193,045	93,259	3,046	33	20	5.6
9+88	107,038	54,534	1,740	40	7	5.0
10+60	200,007	93,114	3,046	30	8	7.1
11+45	50,038	140,251	6,237	44	17	5.1
12+14	50,038	57,145	3,336	30	8	4.9
12+94	212,045	33,794	4,786	--	--	3.0
13+72	50,038	43,366	7,397	--	--	2.9
14+40	175,061	24,656	5,656	40	12	3.0
15+24	252,946	51,053	3,336	20	20	2.9
Average	114,967	61,061	6,064	36	15	4.0
Std. Dev.	69,020	38,615	4,441	6	5	1.0

Note: 1 psi = 0.006894757 MPa
1 inch = 25.4 mm

The average backcalculated AC modulus was 115 ksi (793 MPa); however, the data indicated three distinct regions with different moduli. The moduli for the two extensions were higher than the rehabilitated portion due to cracking in the rehabilitated portion of the runway. The average backcalculated moduli for the base and the subgrade were around 61 and 6 ksi (421 and 42 MPa), respectively.

The number of hammer blows and the depth of penetration were recorded during the DCP tests. A DCP index was computed in terms of mm/blow, and California Bearing Ratio (CBR) values were determined using the following equation, developed by Webster et al.[24,25]:

$$\log (CBR) = 2.81 - 1.32 \log DCPI$$

The estimated CBR for the base and the subgrade were 36 and 15, respectively, as shown in Table 2.3.

2.3.1.3. UTW Thickness Design for SNH

Design traffic for SNH is shown in Table 2.4.

Table 2.4. Aircraft traffic used in SNH structural design calculations.

Aircraft Weight kips (KN)	Annual Departures	Tire Configuration	Contact Pressure, psi (kPa)	Spacing Between Duals, in (mm)
60 (266)	150	Dual-wheel	94 (648)	18 (457)
30 (133)	1000	Dual-wheel	84 (577)	15 (381)

The following approach was used to determine the design life of the 4-inch (100-mm) UTW.

- A two-dimensional finite element (FE) program was used to calculate stresses and deflections in the UTW using a corner load case (one tire of the dual-wheel gear located at a corner) and an edge load case (both tires of the dual-wheel gear located along a joint equidistant from the corners of the slab). The joint spacings considered were 48 inches (1220 mm) and 72 inches (1830 mm).
- The maximum calculated value of the bending stress in the UTW for the corner and edge load cases was subsequently divided by the flexural strength (S_C) of the UTW PCC, 700 psi (4.83 MPa), to obtain the stress ratio (S_R).
- The PCA fatigue equations were used for analysis of fatigue cracking of the UTW. N_f, the number of fatigue cycles, is unlimited for $S_R \leq 0.45$. The fatigue equations are:

    - $\text{Log } N_f = 11.737 - 12.077\ S_R$ for $S_R \geq 0.55$
    - $N_f = ((4.2577 \div (S_R - 0.4325))^{3.2}$ for $0.45 < S_R < 0.55$

- The equivalent annual traffic was determined to be 250 operations of the controlling aircraft. The computed N_f was then divided by 250 operations per year to get service life of 30 years.

2.3.1.4. UTW Construction at SNH

Construction of the UTW on Runway 18-36 started on April 3, 2000, with milling of the existing AC surface. The milling thickness was kept below 0.5 inch (13 mm) to minimize reduction in thickness of AC layer. Multiple sweepings with a mechanical broom removed the residual grit from the milled surface. High-pressure compressed air provided the final cleaning. An on-site plant produced the PCC mix with properties shown in Table 2.5.

Figure 2.5 shows the construction of the UTW; Figure 2.6 shows core samples taken from the UTW on the SNH runway.

Table 2.5. Mix design of PCC used at SNH.

PCC Components	Attributes
Cement	Type I (575 lb total cementitious material)
Fly Ash	≤ 15 % by weight of cementitious material
Strength	700 psi (4.83 MPa) flexural
Slump	≥ ½ inch (13 mm) and ≤ 2 inch (50 mm)
Water/Cement Ratio	0.35
Air Content	6 % by volume
Synthetic Fibers	3 lb/yard^3 (1.78 kg/m^3)

Figure 2.5. UTW placement at SNH followed milling of existing AC pavement.

Figure 2.6. Cores extracted at SNH during construction indicated a good bond.

Observing the success of the UTW construction on the runway, the SNH Airport Authority added the taxiway connectors and the apron to the same contract. No evaluation was made of the existing AC pavement in these areas and the runway UTW design was used. As a result, some unforeseen problems were encountered as discussed in the following sections.

2.3.1.5. Assessment of Current UTW Conditions at SNH Runway 18-36

SNH runway 18-36 was surveyed in December 2001. The PCI ratings are given in Table 2.6, and pavement features and sections are shown in Figure 2.7. The runway was divided into the east shoulder (25ft [7.62m] wide), the keel section (50ft [15.24m] wide) and the west shoulder (25ft [7.62m] wide). Distress conditions were assessed on all slabs on the runway.

All pavement areas had a PCI rating of at least 98 and were categorized as excellent. There were a few slabs with low-severity linear cracks. There was no evidence of any climate or durability-related distress.

Table 2.6. PCI ratings for SNH Runway 18-36 after 20 months service.

Pavement	Feature	Station		PCI Rating		
		From	To	East	Keel	West
Runway	01	0+00	1+53	100	100	100
	02	1+53	2+13	100	100	100
	03	2+13	2+42	100	99	100
	04	2+42	3+36	100	99	100
	05	3+36	4+26	100	98	100
	06	4+26	12+80	100	99	100
	07	12+80	15+24	100	100	100

2.3.1.6. Instrumentation of UTW at SNH

To evaluate the bond between AC and PCC, two slabs were instrumented during UTW construction [26]. Strain gages were installed near the surface and bottom of the PCC (concrete strain gage, EGP-5-120) and on the top of the milled AC surface (WFLM-60), and rosette strain gages (PMR-60-2L) were placed in the corners. In addition to strain gages, thermocouples were installed in the pavement slabs to measure pavement temperature gradients, and a thermistor probe was installed to measure ambient air temperature.

Based on analysis of the strain data and comparison of the summer and winter test results, the following conclusions were drawn [27]:

- Analysis of dipstick data showed no difference between the morning and afternoon measurements during winter and summer tests, indicating that the PCC slabs are bonded to the milled AC surface.

Figure 2.7. Sample unit layout for Runway 18-36 at SNH

DO NOT DELETE; leave this page blank.

This page left blank for reverse side of Figure 2.7. Sample unit layout for Runway 18-36 at SNH

- Analysis of winter data indicated that PCC slabs are bonded to the milled AC surface at the middle of the slabs, along the longitudinal and transverse joints and at the corners.

- Analysis of summer data indicated that some debonding might have occurred at the corners. Based on winter data analysis results, this discrepancy is attributed to incorrect positioning of the loaded truck wheels during summer tests; however, interpretation of corner strain data is problematic due to structural discontinuities present.

- During both winter and summer tests, comparisons of strain data at identical locations show generally slightly higher strains at slower speeds, as would be expected due to rate of loading effects.

- Comparison of summer strain data at identical locations for the morning and afternoon runs indicated that, on the whole, PCC slabs and the milled AC surface are bonded and acting as a composite structure. Winter data did not show such a clear trend; some difference in magnitudes was evident.

- Strains measured across longitudinal and transverse joints between loaded and unloaded slabs suggest that there is a good load transfer across the joints.

In general, the analysis of winter data and comparison of winter and summer analysis results indicate that the PCC slabs and the milled AC surface are bonded together and that the rehabilitated pavement should perform as designed.

2.3.1.7. Lessons Learned from SNH

All pavement areas on Runway 18-36 had a high PCI rating. The runway was the original UTW rehabilitation project and a thorough evaluation of the existing AC pavement and in-depth design analysis was made prior to the UTW construction. Because the runway UTW construction was such a success, the contract was amended to include UTW construction on the taxiways and the apron without any pre-construction testing or any further design analysis. The same design section (4-inch [100-mm] PCC) was used for this additional construction. Several areas on the apron and taxiway contained localized weak spots and deterioration of the AC. Shortly after completion of the UTW construction, these areas exhibited extensive cracking, with the majority of the slabs cracked into two or more pieces, as shown in Figure 2.8.

Figure 2.8. Cracking in SNH apron UTW slabs.

Another problem encountered in the same area was depressed slabs in the general vicinity of the cracked slabs; these are shown in Figure 2.9. Improper joint spacing and slab shapes also caused slabs to crack, especially at the intersection of taxiways and the apron, and taxiways and the runway (Figure 2.10).

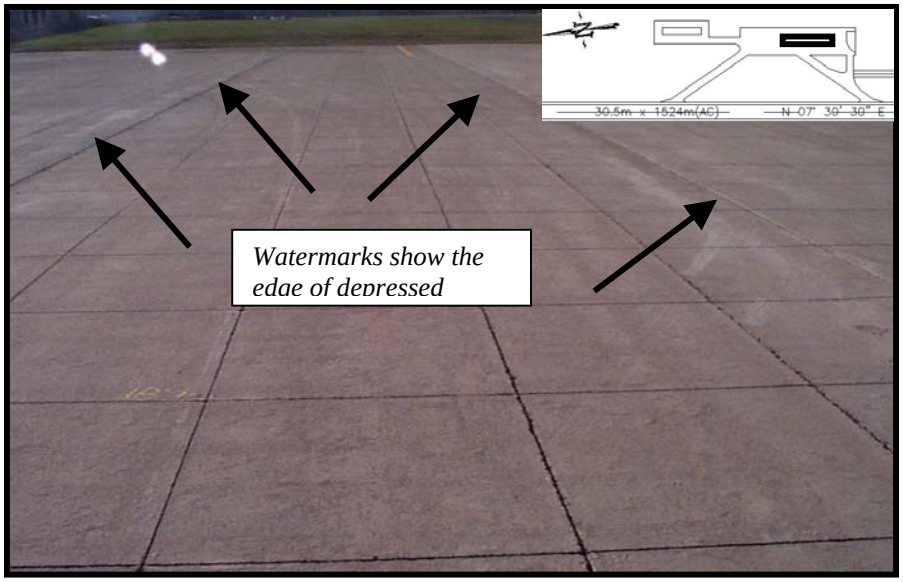

Figure 2.9. Poor subgrade support caused depressions in SNH apron pavement.

Figure 2.10. Improper joint spacing and slab shapes caused SNH slabs to crack.

Surface preparation problems near the airport office caused a few slabs to cracks. This area (13 slabs long and 2 slabs wide) could not be milled properly during construction due to deteriorated AC pavement. All the UTW slabs in this area sounded hollow when tapped using a small hammer, indicating a disbond. However, only the four slabs in front of the access gate (to allow cars and pickup trucks access to apron) exhibited distress, which was in the form of linear cracks. Cracked slabs in other areas of the runway and apron sounded solid when tapped with the hammer.

2.3.2. SPIRIT OF ST. LOUIS AIRPORT, MISSOURI

The SUS GA airport owned by St. Louis County is located in Chesterfield, Missouri, south of U.S. Highway 61. A layout of the airfield pavements is shown in Figure 2.11. The airport master plan called for ramp rehabilitation, highlighted in Figure 2.11. The ramp, originally constructed in 1986, covers approximately 47,800 yd^2 (40,000 m^2).

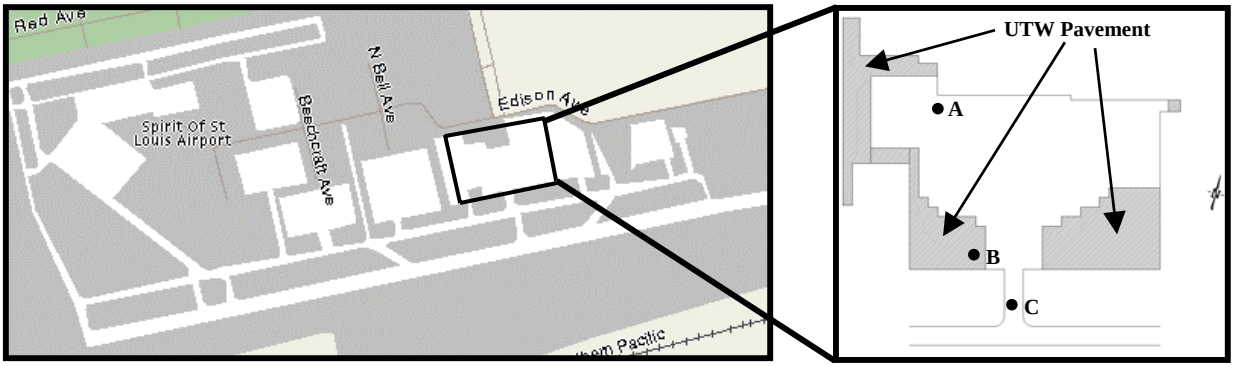

Figure 2.11. Layout of airfield pavements at the Spirit of St. Louis Airport.

2.3.2.1. Pre-UTW Construction Conditions at SUS

The SUS airport master plan called for ramp rehabilitation to carry aircraft ranging from commercial jets, such as DC-9s and 727-100s with a gross weight of 110 kips (50 Mg), to light load aircraft with a gross weight of 12.6 kips (5.7 Mg) [21,28]. The AC-surfaced pavement was in fair to poor condition; an overlay of the apron area was recommended in 1994 [21].

The existing AC surface varied in thickness depending upon whether the base layer was cement stabilized, asphalt stabilized, or granular aggregate base. Fifty cores were taken for pavement layer thickness determination and to assess the condition of the AC pavement and the underlying soils; only three of the cores were taken on the apron as shown on Figure 2.11. Layer thicknesses are shown in Table 2.7.

Table 2.7. Thickness of pavement layers at SUS apron.

Core Location	Layer Thicknesses.			
	AC Surface	AC Base	Soil Cement Base	Granular Base
A	1.0 in (25 mm)	2.0 in (50 mm)	4 in (100 mm)	--
B	1.5 in (38 mm)	2.0 in (50 mm)	--	6 in (150 mm)
C	1.5 in (38 mm)	1.5 in (38 mm)	4 in (100 mm)	--

2.3.2.2. SUS UTW Thickness Design

The design traffic is shown in Table 2.8.

Table 2.8. Design traffic for the SUS apron.

Loading Type	Gross Aircraft Weight	Equivalent Annual Operations
Heavy	110 kips (50 Mg)	200
Medium	70 kips (32 Mg)	3,000
Light	12.6 kips (5.7 Mg)	--

The UTW design for the apron was for light load aircraft, and the design thickness was 3.5 inches (89 mm) with a joint spacing of 50 inches (1270 mm).

2.3.2.3. UTW Construction at SUS

The SUS apron was constructed in February 1995 after milling 0.5 inch (13 mm) of the existing AC. Ready mix concrete with fibers was placed using a slip form paver and textured with a light broom finish; PCC properties are shown in Table 2.9.

Table 2.9. PCC mix design used at Spirit of St. Louis Airport.

PCC Components	Attributes
Cement	Type I, 510 lbs/yd^3 (303 kg/m^3)
Fly Ash	79 lbs/yd^3 (47 kg/m^3)
Strength	650 psi (4.48 MPa) flexural
Sand	1,262 lbs/yd^3 (749 kg/m^3)
#57 Limestone	1,880 lbs/yd^3 (1,115 kg/m^3)
Water/Cement Ratio	0.35
Air Entrainment	1.79 fl oz/100 lbs (53ml/45kg) of cement
Water Reducer	5.5 fl oz/100 lbs (163 ml/45 kg) of cement
Synthetic Fibers	3 lb/yard^3 (1.78 kg/m^3)

2.3.2.4. Assessment of Current UTW Conditions at SUS

The site visit to SUS to evaluate the pavement condition was made in February 2002. The apron features are shown in Figure 2.12, and the condition ratings are shown in Table 2.10. The apron layout showing feature designations is found on Figure 2.12. All PCC slabs were surveyed; all features were rated excellent. Only 204 slabs out of 2,728 slabs (7.48 percent) in Feature A01 had climate/durability related problems; the other four features had no climate/durability related problems.

Table 2.10. PCI ratings for UTW apron at SUS.

Feature	Sample Units	Area	PCI Rating	Distress Types Observed
A01-1	117	10,187 ft^2	97	Some load-related distresses visible
A02-1	12	1,400 ft^2	100	None
A03-1	79	11,145 ft^2	100	One slab with broken corners
A04-1	134	17,487 ft^2	99	Some load-related distresses visible
A05-1	4	282 ft^2	94	Some load-related distresses visible

Note: 1 ft^2 = 0.093 m^2

This page intentionally left blank.

Figure 2.12. Layout of sample units at Spirit of St. Louis Airport.

This page left blank for reverse side of

Figure 2.12. Layout of sample units at Spirit of St. Louis Airport.

2.3.2.5. Lessons Learned from SUS

Despite an excellent overall rating, there were some areas with distresses attributable to traffic loadings. Very few climate or durability-related distresses were observed.

The UTW apron area is designated for aircraft less than 12.6 kips (5.7 Mg), but fuel trucks use a portion of the UTW apron from the entrance gate to their designated parking location. Figure 2.13 shows the path taken by the fuel trucks after entering through the apron access gate.

After entering the apron area, trucks make a left turn on the UTW pavement (Figure 2.13-A). All PCC slabs along the path of the trucks, shown in Figure 2.14, have corner cracks. The fuel trucks make the second left turn (Figure 2.13-B) into the parking area. All slabs in this area are shattered or fractured into three or more pieces as shown in Figure 2.15. Corner breaks and shattered slabs are load-related, not climate or durability-related.Another problem noticed at SUS was cracking of slabs containing aircraft tie downs, shown in Figure 2.16. These slabs were retrofitted with tie down anchors, which are PCC columns extending about 18 inches (457 mm) into the ground below the slab. Stress build-up due to temperature swings have resulted in the cracking shown in Figure 2.16.

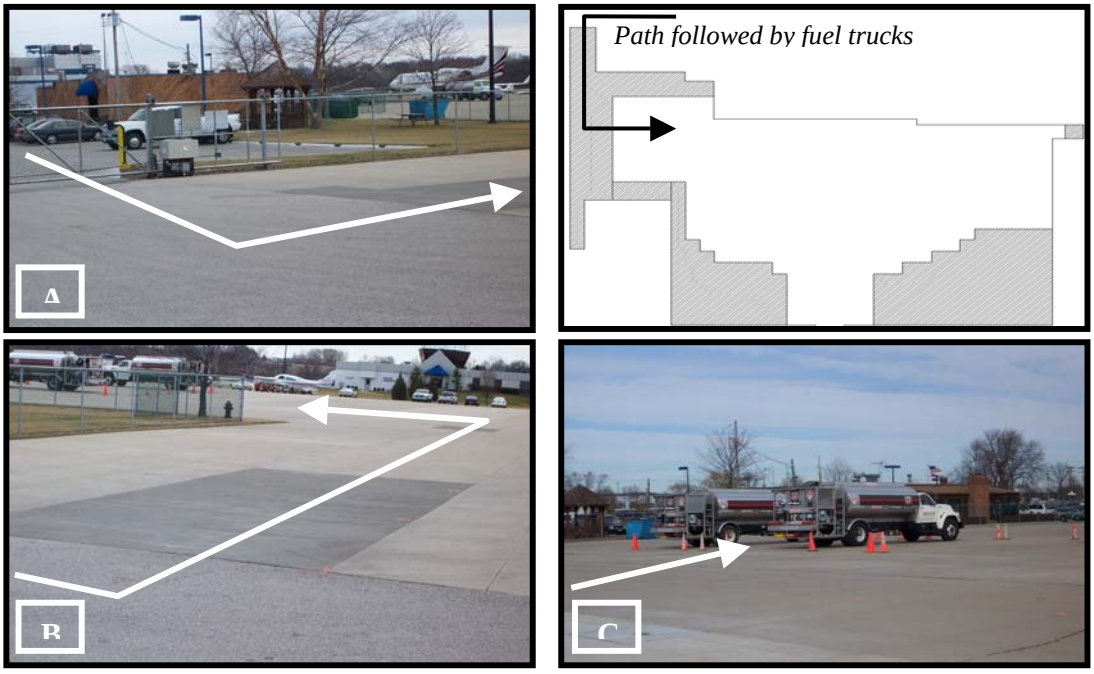

Figure 2.13. Fuel truck path over the UTW apron pavement.

Figure 2.14. All slabs at the first left turn have corner cracks along interior joints.

Figure 2.15. All slabs after the second left turn are shattered into three or more pieces.

Figure 2.16. All slabs containing aircraft tie downs were shattered.

2.3.2.6. Verification of Bond Loss at SUS

SUS was revisited during Track 2 to determine if the hollow sound noticed during the initial site visit indicated a loss of bond between the PCC and AC. Cores, with descriptions provided in Table 2.11, were taken down to the granular pavement layers at selected locations as shown in Figure 2.17.

Table 2.11. Description of cores removed at SUS.

Core	Sound	Average Thickness (inch)		Bond Condition	Slab Distress
		PCC	AC		
1	Hollow	3.3	2.0	No bond	Shattered slab
2	Hollow	3.7	2.5	No bond	No distress
3	Hollow	3.9	Fragmented	No bond	Shattered slab
4	Solid	3.7	Fragmented	No bond	Shattered slab
5	Solid	2.8	3.2	No bond	Corner breaks
6	Hollow	3.0	3.1	No bond	Corner breaks
7	Hollow/Solid	3.1	3.3	Intact bond	Corner breaks
8	Solid	3.3	3.3	Intact bond	Corner breaks
9	Solid	3.1	3.6	No bond	Shattered slab
10	Hollow	3.0	3.8	No bond	Opposite corner broken
11	Hollow/Solid	3.3	2.6	No bond	Shattered slab
12	Solid	3.3	3.0	Intact bond	No distress

Note: 1 inch = 25.4 mm

The revisit to SUS used sounding with a hammer to locate areas of disbond. Hollow sounds indicated a disbond and was verified by the removal and examination of pavement cores in these locations. A solid ringing sound indicated a bond between the AC and PCC if the core was away from the distressed location. A solid sound indicated a bond between the PCC and AC if the slab was not distressed, as was the case of core location 12 at SUS. Even in the case of distressed slabs, a solid sound away from the distresses indicated an intact bond, as was the case with core location 8.

A solid sound does not always indicate an intact bond. An example of this is cores taken near corner breaks. The traffic action tends to press the broken part of the corner break into the AC, thus creating a bond that cannot be detected with sounding with a hammer. Examples of such cases are cores taken at locations 5 and 9. A solid sound outside the corner break area indicated a bond; an example of this is core location 7.

Figure 2.17. Location of cores taken at the Spirit of St. Louis Airport.

This page left blank for

Figure 2.17.

2.3.3. NEW SMYRNA BEACH MUNICIPAL AIRPORT, FLORIDA

The NSB GA airport is located in southeast Volusia County, Florida, along an 8-mile (12.87-km) stretch of the Atlantic coast (see Figure 2.18). NSB faces U.S. Highway 1, 2 miles (3.22 km) north of downtown New Smyrna Beach and about 12 miles (19.31 km) south of Daytona Beach. Originally constructed during World War II, the UTW apron covers approximately 17,000 yd^2 (14,200 m^2).

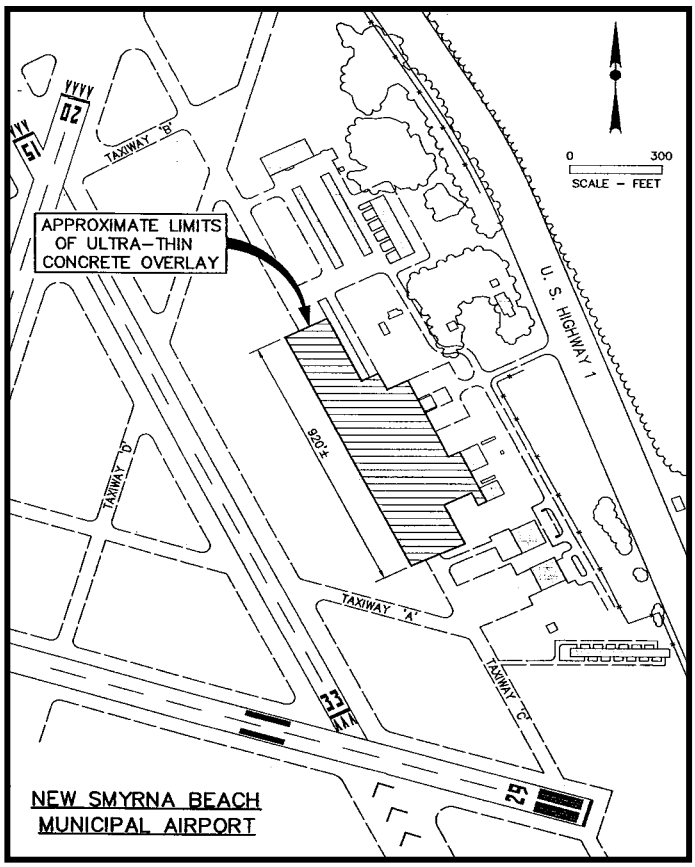

Figure 2.18. Layout of airfield pavements at the New Smyrna Beach Airport

2.3.3.1. Pre-UTW Construction Conditions at NSB

A 1995 PCI survey of the NSB apron indicated sections with ratings of "poor" and "very poor." There were several areas with grass growing between the cracks. The AC surface, where UTW would later be placed, was severely oxidized and cracked, and had alligator cracking on the taxiway portion (Figure 2.19) [8,29,23]. About half of the apron had a 1- to 2-inch (50- to 100-mm) AC surface on top of a 5- to 8-inch (125- to 200-mm) thick base built on a compacted, well-draining coquina shell soil.

Figure 2.19. Alligator cracking of AC surface at New Smyrna Beach Airport.

2.3.3.2. NSB UTW Thickness Design

The University of Central Florida (UCF) conducted a study at their Circular Accelerated Test Track (CATT) to determine PCC durability and performance and the type and amount of fiber additive for UTW to be placed at the NSB demonstration project. Eight test sections were constructed at CATT; section details are available elsewhere [8,29]. The study concluded that fiber reinforced concrete retarded the initial formation of cracks and reduced the propagation of cracks. Compared to the fiber reinforced concrete, plain PCC had significantly wider cracks.

The NSB project was designed based on the results of the CATT tests. The primary objective of the NSB demonstration project was to resurface the apron, and the secondary objective was to evaluate different UTW characteristics. The project variables included [23]:

- PCC thickness of all sections, 2 to 3.5 inches (50 to 89 mm)
- PCC–AC interface conditions (bonded, not bonded, and stress-relieving layer)
- Polypropylene or polyolefin fibers (different application rates)
- Joint spacing, 4 ft by 4 ft or 5 ft by 6 ft (1.2 m by 1.2 m or 1.5 m by 1.8 m)

PCC with a flexural strength of 650 psi (4.48 MPa) was specified; Figure 2.20 shows the location of various characteristics.

Figure 2.20. UTW thickness, location of areas with fibers, and different surface preparation methods at NSB.

This page left blank for Figure 2.20. UTW thickness, location of areas with fibers, and different surface preparation methods at NSB.

2.3.3.3. UTW Construction at NSB

Pre-construction site preparation included cleaning and removing of loose material from the pavement surface. Pavement damage was not to such an extent that it warranted repair prior to UTW construction. Before PCC placement, all apron areas where bonding agent was required were prepared by applying acrylic latex based bonding agent. Other areas were left untreated or covered with a stress-relieving interlayer if required (see Figure 2.20).

Ready mix concrete was hand-placed, and a vibrating roller screed was used to strike off and consolidate the PCC. A "roller bug" [29] consisting of one or two cylinder shaped rollers of coarse expanded material was used on the freshly struck-off PCC surface to force the fibers down.

The mix design properties are provided in Table 2.12.

Table 2.12. Properties of UTW design mix for New Smyrna Beach Airport.

PCC Components	Attributes
Cement	Type I, 564 lbs/yd^3 (334 kg/m^3)
Fly Ash	None
Strength	650 psi (4.48 MPa) flexural strength
# 67 stone (PCC)	≤ 50 percent of total aggregate by weight
Water/Cement Ratio	≤ 0.50
Air Entrainment	4.5 %
Synthetic Fibers	Various rates, see

2.3.3.4. Assessment of Current Conditions at NSB

Results of a PCI survey in February 2002 are shown in Table 2.13. Figure 2.21 shows the feature designations and sample units. A total of 7,660 UTW slabs divided into 26 features were surveyed. Of these, only 62 slabs (0.81 percent) exhibited any climate/durability-related distress. Linear cracks and broken corners were the most common load-related distress observed. Twenty-three of the 26 features had no climate/durability distress.

Apron areas designated as Features A01, A02, A03, A11, and A12 (see Figure 2.21) are also used as a taxiway; Features A01, A02, A03, and A11 provide access to Taxiway D towards the north end, and Features A11 and A12 provide access to Taxiway A and C towards the south end of the apron (see Figure 2.21). The traffic pattern on the apron during the site visit and discussions with the airport manager suggested that access to Taxiway D is the least used, and only by small aircrafts.

Features A01, A02, and A03 have no load-related distresses. Features A11 and A12, used most often, have some load-related distresses.

This page intentionally left blank.

Figure 2.21. The NSB apron was divided into 26 features to encompass all variables.

This page left blank for the reverse side of

Figure 2.21. The NSB apron was divided into 26 features to encompass all variables.

Table 2.13. PCI survey results on UTW apron at NSB.

Feature	Sample Units	Total Slabs	Area, ft^2	PCI Rating	Distress Types Observed
A01-1	12	2,400	8,450	100	None
A02-1	1	24	495	100	None
A03-1	9	216	5,436	100	None
A04-1	5	120	495	100	Four slabs with small patch.
A05-1	5	120	1,055	100	None
A06-1	1	2	1,249	47	Large (8-m) slabs divided in the middle.
A07-1	1	12	3,746	80	Linear cracks in half the slabs.
A08-1	25	600	17,373	96	Linear cracks and some broken corners.
A09-1	12	288	11,248	95	Twelve slabs with linear cracks.
A10-1	18	432	12,120	94	Twenty slabs with linear cracks.
A11-1	38	912	25,833	99	Sixteen slabs with linear cracks.
A12-1	25	600	5,005	98	Twenty-five slabs with climate/durability distresses.
A13-1	14	280	7,298	93	Seven slabs with broken corners.
A14-1	7	168	4,176	89	Twenty-one slabs with linear cracks.
A15-1	3	56	603	96	Two slabs with linear cracks.
A16-1	5	100	2,357	92	Six slabs with linear cracks.
A17-1	1	31	914	98	All slabs with joint seal damage.
A18-1	3	62	2,013	86	Ten slabs with corner breaks.
A19-1	6	144	4,306	100	None.
A20-1	2	48	1,324	100	None.
A21-1	2	48	1,745	100	One slab with a small patch.
A22-1	1	28	872	100	None.
A23-1	15	294	8,622	95	Six slabs with climate/durability distresses.
A24-1	19	399	14,100	98	Nine slabs with broken corners.
A25-1	19	228	9,871	100	One slab each-corner spall and small patch
A26-1	2	48	5,726	95	One slab broken corner, one slab linear crack.

Note: 1 ft^2 = 0.093 m^2

2.3.3.5. Lessons Learned from NSB

The NSB apron is performing well to date, except for a few areas with some localized problems. The PCI ratings of most of the apron features were excellent, with a few very good ratings. The only low PCI rating was a 47 on Feature A-06, which was comprised of only two 26-ft (8-m) square slabs. These slabs cracked in the middle, dividing each slab into four equal size pieces. These slabs were rated as shattered slabs, which produced a PCI of 47. Feature A07 used 26 ft (8 m) by 13 ft (4 m) slabs, and these slabs cracked into two pieces, as shown in Figure 2.22.

Ten cracked and non-cracked slabs each were tapped with the hammer along the joints, cracks, and the middle of the slab. In all instances the slabs sounded solid, indicating a good bond.

Figure 2.22. Large 26-ft by 13-ft (8-m by 4-m) slabs cracked into two pieces.

2.4. FIELD PERFORMANCE OF UTW ON VEHICULAR PAVEMENTS

2.4.1. COMPARISON OF HIGHWAY AND AIRPORT LOADS

SUS, STL, and SNH are the three GA airports that have used UTW for pavement rehabilitation. Among the airport UTW projects, SNH is the only airport that has used UTW for runway rehabilitation; the other two airports used UTW apron rehabilitation.

Due to similarities in wheel loads and contact stresses applied to the pavement surface, the information gained from highway UTW projects can be applied to GA airports (after careful analysis). For example, the current Federal truck weight regulations limit the weights on single axles to 20 kips (89 kN) and tandem axle loads to 34 kips (151 kN). Three-axle single unit trucks and 5-axle tractor-semi trailers constitute approximately 25 and 43 percent of the U.S. truck fleet [30]. Table 2.14 compares the imposed loads, contact areas, and pressures for these wheel axle combinations to UTW design aircraft load parameters used at SUS, SNH, and NSB airports.

Table 2.14. Comparison of axles-wheel combinations

Axle-Wheel Combination	Gross Imposed Load	Load Per wheel	Tire or Contact Pressure	Contact Area
	kips (kN)	kips (kN)	psi (kPa)	inch^2 (cm^2)
Single axle Dual tires [a]	20.0 (89.0)	5.00 (22.25)	100 (689)	50 (323)
Tandem axle Dual tires [a]	34.0 (151.2)	4.25 (18.88)	100 (689)	277 (43)
SNH, TN Dual tires [b]	30.0 (133.4) [c]	6.75 (29.93) [d]	85 (586)	510 (79)
SUS, MO Single tire [b]	12.5 (55.6) [c]	5.63 (25.04) [d]	60 (414)	605 (94)
NSB, FL Dual tire [a]	33.0 (146.8) [e]	5.5 (24.47) [f]	100 (689)	355 (55)

Notes: [a] Truck tire
[b] Aircraft tire
[c] Gross aircraft weight.
[d] Assumes that 90 percent of total load is on the main gear, 45 percent on each side.
[e] Gross load imposed on the accelerated pavement testing machine assembly
[f] 3-half axle boogies with dual tires.

The gross weights on the trucks and aircrafts vary widely but are quite similar in terms of load on a single wheel; design aircraft wheel loads are slightly higher than the truck wheel loads. However, trucks tires are usually inflated to a higher tire pressure and have smaller contact areas. The aircraft wheel loads are being applied with a relatively lower contact pressure and larger contact area, which is relatively less damaging to the pavement structure. Also, in terms of number of load applications, highway pavements experience a higher number of load repetitions compared to pavements at a typical GA airport. So the comparison of performance is slightly conservative since the truckloads should tend to cause more damage than the aircraft loads.

2.4.2. IOWA HIGHWAY 21, IOWA COUNTY, IOWA

A 1994 Iowa research project constructed a 7.2-mile (11.6-km) stretch of PCC overlays on Iowa Highway 21 from US 6 to Iowa Highway 212 (Figure 2.23). A total of 65 test sections, each 700 ft (213 m) long, were constructed. Major research variables in the sections were:

- Three PCC overlay thicknesses: 2, 4, and 6 inches (50, 100, and 150 mm)
- Four joint spacings: 2, 4, 6, and 15 ft (0.6, 1.2, 1.8, and 4.6 m)
- Use of fibers: PCC with and without polypropylene fibers
- Surface preparation: Patching, surface scarification, and cold-in-place recycling

2.4.2.1. Iowa Highway 21 Construction History

The original construction of Iowa Highway 21 was in 1961, and rehabilitation projects were performed in 1976 and 1987. The pavement section is shown in Figure 2.24. Iowa 21 is 24 ft (7.3 m) wide with 9-ft (2.75-m) wide shoulders and open ditch drains on both sides.

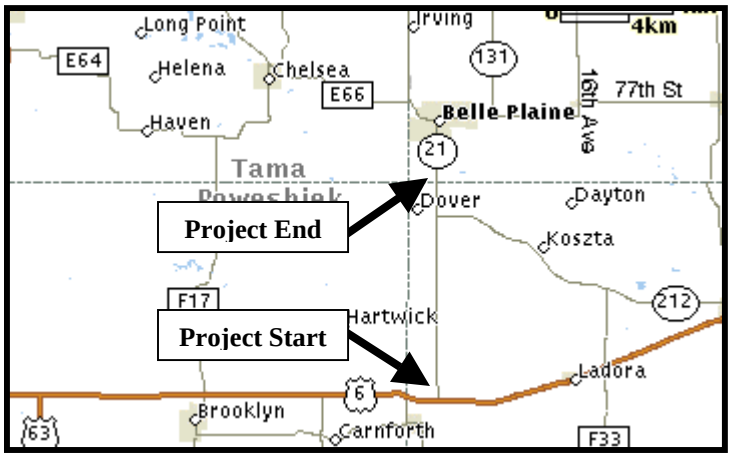

Figure 2.23. Location of Iowa DOT PCC overlay research project.

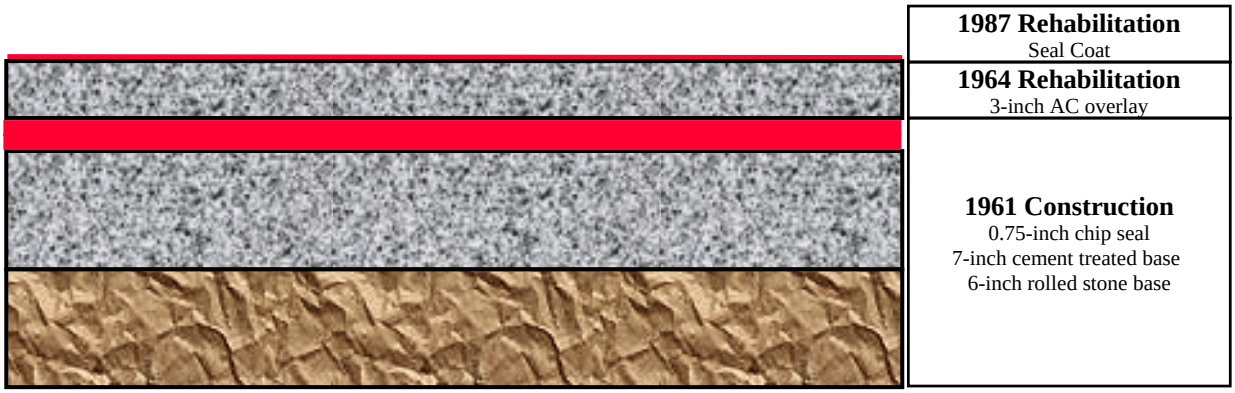

Figure 2.24. Pre-UTW construction history of Iowa Highway 21.

2.4.2.2. UTW Construction at Iowa 21

Construction of the PCC overlays (using a conventional mix) extended from June 24 through July 18, 1994. Of the 65 total sections, only 41 test sections were considered for monitoring; others were transition sections. Of the selected 41 monitoring sections, only 19, as shown in Table 2.15, had PCC thicknesses less than or equal to 4 inch (100 mm).

The initial research lasted for 5 years and was then extended for another 5 years. Only 2-inch (50-mm) panels had shown any distress during the initial 5 years; distressed panels were replaced with 3-inch (75-mm) panels as part of the project extension. The objective of the project extension was to provide additional information about the AC–PCC bond and the behavior of the newly rehabilitated areas [17]. The replaced panels were filled with high early strength concrete mix composed of 50 percent coarse aggregate and 50 percent fine aggregate. Mix properties of the original PCC overlays and the replacement panels are shown in Table 2.16.

Table 2.15. Characteristics of UTW section at Iowa 21.

Section	Station (m)		Thickness (inch)	Fiber Use	Joint Spacing (ft)	Surface Preparation
	Start	End				
6	2357+00	2364+00	4	F	6	P&S
7	2364+00	2371+00	4	F		P&S
8	2371+00	2378+00	4	F	4	P&S
10	2378+00	2387+00	2	F	2	P&S
11	2387+00	2394+00	2	F	4	P&S
23	2449+00	2456+00	2	NF	2	P&S
29	2480+00	2487+00	4	NF	4	P
38	2540+00	2547+00	2	F	2	P
39	2547+00	2554+00	2	F	4	P
41	2555+00	2562+00	4	F	4	P
42	2562+00	2569+00	4	F	2	P
43	2569+00	2576+00	4	F	6	P
48	2594+00	2601+00	4	F	6	CIP
49	2601+00	2608+00	4	F	2	CIP
50	2608+00	2615+00	4	F	4	CIP
52	2616+00	2624+00	2	F	2	CIP
53	2624+00	2631+00	2	F	4	CIP
58	2654+00	2661+00	4	NF	6	CIP
62	2691+00	2698+00	2	NF	4	CIP

Notes: 1 inch = 25.4 mm, 1 m = 3.281 ft
Fiber Use: F=Fiber, NF=No Fibers
Surface preparation: P&S=Patch and scarify, P=Patch only, CIR=Cold-in-place recycling

Table 2.16. Properties of PCC used at Highway 21 in Iowa.

PCC Components	Original Construction		Replacement Mix
	Fly Ash	No Fly Ash	
Fine Aggregate	0.307	0.309	0.312
Coarse Aggregate	0.375	0.377	0.311
Minimum Cement	0.092	0.108	0.156
Water	0.147	0.146	0.161
Entrained Air	0.060	0.060	0.060
Fly Ash	0.019	--	--
Water/Cement Ratio – min/max	0.430/0.480	0.430/0.480	--

Note: Ratios are absolute volumes of materials to unit volume of concrete

2.4.2.3. Assessment of Current Condition at Iowa 21

A PCI survey of UTW sections on Iowa 21 was conducted in February 2002. All surveyed areas were in excellent condition. Many of the original sections had been replaced. Results of the PCI survey are shown in Table 2.17. Most sections had medium-severity joint seal damage. Each feature had a few slabs with load-related distresses such as linear cracks, corner breaks, and a rare shattered slab.

Table 2.17. PCI survey of UTW sections on Iowa 21 indicated excellent performance.

Section	Station (m)		Thickness (inch)	Fiber Use	Joint Spacing (ft)	Surface Preparation	Feature	PCI
	Start	End						
6	2357+00	2364+00	4	F	6	P&S	RD01-1	95
7	2364+00	2371+00	4	F	2	P&S	RD01-2	96
11	2387+00	2394+00	2	F	4	P&S	RD01-3	88
21	2441+00	2448+00	4	NF	2	P&S	RD01-4	92
38	2540+00	2547+00	2	F	2	P	RD01-5	92
39	2547+00	2554+00	2	F	4	P	RD01-6	94
40T	2554+00	2555+00	2-4	F	4	P	RD01-7	95
62	2695+53	2696+97	2	NF	4	CIP	RD01-8	95

Notes: 1 inch = 25.4 mm, 1 m = 3.281 ft, 1 ft = 0.3048 m
Fiber Use: F=Fiber, NF=No Fibers
Surface preparation: P&S=Patch and scarify, P=Patch only, CIR=Cold-in-place recycling

2.4.2.4. Lessons Learned from Iowa 21

All UTW sections are currently performing well, with no apparent climate/durability-related problems. Earlier work (prior to replacement of panels in August 1999) found some UTW sections performing poorly; disbonding between AC and PCC was found in UTW sections without fibers and in areas where the UTW was placed after broom cleaning only or after cold in-place recycling [17].

Slabs with cracks were tapped with the hammer along the cracks and joints, and these did not sound hollow or any different from slabs without cracks. When the 2-inch (50-mm) thick panels were replaced in August 1999, most panels were well bonded to the AC layer and pulled a portion of the AC out when extracted using a backhoe.

2.4.3. COLORADO STATE ROAD 119, LONGMONT, COLORADO

Whitetopping on State Road 119 involved rehabilitation of a 1-mile (1.6-km) long section of a 2-lane AC pavement. The objective of this research project was to develop mechanistic design guidelines for UTW, and incorporated several important variables indicated below:

- Surface preparation: old AC, new AC, milled AC

- Slab dimensions: 6 ft x 6 ft, 10 ft x 12 ft, 6 ft x 12 ft, and 12 ft x 12 ft (1.8 m x 1.8 m, 3.0 m x 3.7 m, 1.8 m x 3.7, and 3.7 x 3.7 m)
- PCC thickness: 4.5, 5.0, and 6.0 inches (113, 125, and 150 mm)

The project location is shown in Figure 2.25. The UTW pavement was placed on the passing lane of the eastbound lanes, directly on top of the old AC pavement. The old AC pavement was not milled but was washed and cleaned prior to PCC placement.

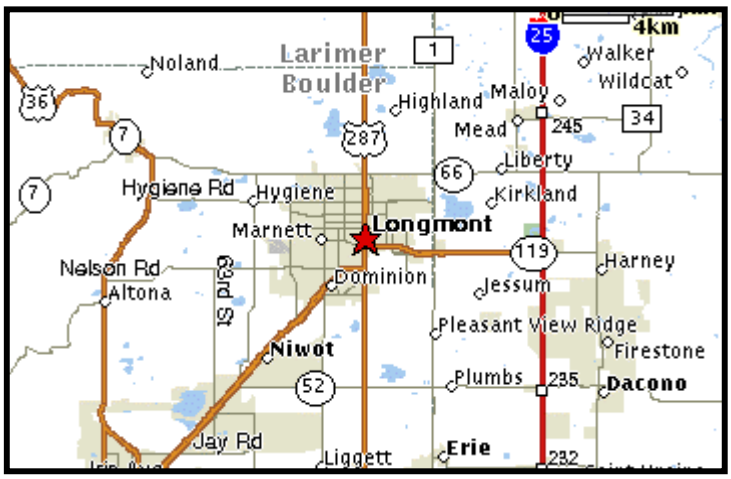

Figure 2.25. Location of Colorado DOT PCC overlay research project.

2.4.3.1. State Road 119 Design and Construction

UTW placement on State Road 119 was part of a larger project for developing a procedure for the design of PCC overlays. In 1994, the PCA developed design guidelines for UTW pavements; however, these were not considered appropriate for Colorado conditions, and it was felt that Colorado traffic would require pavements thicker than 4 inches (100 mm) with joint spacings in excess of 6 ft (1.8 m).

The UTW sections were placed in August 1996 using a slip form paver. The project was delayed by several weeks due to rainy days and construction equipment problems [20]. PCC cylinders were cast and later tested for compressive strength; the average compressive strength was 4,100 psi (28.5 MPa). PCC mixture composition for this project is not available, but Table 2.18 shows similar mix used at another UTW research project (part of this overall project) constructed at the same time on Santa Fe Drive in Denver [20].

Table 2.18. Typical PCC proportions used in Colorado.

PCC Components	Attributes
Cement	Type I, 565 lbs/yd^3 (335 kg/m^3)
Fly Ash	67 113 lbs/yd^3 (kg/m^3)
Sand	1,300 lbs/yd^3 (771 kg/m^3)
Intermediate Aggregate	920 lbs/yd^3 (546 kg/m^3)
Coarse Aggregate	710 lbs/yd^3 (421 kg/m^3)
Water/Cement Ratio	0.41
Water	280 lbs/yd^3 (166 kg/m^3)
Synthetic Fibers	None used

2.4.3.2. Assessment of Current UTW Conditions at State Road 119

A condition assessment of the UTW on State Road 119 in March 2002 rated the pavement as excellent. The UTW section was divided into six features for the PCI survey, as shown in Table 2.19; the table also provides distress survey results.

Table 2.19. PCI ratings of State Road 119 indicated excellent performance.

Feature	Sample Units	Slab Dimensions (m)			Total Slabs	Area ft^2	PCI Rating	Distress Types Observed
		Length, ft	Width, ft	Thick, inch				
1	23	6	10	4.5	456	27,360	99	2 slabs each with spalling joints, corners/shrinkage cracks.
2	10	10	12	5.0	228	27,360	100	None.
3	14	10	10	5.0	456	45,699	100	None
4	22	6	6	4.5	440	15,840	100	Three slabs with corner spalling.
5	6	12	12	6	110	15,840	98	1 slab with spalling joints and one slab with corner breaks.
6	6	12	9.8	6	110	12,936	99	Two slabs with spalling corners.

Note: 1 ft = 0.3048 m, 1 inch = 25.4 mm, 1 ft^2 = 0.093 m^2

2.4.3.3. Lessons Learned at State Road 119

All UTW sections at State Road 119 are performing well, and no unusual observations were made during the site visit. The traffic on State Road 119 has grown significantly due to housing developments in the area, but after 6 years in service the pavement is in excellent condition.

2.4.4. WILLIAMSTOWN JUNIOR AND SENIOR HIGH SCHOOL, KENTUCKY

The Williamstown Junior & Senior High School parking lot, shown in Figure 2.26 was rehabilitated using UTW in 1990. Williamstown in located about 50 miles (80 km) south of Cincinnati, Ohio, just off of IH-75.

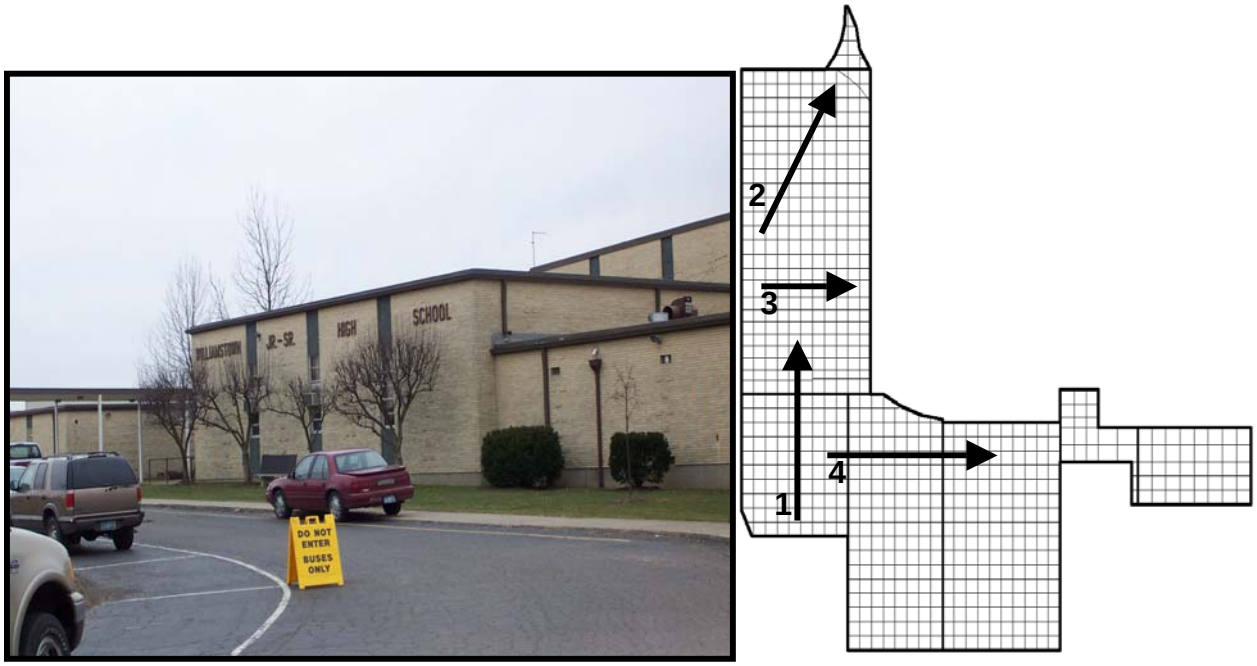

Figure 2.26. Williamstown school parking lot surrounds the school building.

The existing AC at the parking lot was severally distressed and in immediate need of rehabilitation.

Figure 2.27 shows distresses at various locations in the parking lot (viewing directions are indicated on Figure 2.26). The existing AC had oxidized, and almost all the pavement section had block cracking. Several places had severe alligator cracking and patches where potholes had been repaired.

Figure 2.27. AC pavement at the Williamstown School was severely distressed.

2.4.4.1. UTW Construction at Williamstown Jr. and Sr. High School

UTW of 4-inch (100-mm) thickness was placed over the existing AC pavement. Potholes in the existing pavement were filled with bituminous cold mix to provide for a uniform surface for PCC slab construction.

PCC mix proportions and material properties conformed to typical Kentucky DOT specifications. The mix used 440 lbs/yd^3 (260 kg/m^3) of Type I cement with a target air content of 5.5±1.5 percent. PCC slump was limited to a maximum of 5-inches (150-mm), and fibers were added at a rate of 1.5 lb/yd^3 (0.9 kg/m^3). The concrete was specified to have a compressive strength of 4000 psi (27.5 MPa) at 28 days.

Ready mix concrete was placed in fixed forms as shown in Figure 2.28-A. Paving was accomplished in alternate lanes; the first lanes were placed in wooden forms, and subsequent lane pours used already placed lanes as forms (Figure 2.28-B). The concrete was spread manually and finished using a vibrating screed (Figure 2.28-C). Figure 2.28-D shows the finished product. The concrete was given a broom textured finish.

2.4.4.2. Assessment of Current UTW Conditions at Williamstown School

The PCI survey in February 2002 divided the parking lot into eight features, as shown in Figure 2.29; Table 2.20shows survey results. All slabs in Feature A01 were shattered, which resulted in a low PCI of 43.

Figure 2.28. PCC was placed manually at Williamstown Jr. & Sr. High School.

This page intentionally left blank.

Figure 2.29. Williamstown school parking lot was divided into eight features.

This page left blank for

Figure 2.29

Table 2.20. PCI ratings of school parking indicated very good performance.

Feature	Sample Units	Slab Dimensions, m	Total Slabs	Area ft^2	PCI Rating	Observed Distress Types
PK01-1	1	Various sizes, see Figure 2.29 for details	100	3,337	43	All slabs with load-related distresses.
PK01-2	7	All were 10 ft square, last row was 10 ft by 9 ft	154	12,594	81	All sample units with load-related distresses.
PK01-3	4	8.5 ft by 10 ft; some 6 ft, 11 ft, 12 ft by 12 ft	86	10,990	82	All sample units with load-related distresses.
PK01-4	4	10 ft by 10 ft	90	9,000	84	Three sample units with load-related distresses.
PK01-5	5	10 ft by 10 ft	140	14,000	92	Four sample units with load-related distresses.
PK01-6	6	10 ft by 10 ft	160	16,000	87	Four sample units with load-related distresses.
PK01-7	1	Various sizes, see Figure 2.29 for details	22	2,928	86	Three slabs with load-related distresses.
PK01-8	2	10 ft by 12 ft 12 ft by 12 ft	40	4,800	100	None.

Note: 1 ft = 0.3048 m, 1 inch = 25.4 mm, 1 ft^2 = 0.093 m^2
All slabs were 4 inch (100 mm) thick.

2.4.4.3. Lessons Learned from Williamstown Jr. and Sr. High School

There was no climate/durability-related distress observed at the school parking lot. Of all the load-related distresses observed, the majority consisted of slabs with broken corners and linear (longitudinal/transverse/diagonal) cracks.

Slabs in Feature 1 (see Table 2.20, Figure 2.29) were badly deteriorated at the transition from AC to PCC pavement. PCC slabs in this area were badly cracked (see Figure 2.30), which led to a low PCI of 43.

Figure 2.30. PCC Slabs on transition from AC to PCC were severely distressed.

Slabs in the path followed by school buses were also distressed, with most slabs having corner breaks and linear cracks. Figure 2.31 shows the path followed by the buses as they drop off students in the morning and pick them up in the afternoon. Figure 2.32 shows the distresses in the area where buses stop, turn, and back up to their designated parking area.

Distressed and non-distressed slabs were tapped with a hammer; none of the slabs sounded hollow. This was true for slabs with corner cracks as well as slabs with no corner cracks. When this procedure was used next to the broken corner crack, the slab still sounded solid.

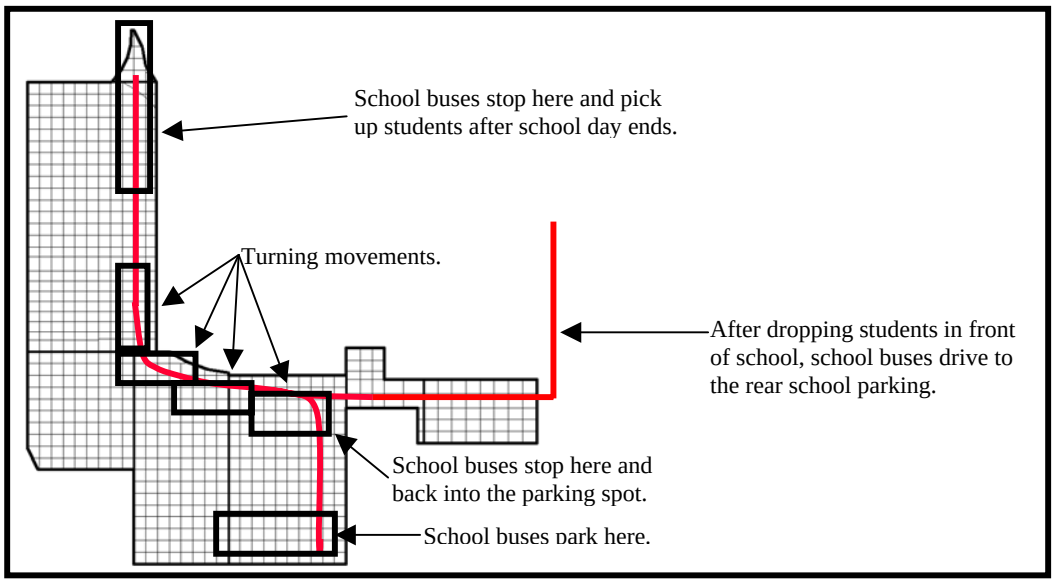

Figure 2.31. The path followed by school buses was severely distressed.

Figure 2.32. Most slabs where buses made turns had broken corners.

2.4.4.4. Verification of Bond Loss at Williamstown Jr. and Sr. High School

A second site visit was made to the Williamstown Jr. and Sr. High School to further investigate the bond condition. Cores were taken down to the granular pavement layers at selected locations, as shown in Table 2.21 and Figure 2.33.

Table 2.21. Description of cores removed at Williamstown Jr. and Sr. High School.

Core	Sound	Average Thickness (inch)		Bond Condition	Remarks
		PCC	AC		
1	Solid	4.4	1.5	No bond	AC stripping
2	Hollow	4.5	-[1]	No bond	AC stripping
3	Hollow	4.7	1.1	No bond	Corner break
4	Hollow	5.0	-[1]	No bond	Joint damage
5	Solid	4.9	1.2[1]	Intact bond	AC bottom stripped
6	Hollow	5.7	-[1]	No bond	Faulted slab
7	Solid	5.7	0.9	No bond	Corner break
8	Hollow	5.3	1.1	No bond	Corner break
9	Hollow	4.4	-[1]	No bond	AC stripping
10	Hollow	4.4	0.9[1]	No bond	No distress
11	Solid	4.6	1.2[1]	No bond	No distress
12	Hollow	4.6	-[1]	No bond	Faulted slab

Notes: [1]AC disintegrated
1 inch = 25.4 mm

The revisit to the school parking lot indicated that sounding with a hammer could be used to determine if the PCC is bonded to the underlying AC only if the slab distress conditions are also taken into account. There was always a lack of bond between the UTW and AC when a hollow sound was observed, and sometimes there was no bond when a solid sound was heard if the test was made near a distressed slab.

This page intentionally left blank.

Figure 2.33. Location of cores taken at the Williamstown Jr. and Sr. High School.

This page left blank for

Figure 2.33. Location of cores taken at the Williamstown Jr. and Sr. High School.

2.4.5. HOLIDAY INN PARKING LOT, DECATUR, ILLINOIS

The Decatur Holiday Inn and Conference Center, located on US 36, rehabilitated the existing AC parking lot with 3-inches (75-mm) of UTW in 1994. Decatur is located about 50 miles (80 km) east of Springfield, Illinois; Figure 2.34 shows the hotel view and the parking lot layout.

2.4.5.1. Pre-UTW Construction Conditions

The condition of the parking lot before UTW construction is shown in Figure 2.35. The parking lot had block cracking in all areas and severe alligator cracking, especially in areas with high traffic. The pavement surface was raveled and oxidized.

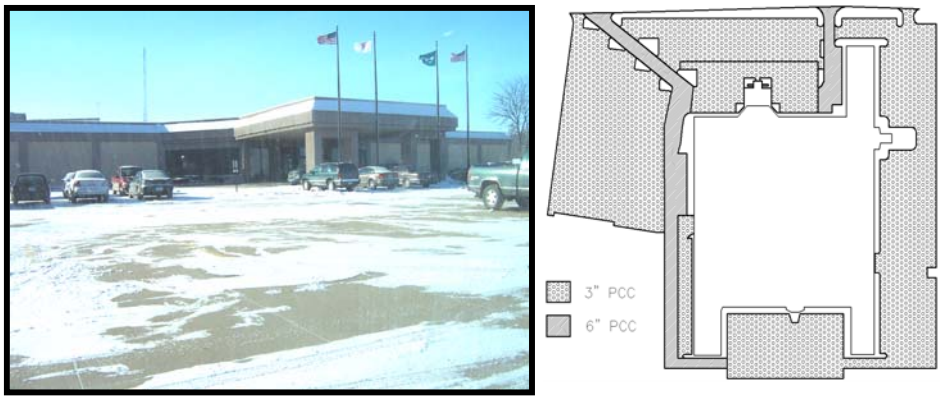

Figure 2.34. View and parking lot layout of Decatur Holiday Inn parking lot.

Figure 2.35. AC pavements at Holiday Inn parking lot exhibited alligator cracking.

The original parking lot was constructed during the 1960's with an AC surface over a crushed stone base. It was rehabilitated 10 years later with a 1.5-inch (38-mm) thick AC overlay.

2.4.5.2. UTW Construction at Holiday Inn Parking Lot

The UTW at the parking lot was constructed in 1994 during a 3-month period. Ready mix concrete (Figure 2.36-A) was placed in 3-inch (75-mm) thickness all over the parking lot area, except for the service roads where the thickness of the PCC was 6 inches (150 mm). The joint spacing was 6 ft (1.83 m). Before PCC placement, the existing AC surface was milled using conventional milling equipment, then the PCC was placed using a slip form paver (Figure 2.36-B). The PCC surface was given a light broom finish. Mix proportions and material properties conformed to Illinois DOT specifications.

Figure 2.36. Slip form paver was used at the Holiday Inn parking lot.

2.4.5.3. Assessment of Current Condition and Lessons Learned at Holiday Inn

At the time of site visit in February 2002, the area was partially covered with snow. A cursory survey was made and information was obtained from the groundskeeper. No distresses were found during the survey; Figure 2.37 shows the overall pavement condition.

The only crack observed was located with the help of the groundskeeper (see Figure 2.38). A few slabs and this crack were tapped with the hammer, and they all sounded solid. However, due to prevailing freezing temperatures, no statement can be made about the bond.

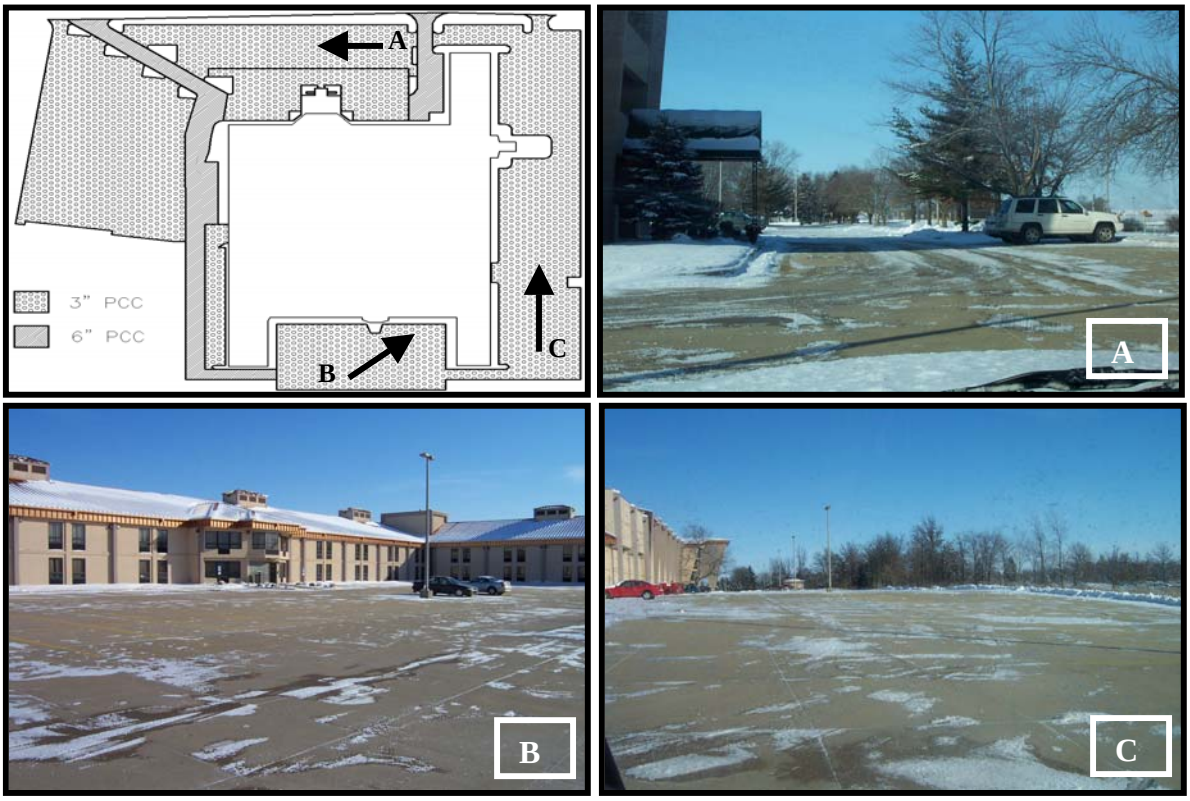

Figure 2.37. Adequate area was snow free to assess the parking lot condition.

Figure 2.38. A single crack in front of a rear hotel entrance was observed.

2.4.6. LIFE BRIDGE CHRISTIAN CHURCH, LONGMONT, COLORADO

Life Bridge Christian Church parking lot, shown in Figure 2.39, was rehabilitated in 1998 using 3.5-inches (89-mm) of UTW pavement placed over the existing AC surface. The church is located about 40 miles north of Denver, Colorado.

2.4.6.1. Pre-UTW Construction Conditions

The existing AC parking lot was severely distressed with alligator cracks covering all areas, as shown in Figure 2.40. There were areas of the parking lot where the pavement had rutted after the formation of alligator cracks; these areas were repaired using full-depth patches before UTW placement.

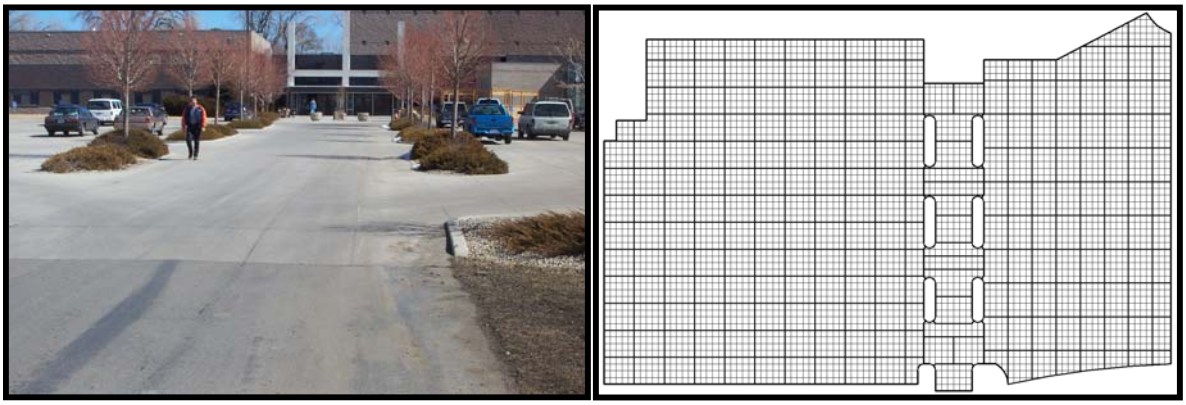

Figure 2.39. View and parking lot layout of the Life Bridge Christian Church.

Figure 2.40. Life Bridge Christian Church parking lot was severely cracked.

2.4.6.2. UTW Construction at Life Bridge Christian Church

The UTW at the church parking lot was constructed using ready mix concrete and fixed forms. The existing AC pavement surface was broom cleaned prior to PCC placement.

Potholes in the existing pavement were filled, and large depressed areas were filled with crusher fines (Figure 2.41-A). If the depressed areas showed an indication of fatigue (depressed with severe fatigue cracking), the surface was strengthened using a welded wire mesh (Figure 2.41-B).

Figure 2.41. Severely distressed areas were repaired before UTW construction.

Ready mix concrete was placed in steel forms (Figure 2.42-A), and spread manually using a vibrating screed (Figure 2.42-B). The concrete was given a burlap drag finish (Figure 2.42-C) before cutting joints. The entrance to the church between the two parking lots was placed last (Figure 2.42-D).

The PCC mix contained 440 lbs/yd^3 (260 kg/m^3) of Type I cement with a target air content of 6 ± 2 percent. PCC slump was approximately 3-inches (75-mm) and fibers were added at a rate of 3.0 lb/yd^3 (1.8 kg/m^3). Test cylinders made using field mix indicated a compressive strength of 4,600 psi (32 MPa) at 28 days.

2.4.6.3. Assessment of Current UTW Condition at Church Parking Lot

A site visit was made to the church parking lot in March 2002. The parking lot was divided into three features and sample units for the condition survey (see Table 2.22 for survey results), as indicated in Figure 2.43. No significant climate/durability-related problems were observed during the condition survey.

Figure 2.42. PCC was manually placed at church parking lot.

Table 2.22. PCI rating of church parking lot indicated excellent rating.

Feature	Sample Units	Total Slabs	Area, ft^2	PCI Rating	Distresses
PK-01	16	366	5,856	99	No climate/durability-related distresses were found. Two slabs were categorized as shattered slabs, and two slabs each were determined to have corner breaks and linear cracks.
PK-02	141	2,532	12,594	100	One slab had climate/durability-related joint spalling. Twelve slabs had load-related linear cracks, and one slab had load-related corner breaks.
PK-03	82	1,482	10,990	99	No climate/durability related-distresses were found. Eight slabs had low to medium-severity corner breaks.

Note: 1 ft = 0.3048 m, 1 inch = 25.4 mm, 1 ft^2 = 0.093 m^2
PCC thickness = 3.5 inch (89 mm); slab size = 4 ft (1.22 m) square

Figure 2.43. The church parking lot was divided into three features.

This page left blank for Figure 2.43. The church parking lot was divided into three features.

2.4.6.4. Lessons Learned at Life Bridge Christian Church

There were no significant climate or durability-related distresses at the church parking lot. A number of slabs with and without corner cracks were sounded with a hammer. There were no indications of a disbond using this method, even when tested along slab edges and the cracked corner.

A construction-related problem was noted at the driveway leading to the church. The driveway between the parking lots was placed last and, due to an error in slope calculations, a portion of the driveway had a slab thickness of only 2-inches (50-mm). This area has failed, as shown in Figure 2.44.

Figure 2.44. Thinner slabs led to premature failure.

Cracked slabs in the parking lot sounded solid when tapped with the hammer. However, some of the 2-inch (50-mm) slabs in the driveway, which contained corner cracks, sounded hollow along the edges of the corner cracks. Adjacent non-cracked slabs sounded solid.

Trucks delivering food and other supplies to the church school make turning movements similar to those observed at SUS and Williamstown Jr. and Sr. High School (Figure 2.45). However, no distresses were observed in these areas at the church parking lot.

2.4.6.5. Verification of No Bond at Life Bridge Christian Church

The church parking lot was another site selected to determine if the hollow sound noticed during the initial site visit indicated a loss of bond between the PCC and AC. Cores were

taken at selected locations down to the granular pavement layers as shown in Table 2.23 and Figure 2.46.

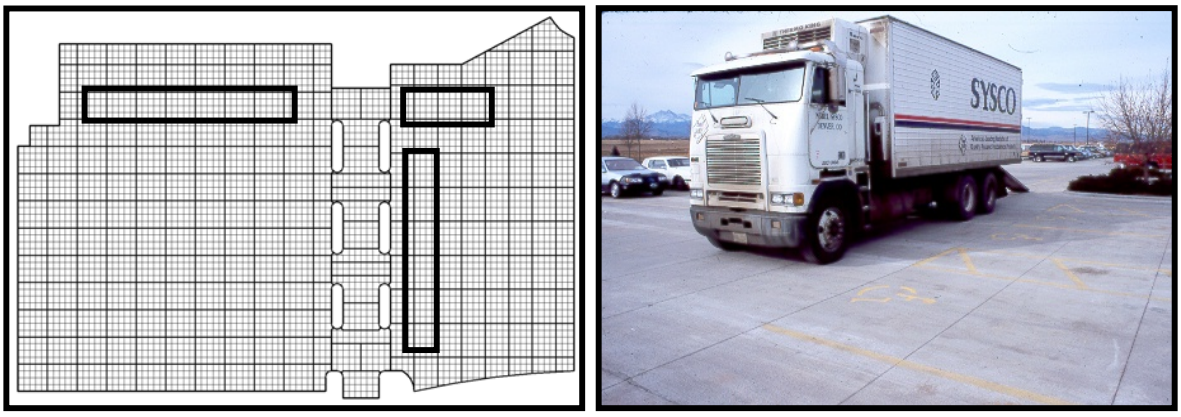

Figure 2.45. Turning movements at the church parking lot did not cause any distresses.

Table 2.23. Description of cores removed at Life Bridge Christian Church.

Core	Sound	Average Thickness (inch)		Bond Condition	Slab Distress
		PCC	AC		
1	Solid	2.72	2.80	unbonded	Opposite corner broken
2	Hollow	2.60	2.72	unbonded	Corner break
3	Solid	2.87	2.80	unbonded	Corner break
4	Hollow	3.39	2.52	unbonded	Corner break
5	Hollow	No core removed			
6	Hollow	3.15	2.95	unbonded	Longitudinal crack
7	Hollow	No core removed			No distress
8	Solid	2.72	4.76	unbonded	Corner break
9	Hollow	3.35	--	unbonded	No distress
10	Solid	3.70	2.40	unbonded	Corner break
11	Solid	4.33	2.40	unbonded	No distress
12	Solid	No core removed			Cracks
13	Solid	No core removed			Corner break

Note: 1 inch = 25.4 mm

During UTW construction the existing AC pavement surface was broom cleaned prior to PCC placement; no bond between the PCC and AC was expected, and all the cores taken from the parking lot indicated the absence of a bond.

All core locations sounded solid when tapped with a hammer, even near locations that were distressed. Cores taken from slabs with no distress indicated good contact between the PCC and AC but there was no bond. Cores taken from distressed slabs also indicated a good contact (solid sound) between the PCC and AC. For example, several corner breaks gave solid sound but were not bonded.

Figure 2.46. Location of cores removed at the Life Bridge Christian Church.

This page left blank for Figure 2.46. Location of cores removed at the Life Bridge Christian Church.

3. APPLICABILITY OF HIGHWAY PROJECTS TO AIRPORTS

3.1. UTW PROJECTS IN THE UNITED STATES

There are only three known airports in the U.S. with UTW pavement, as shown in Table 2.1. Most UTW pavements have been built for highway and parking lot applications. During the last 12 years approximately 2 million ft^3 (56,500 m^3) of UTW pavement were placed, representing a surface area of approximately 7,158,000 ft^2 (665,000 m^2). The airport UTW projects represent approximately 14 percent of the total UTW pavement, with most of it placed at SNH.

The purpose of Phase I of the current research was to survey field performance of UTW projects and determine if there is any evidence of a loss of bond between the PCC and AC and, if so, whether it has contributed to cracking or other distress. Because only three airports were available, some UTW highway and parking lot projects were selected to obtain additional performance data.

3.2. BRIEF HISTORY OF UTW PAVEMENT RESEARCH IN THE U.S.

The first experimental UTW section was constructed on the access road to a waste disposal facility in Louisville, Kentucky [1,3,8,11,12,13,20]. PCC thicknesses for this project were 2 inches (50 mm) and 3.5 inches (89 mm) and each section was 275 ft (84 m) long. Slab sizes were 6 ft (1.8 m) square and 2 ft (0.6 m) square. The PCC had a compressive strength of 3,500 psi (24 MPa) at 36 hours and incorporated fibers. The AC surface was milled before PCC placement. This project led the way with its successful construction and performance. Other researchers have reported highway applications of UTW in Tennessee, Georgia, North Carolina, Kansas, Iowa, Pennsylvania, New Jersey, Colorado, Missouri, and Florida [3,31]. Some details of various UTW projects are provided below.

3.2.1. TENNESSEE DOT – STARTING 1992

Tennessee DOT has constructed many UTW sections on highways [3,14]. The first project was built on a city street in Nashville in 1992. The as-built PCC thickness ranged from 64 to 76 mm, and a constant panel size of 5 ft (1.5 m) square was used. The 1992 Nashville project was followed by projects in other major cities in Tennessee.

The latest Tennessee DOT UTW project is runway, apron, and connector taxiways at SNH. SNH was visited as part of the field visits during the course of this project.

3.2.2. IOWA DOT – STARTING 1994

Iowa DOT constructed a whitetopping project in 1994 on Iowa Highway 21 near Belle Plaine [8,16,17,18,20]. This is one of the projects visited during the course of this research.

3.2.3. KANSAS DOT – STARING 1994

In 1994, Kansas DOT participated in a UTW demonstration project. The project used a 2-inch (50-mm) thick PCC with panel sizes of 3 ft (0.9 m) and 4 ft (1.2 m). The project was monitored for 5 years and performed fairly well. The project demonstrated that UTW could be built with conventional paving equipment and locally available materials [15].

3.2.4. NEW JERSEY DOT – STARTING 1994

New Jersey DOT built a UTW test section on a ramp connecting northbound 1-295 and Route 130 in 1994. The project, with a total length of 900 ft (275 m), tried panel sizes of 3, 4, and 6 ft square (0.9, 1.2, and 1.8 m square); the average as-constructed PCC thickness was 3.82 inches (97 mm). An evaluation conducted by New Jersey DOT in 1997 indicated that the smallest panels had the best performance and the largest panels had the most distresses [3].

3.2.5. FLORIDA DOT – STARTING 1996

Florida DOT has conducted considerable research into different UTW applications, including at the NSB airport apron visited during the course of this research. In 1996, Florida DOT evaluated the construction, materials, and performance of UTW pavement by conducting tests at the UCF CATT facility [3,4,8,31]. This research investigated the type and optimum fiber content for UTW, conducted accelerated testing to determine UTW durability and performance characteristics, and implemented the results at NSB demonstration project [7].

During the same time period, Florida DOT constructed three test tracks behind the Florida DOT Materials Office in Gainesville and loaded the UTW pavement with trucks of different weights and wheel configurations for 18 months [4,8,22,31]. The UTW panels were 2, 3¼, and 4 inches (50, 83, and 100 mm) thick with a panel size of 3, 4, and 6 ft square (0.9, 1.2, and 1.8 m square). Pre- and post-construction FWD tests indicated a significant improvement in load carrying capacity. No load-related distresses were observed during testing. The results of this research led to UTW implementation at the Ellaville Weigh Station on I-10 in North Florida. The UTW pavement there incorporated the following combinations:

- Thickness: 3 inches (75 mm) and 4 inches (100 mm)
- Slab size: 4 ft (1.2 m) and 6 ft (1.6 m)
- Fibers and no fibers

The project concluded that, during UTW design, emphasis should be placed on achieving bond strength between the PCC and existing AC. Moreover, joint sawing must be timely, as any delayed sawing will lead to cracking of the UTW panels. The two larger panel sizes appeared to provide similar performance, as did PCC with or without fibers [4].

3.2.6. COLORADO DOT - STARTING 1995

The Colorado DOT instrumented two sites near Denver (Santa Fe Drive and Route 119 in Longmont) and used instrumentation data from these sites combined with data from the SUS airport to develop mechanistic UTW design guidelines. The Santa Fe Drive test sections were 4 inches (100 mm) and 5 inches (125 mm) thick, and the Route 119 test sections were 4.5 inches (113 mm) and 5 inches (125 mm) thick. Route 119 test sections in Longmont were visited during this project [19,20,28,31, 32].

The Route 119 test sections were placed on new and old AC with and without milling; the research recommended that when PCC is to be placed over new AC it needs no milling to enhance the PCC–AC bond. Another significant finding, contrary to popular belief—load testing indicated that all section behaved as partially bonded and not fully bonded [20,28,32].

3.2.7. MINNESOTA DOT - STARTING 1995

The Minnesota DOT constructed two 100-ft (30-m) long UTW test sections in 1995 on a 4-lane divided highway near North Mankato. A 1999 evaluation indicated that all sections had cracked, but the cracks in the fiber reinforced PCC were relatively tighter than the cracks in PCC without any fibers. Another project constructed in North Mankato in 1996 is still performing well [3,10,33]. In 1997, a UTW project was constructed as part of the Mn/ROAD facility. The project incorporated the following variable combinations:

- PCC thickness: 3 inch, 4 inch, and 6 inch (75 mm, 100 mm, and 150 mm)
- Slab size: 13-ft square, 16 ft x 19.4 ft, 33.4-ft square (1.2-m square, 1.5 m x 1.8 m, and 3.1-m square)
- Polyolefin and polypropylene fibers

The PCC mix used was similar to conventional PCC mixes. The test sections were instrumented, and the results indicated that a good bond was achieved [10].

3.2.8. MISSOURI DOT - STARTING 1996

The SUS airport in Missouri (visited during this research effort) used UTW for a light load aircraft (12.6 kips, 5.7 Mg) apron. During PCC placement, six slabs were instrumented with 20 sets of PCC strain gages that were installed at different depths. Load tests conducted during the spring and fall seasons were used to develop a mechanistic design procedure for UTW pavements. Data from SUS and Colorado DOT test sites were used for this purpose [20,21,28,31].

3.2.9. MISSISSIPPI DOT – STARTING 1997

The Mississippi DOT started its involvement with UTW research in 1997 by constructing a test section on I-20 eastbound near Jackson. The research desired to test a thickness and joint spacing that was thought to be competitive with conventional rehabilitation using a hot mix

asphalt (HMA) overlay. This project used a UTW PCC thickness of 4 inches (100 mm), but the joint spacing had a rather large range, from a minimum of 6 ft (1.8 m) to a maximum of 40 ft (12.2 m). The plain concrete control section performed well, whereas corner cracks were observed in UTW sections at about 1 year of age [3,13,31]. These sections were recently overlaid using HMA. After this 1997 project, the Mississippi DOT built several additional UTW sections on city intersections and rural highways.

3.2.10. FHWA – STARTING 1998

In 1998, the FHWA constructed eight UTW test sections and subjected them to accelerated load testing until 2000. The test sections had two PCC thicknesses (2.5 and 3.5 inches [64 and 89 mm]), two remaining AC thicknesses (5.5 and 4.5 inches [140 and 114 mm]), and PCC with and without polypropylene fibers. Study results indicated the significance of bond on UTW performance [9]. The primary distress types observed were corner breaks, transverse and longitudinal cracks, and joint spalling and faulting [34].

3.3. COMPARISON OF UTW DESIGNS

There are only minor differences in the design of UTW for GA airports and highway pavements. Most UTW designs use 3.5-inch (89-mm) thick PCC over a milled AC surface, slab dimensions of 3 ft (0.9 m) square or 4 ft (1.2 m) square, concrete mix with fibers, and a flexural strength of approximately 700 psi (4.83 MPa). Table 3.1shows how these designs compare. Aircraft wheel loads are slightly higher than truckloads, but the number of aircraft repetitions is less.

3.4. PERFORMANCE SUMMARY

The research team visited three airport and five highway/parking lot UTW projects to gain first-hand knowledge about their performance over the years. These projects ranged in age from almost new (SNH, 2000) to fairly old (Williamstown School, 1990). The oldest project, despite being 12 years old, is still performing well, with some areas showing fatigue damage in terms of corner breaks and linear cracking (transverse, longitudinal, and diagonal). In fact, corner breaks and linear cracks, followed by shattered slabs, were the predominant distresses at all the sites visited, and most of the distresses were in areas subjected to heavy traffic. There is a correlation between pavement thickness and predominant distresses (most were fatigue related); however, this aspect of UTW performance is beyond the scope of this research. There was no evidence of loss of bond due to climate; a brief discussion of observed load-related (fatigue) distresses is provided here.

Table 3.1. Comparison of airport and highway UTW designs.

Agency	Location	Const. Year	Use	Wheel Configuration	Design Load	PCC Thickness	Slab Size	Concrete Strength	Fiber Use	Surface Prep.
ACPA	Louisville, KY	1991	Landfill access	Single axle, Dual wheel	18 kips	2 inch 3.5 inch	19.4 ft^2 6.5 ft^2	3.5 ksi (compressive)	PPL	Milling
TNDOT	Nashville, TN	1992	City streets	Single axle, Dual wheel	18 kips	2.5-3 inch	16 ft^2	--	PPL	Milling
IADOT	Belle Plaine, IA	1994	Rural Highway	Single axle, Dual wheel	18 kips	2 inch 4 inch	6.5, 13.0, 19.4 ft^2	--	PPL	No milling
KSDOT	Leawood, KS	1994	City street	Single wheel, mostly passenger cards		2 inch	9.7 ft^2, 13.0 ft^2	5.0 ksi (compressive)	PPL	Milling
NJDOT	I-295 & Route 130	1994	Highway ramp	Single axle, Dual wheel	18 kips	4 inch (Average)	9.7, 13.0, 19.4 ft^2	--	None	None
CODOT	Denver	1996	City street	Single axle, Dual wheel	18 kips	4 inch	16.1 ft^2	4.3 ksi (compressive)	None	New surface
MSDOT	Edwards	1996	Interstate Highway	Single axle, Dual wheel	18 kips	4 inch	26.2 ft – 40.0 ft	--	None	Milling
FDOT	Ellvile	1997	Weigh-station	Single axle, Dual wheel	18 kips	3 inch, 4 inch	12.9 , 17.2 ft^2	--	PPL	Milling
MnDOT	Mn/ROAD	1997	Highway	Single axle, Dual wheel	18 kips	3 inch, 4 inch	12.9 ft^2, 4.9 x 5.9 ft	4.3 ksi	PPL, POF	Milling
FDOT	New Smyrna Beach	1995	GA apron	Dual-wheel	APT Results	2 –3.5 inch	12.9 ft^2, 4.9 x 5.9 ft	4.5 ksi	PPL, POF	Cleaning
MnDOT	Spirit of St. Louis	1995	GA apron	Single wheel	12.5 kips	3.5 inch	14 ft^2	4.5 ksi	PPL	Milling
TNDOT	Savannah	2000	GA apron runway, taxiways	Dual-wheel	30 kips	4 inch	4 by 4.2 ft	4.8 ksi	PPL	Milling

Note: PPL=Polypropylene fibers, POF=Polyolefin fibers

3.4.1. CORNER BREAKS

Corner breaks were the most commonly observed distress during all site visits. These are caused when the fatigue limit (defined as a stress to strength ratio) of the PCC is exceeded. During field testing, all the corners sounded solid when tapped with a hammer. Researchers associated with the Iowa Highway 21 research project identified corner breaks that, after breaking, bonded back to AC after a few hot summer days. For such a situation, the corner will sound fully intact and will be bonded to the underlying AC (and may appear to be bonded even when cores are extracted); researchers have called this loss of support a "virtual void" [34]. Some corner breaks were observed that appear to have started as linear cracks but then propagated to the nearest joint in the diagonal direction, forming a corner break.

3.4.2. LINEAR CRACKS/SHATTERED SLAB

Longitudinal and transverse cracks are often caused when the fatigue limit of the PCC is exceeded. The reasons for this could be the disbond between the AC and PCC exceeding the UTW design load limit (the slab should still sound solid).

PCC slabs will crack, even when bonded to the underlying AC, if the UTW design load is exceeded. An example of this was observed at SUS, where fuel trucks use a portion of the UTW pavement designed for 12.6-kip (5.7-Mg) gross weight aircrafts; Figure 3.1 shows the fuel truck and the gross vehicle weight rating (GVWR). The UTW distresses are shown in Figure 2.14 and Figure 2.15.

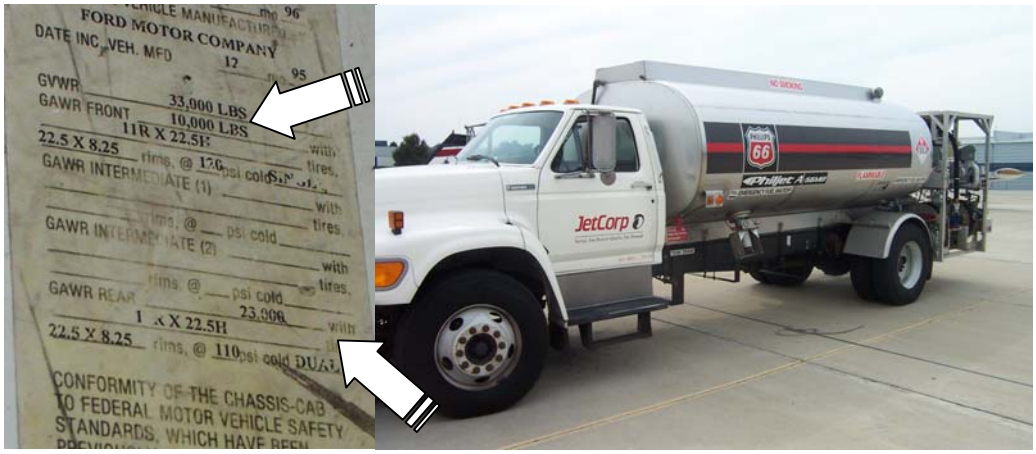

Figure 3.1. Photograph of fuel truck at SUS with GVWR.

SNH personnel noted an area on Apron Feature A03 where surface preparation problems led to inadequate bond between the AC and PCC. The slabs in this area sound hollow when tapped with a hammer, but some were already showing linear cracks.

There were a few instances at SNH, as shown in Figure 3.2, where cracks, once started, continued on for several slabs. There did not appear to be a loss of bond between the PCC

and AC when tapped with a hammer; all slabs sound solid when tapped at mid-slab and along the crack. Once a crack started it progressed on to adjoining slabs.

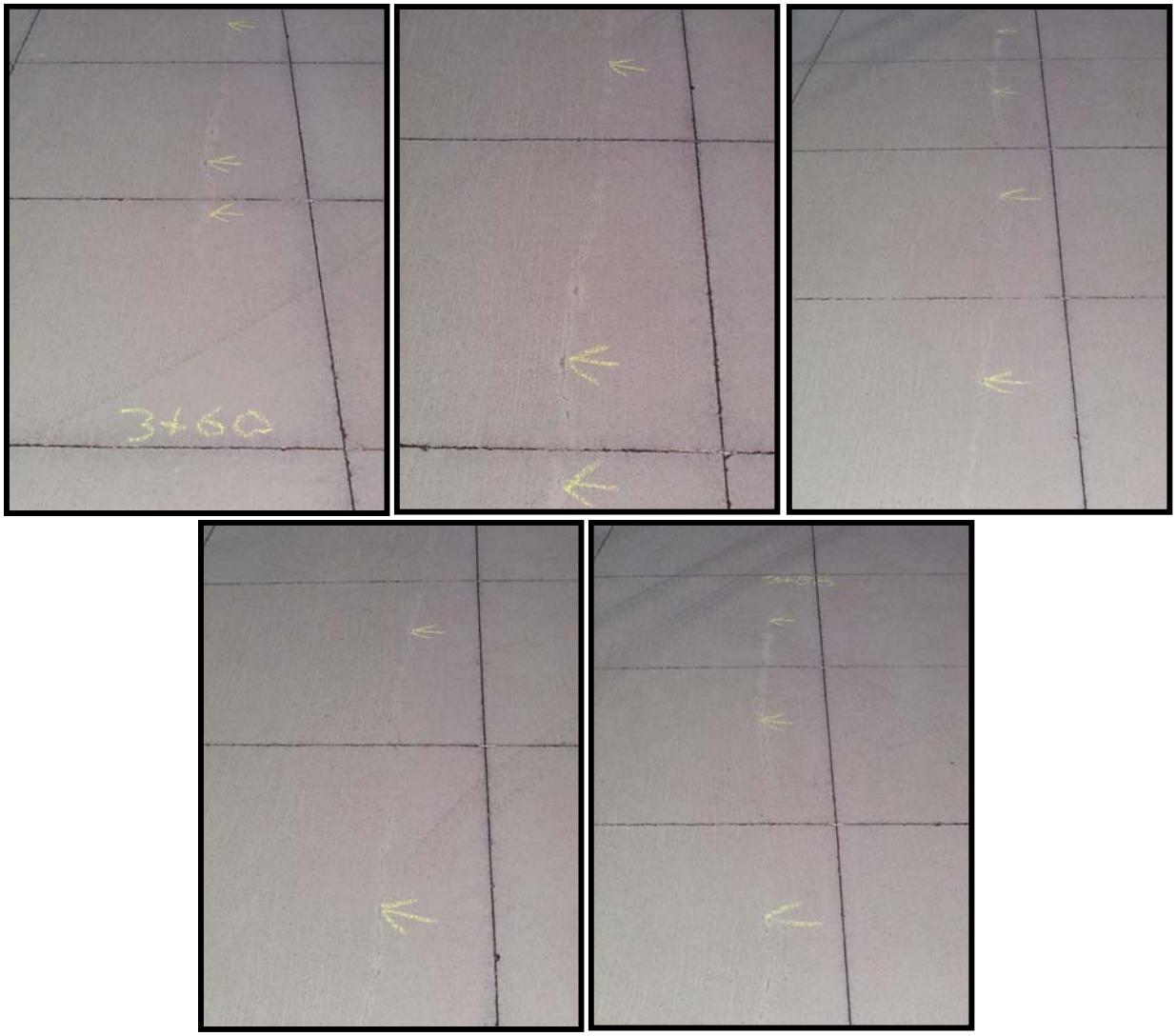

Figure 3.2. Linear cracks, once started, may continue for several slabs.

This page intentionally left blank.

4. TEST SECTION CONSTRUCTION

4.1. INTRODUCTION

The Track 2 research evaluated the deterioration of bond between PCC and AC by subjecting field-prepared samples to laboratory simulated environmental exposure conditions of F&T and W&D. Track 2 research began by construction of test section to obtain samples for laboratory testing.

4.1.1. RECOMMENDATIONS FOR TEST SECTION CONSTRUCTION

4.1.1.1. PCC Thickness

The PCC thickness of most UTW projects in the U.S. have ranged between 2 inches (50 mm) and 4 inches (100 mm). The recommended PCC thickness for the test section was 3.5 inches (89 mm). To represent the typical UTW construction, wooden 2x4's were used as forms.

4.1.1.2. PCC Mix Design

The PCC mix design for the test section was formulated to represent the typical UTW mixes used in the field. Table 4.1 shows the PCC mixes for the various projects reviewed during Track 1 research. The PCC mix used in construction of the Track 2 test section is shown in Table 4.2.

Table 4.1. PCC mixture proportions used at UTW projects.

PCC Component	UTW Project Location				
	SNH	SUS	NSB	Colorado DOT	School Parking
Type I Cement	22.5 – 26.0 pcf	18.9 pcf	20.9 pcf	20.9 pcf	16.2 pcf
Fly Ash	≤ 15 %	2.9 pcf	0 pcf	4.2 pcf	--
Strength (flex)	700 psi	650 psi	650 psi	--	400 psi
Fine Aggregate	--	46.8 pcf	--	48.1 pcf	--
Inter Aggregate	--	--	--	34.1 pcf	--
Coarse Agg	--	69.6 pcf	≤ 50 % of agg. wt.	26.3 pcf	--
Slump	0.5 – 2.0 inch	--		--	5 inch
Water/Cement	0.35	0.35	≤ 0.50	0.41	--
Water	--	--	--	10.4 pcf	--
Air Content	6 % by volume	--	4.5 %	--	5.5±1.5 %
Air Entrainment	--	53ml/45kg	--	--	--
Water Reducer	--	163ml/45kg	--	--	--
Synthetic Fibers	0.111 pcf	0.111 pcf	Various rates	None used	0.056 pcf

Note: 1 pcf (lbs/ft^3) = 16.02 kg/m^3

Table 4.2. Mix design information for PCC mix used for test section construction.

Material	Test Section Mix
Cement, lbs/yd^3	580
Fly Ash, lbs/yd^3	0
Mix Water, lbs/yd^3	261
Coarse Aggregate, lbs/yd^3	1,830
Fine Aggregate, lbs/yd^3	1,232
Air Content, %	5.0
Air Entraining Agent, oz/yd^3	5.5
Water Reducer, oz/yd^3	35
MRWR, oz/yd^3	70
Defibrillated fibers, lbs/yd^3	3.0
Total, lbs/yd^3	3,906
Water/cement ratio	0.45

4.2. TEST SECTION CONSTRUCTION

A UTW test section was constructed at ERDC following the Track 1 recommendations. The test section was constructed on an AC pavement test track constructed between 1986 and 1989. The area selected for the UTW test section, shown in Figure 4.1 had a 5-inch (125-mm) thick AC pavement placed directly on the lean clay subgrade. The available length was approximately 125 ft (38 m), which was sufficient for the purposes of this research. Figure 4.2 shows a view of the test road.

4.2.1. TEST SECTION LAYOUT

The old AC pavement at the site for the UTW test section contained longitudinal cracks that run the length of the old pavement in both wheel paths (at about 4.5 ± 0.5 ft [1.37 ± 0.15 m] from each edge) as shown in Figure 4.3. The UTW test section was placed such that the cracks are not included in test samples, as indicated in Figure 4.4.

The test section was three slabs wide and eight slabs long to provide the required number of test samples and an adequate number of extra samples. This size provided six extra panels so that additional samples were available to replace any that might have been damaged in handling.

The test section layout allowed a 1-ft (0.3-m) edge to be sawed around the perimeter of the test section. Each UTW panel was 34 inches (864 mm) square and was sawed with the saw cut going completely through the PCC and underlying AC.

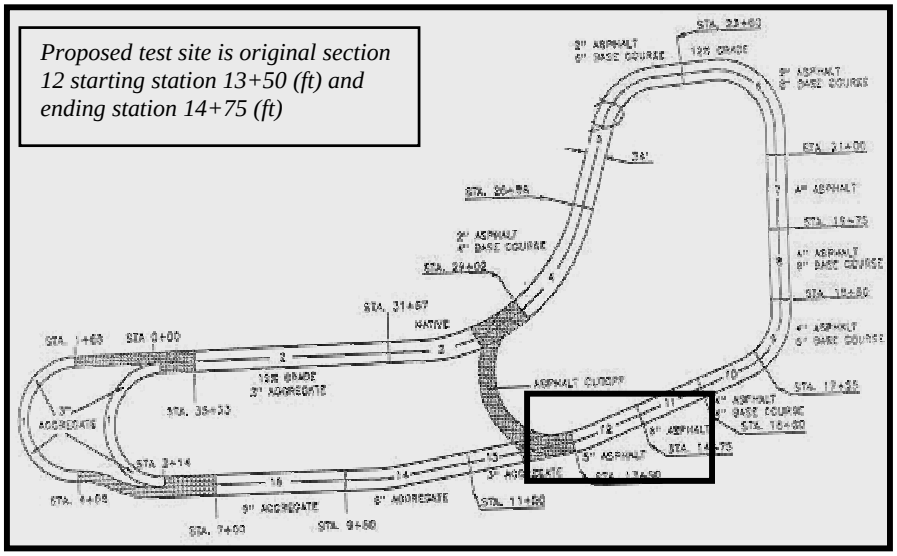

Figure 4.1. The test section was built at ERDC test track.

Figure 4.2. Approximately 125 ft (38 m) are available for test road construction.

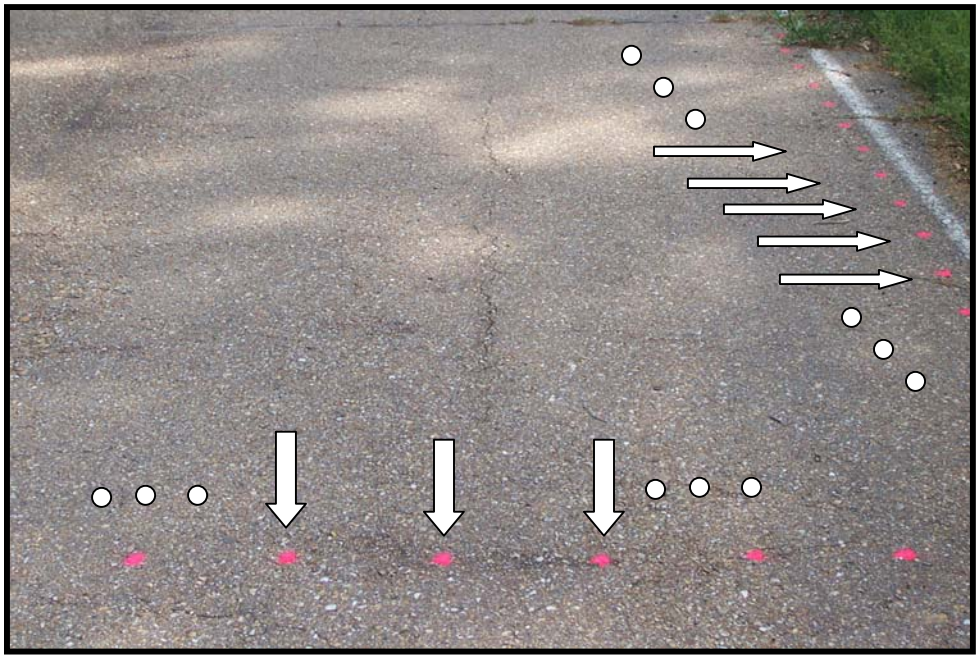

Figure 4.3. Test section distresses were mapped on a 0.3-m square grid.

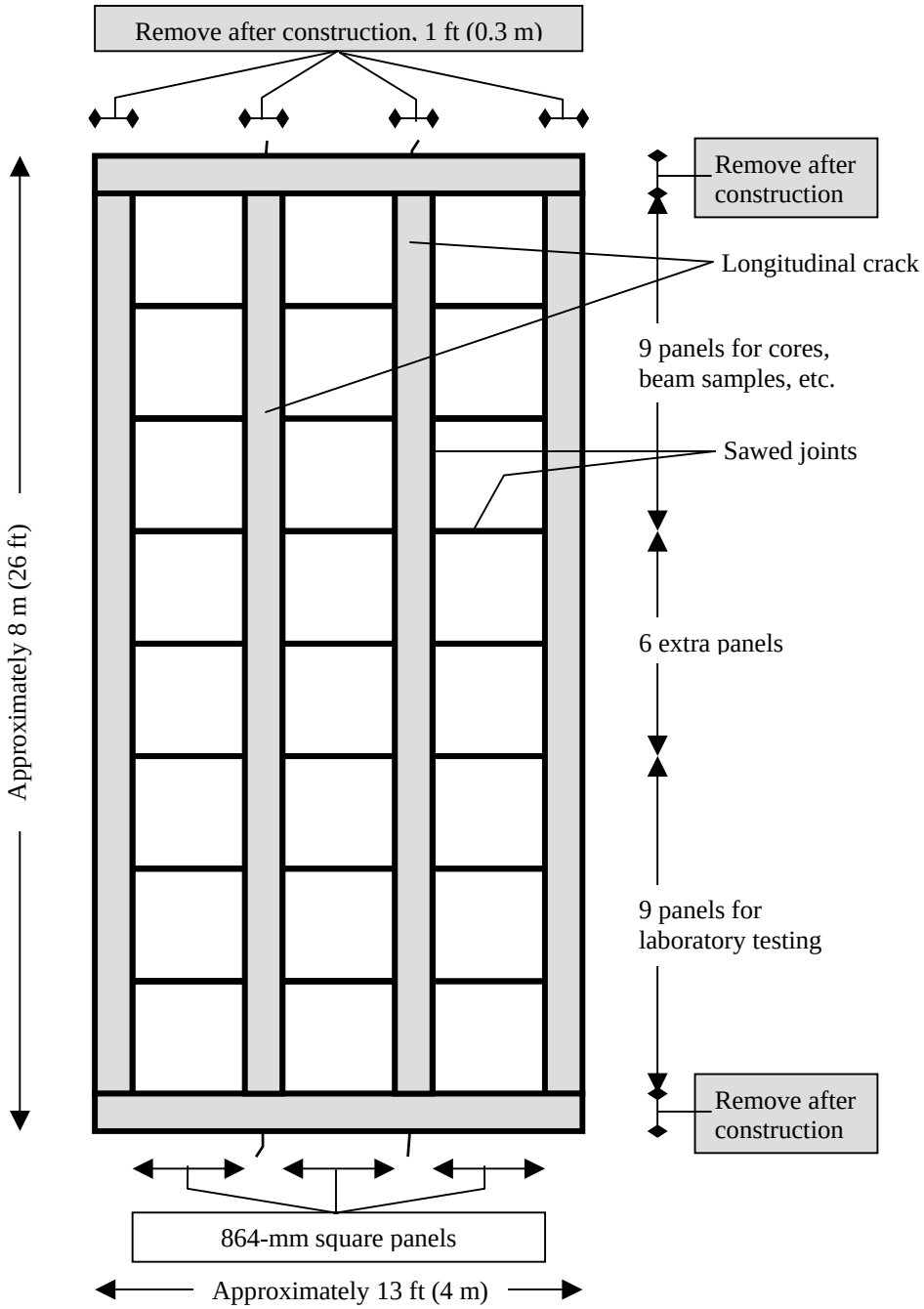

Figure 4.4. Test sample layout avoided longitudinal cracks in AC pavement.

4.2.2. MILLING AND UTW CONSTRUCTION

4.2.2.1. Milling of Existing AC Surface

Core samples of the AC pavement were taken outside the construction area to determine the thickness of the AC layer. Cores were taken "between" and "within" the wheel path (see Figure 4.5); the thickness of the AC layer was 4.5 inches (114 mm). Despite being placed in two lifts, generally the interface could not be located.

The existing AC surface was milled using a milling head attached to a bobcat the produced a typical milling pattern shown in Figure 4.6. Before milling at the test site, three milling depths of 0.25, 0.5, and 0.75 inch were investigated as shown in Figure 4.7. The 0.5-inch (13-mm) milling depth gave the best-milled surface texture and was selected. The milling operation is shown in Figure 4.8, and the milling pattern is shown in Figure 4.9. The milled surface was thoroughly cleaned using compressed air as shown in Figure 4.10.

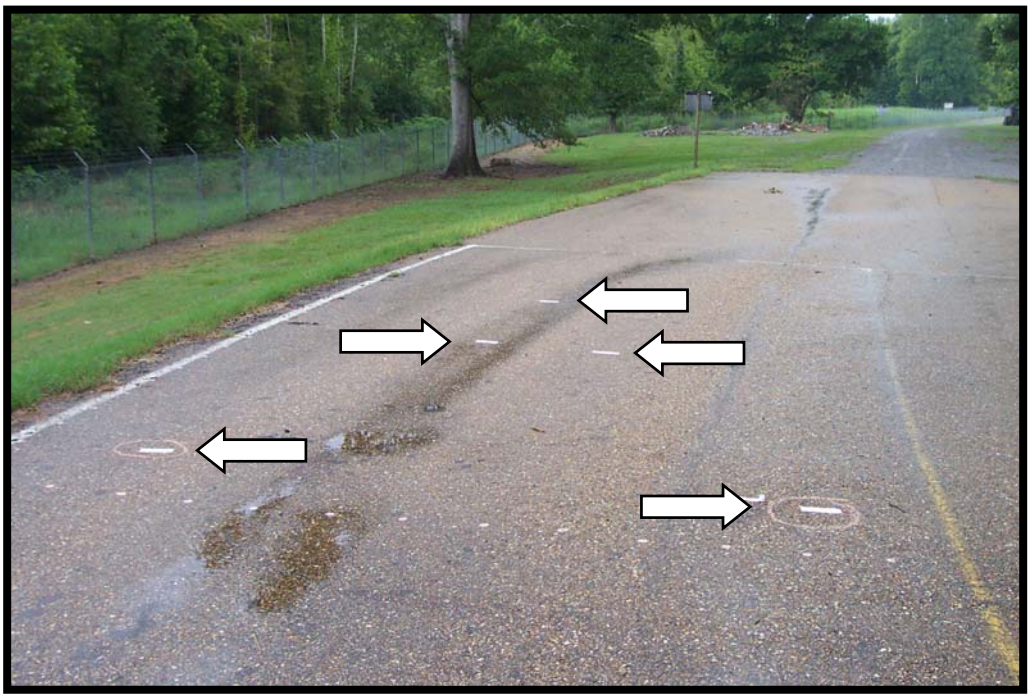

Figure 4.5. Cores were taken outside the test section area to determine AC thickness.

Figure 4.6. Milling pattern and texture depth using a milling head on a bobcat.

Figure 4.7. After trying three milling depths, a 0.5 inch milling depth was selected.

Figure 4.8. A bob-cat® was used for AC milling at the test section.

Figure 4.9. Milling at the test section resembled milling at a typical UTW project.

Figure 4.10. Compressed air was used to clean the milled surface at the test road.

4.2.2.2. PCC Placement

Fixed forms were used to obtain a PCC slab thickness of 3.5 inches (89 mm). The concrete was delivered by ready mix truck and was manually placed and finished (see Figure 4.11).

The concrete was given a smooth finish with no texture. Figure 4.12 shows curing compound being applied; the curing compound was applied at the manufacturer's specified rate for thin PCC sections (twice the rate for standard thickness concrete).

Figure 4.11. Concrete was manually placed and finished at the test site.

Figure 4.12. Curing compound was applied at twice the normal rate.

4.2.2.3. Joints and Saw Cutting

Joints were cut using a Soff-cut® non-raveling saw to a depth of 1 inch (25 mm) as soon as the concrete has hardened sufficiently as shown in Figure 4.13; the joint pattern was in accordance with the test section layout shown in Figure 4.4. The test section was then covered with polyethylene for a period of 14 days (see Figure 4.14).

After curing, wet saws were used to cut through the PCC and AC into the subgrade to form isolated panels.

4.2.3. SAMPLE PREPARATION AND HANDLING

The 34-inch by 34-inch (866-mm by 866-m) composite samples of UTW and underlying AC required special care while extracting in the field. The extraction plan is shown in Figure 4.15. The shaded areas were carefully removed without disturbing the edges or the corner of the sections. The samples were lifted from the bottom using a forklift (see Figure 4.16) and placed on wooden pallets (Figure 4.17) for transportation to the laboratory on a flatbed truck.

Figure 4.13. A Soff-cut® saw was used to cut joints at the test site.

Figure 4.14. The PCC was covered with a plastic sheet after initial joint cutting.

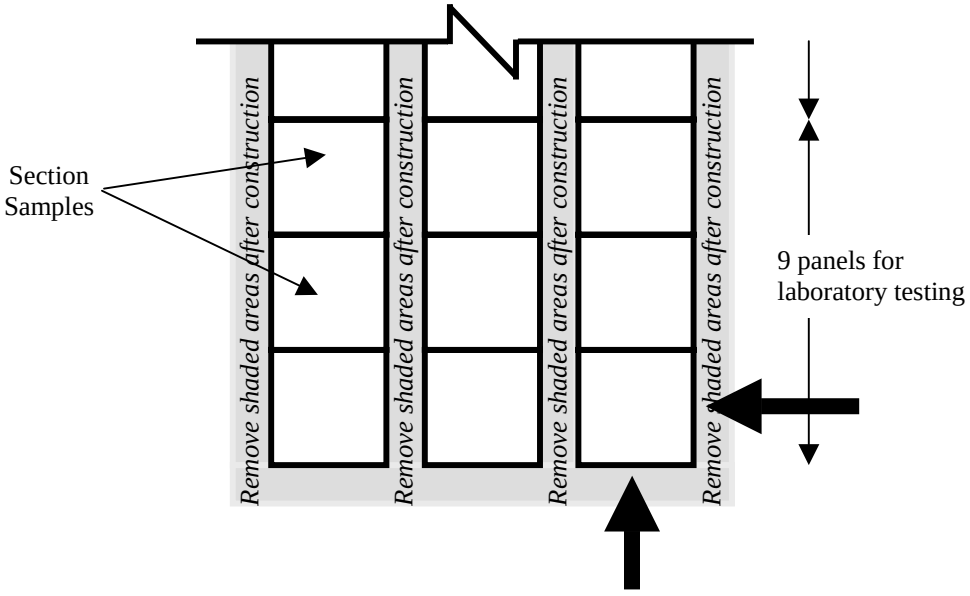

Figure 4.15. Section samples will be extracted using a front-end loader.

Figure 4.16. A forklift was used to remove large 34 inch by 34 inch samples.

Figure 4.17. Samples were tied to pallets to prevent damage during transportation.

This page intentionally left blank.

5. LABORATORY INVESTIGATION PLAN AND APPROACH

5.1. OBJECTIVE OF LABORATORY TESTS

A plan was formulated for a laboratory investigation using the field samples taken from the test section. The objective of the laboratory investigation was to determine if the bond between PCC and HMA has long-term durability when subjected to various types of environmental exposure. Laboratory tests were developed to simulate field conditions of F&T, W&D, and H&C exposures. The field size (34 in by 34 in) specimens were subjected to the various environmental factors by accelerating the time scale in a laboratory environment and determining the long-term durability of the bond by nondestructive means. The H&C tests were not conducted as will be discussed further in the report. The bond evaluation was performed using USUMS.

5.2. MEASUREMENT STANDARD FOR DURABILITY

One of the first challenges in the laboratory investigation was the development of a standard of comparison for measuring bond durability. A standard of comparison is always necessary when making a measurement. A measurement is only useful if a standard is available so that the measured value can be compared against it.

For the laboratory investigation, the two numbers are required for the definition of bond durability. The definition of durability means to be capable of maintaining its quality (percentage of remaining strength) with time (number of cycles of exposure). (The implication is that the repetitive exposure cycles are identical in all respects.) Bond durability, therefore, requires a measure of quality with respect to time to t when subjected to a particular type of environmental exposure. This definition of durability applies to all types of environmental exposure (F&T, W&D, H&C).

5.2.1. FIELD VERSUS LABORATORY DURABILITY

The durability of the bond of a particular UTW construction can have different combinations of quality and exposure time (cycles) based on the parameters of the exposure test. Although the field durability may be considered a constant (example: 60 percent remaining bond area for 30 years of service) for a given specimen under a set of typical weather conditions in a certain region of the country, the value of the laboratory durability can be modified to produce different values by varying the parameters of the laboratory exposure station.

To create an exposure test that is properly accelerated and severe enough to provide data in a reasonable time frame, the temperature extremes in the laboratory need to match or exceed those in the field. Based on the particular parameters (e.g., specimen size, specimen shape, temperature range, rate of change of a variable) chosen for the exposure station for a given type of specimen, the laboratory durability numbers can have different values. To complicate matters further, a standardized exposure test does not exist for any one of the

three environmental exposure conditions. Therefore, it is not known *a priori* whether a satisfactory bond has a durability of 90 percent remaining area in 100, 500, or 1000 cycles of a given exposure condition.

The relationship between the measured laboratory durability and the field durability cannot be determined precisely due to the many variables operating in an exposure test even though the test has been standardized (calibrated). ASTM test method C666, "Standard Test Method for Resistance of Concrete to Rapid Freezing and Thawing," provides a good example. Even though ASTM C666 has been used for over 40 years, it only places the tested specimens into two categories of condition for the field: durable or non-durable. If the specimen has 60 percent or more remaining dynamic modulus after 300 cycles of exposure, then the specimen is considered field durable. If it has less than 60 percent remaining dynamic modulus after 300 cycles, then it is considered non-durable for the field. The standard also states that the test procedure is not intended to provide a quantitative measure of the length of service that may be expected from a specific type of concrete. The implications for this research effort are that, even though the laboratory durability can be determined for a particular condition and test set-up, the exact relationship between the laboratory durability and field durability is still an unknown.

5.2.2. STANDARDIZED DURABILITY TEST

A standardized test procedure requires a "measurement standard." No such standard exists for bond between PCC and AC in UTW. The approach taken to overcome this problem is to compare the bond durability with the durability of other system components, i.e., the PCC and the AC layers.

If the bond between the PCC/AC composite is not the first component of the structure to fail under exposure to cyclic environmental factors for what is otherwise sound materials, then it can safely be assumed that the bond is not the weakest component in the structure. Based on what is known about stress concentration at discontinuities, it would appear likely that deterioration would first take place at the edges and corners of the interfacial bond.

In case of UTW, bond between PCC and HMAC has to last as long as the component materials for the whole UTW system to be durable. The UTW pavement system will fail under field conditions if either one of the two materials fail or the bond between the two materials fails. If the bond structure is the first to fail then the PCC surface may quickly develop cracks under loads due to tensile stress at the interface. Likewise, deterioration of the AC material would cause a loss of bond with the PCC, which would in turn cause failure of the PCC. The plan adopted for this research compares the durability of both the AC and the PCC against the durability of the bond.

A valid test procedure requires the following:

- Field durable material for testing
- Deterioration during testing

- Calibration

For the test on UTW bond durability to be valid, it requires that both material components of a composite pavement specimen be field durable. Questions about the quality of bond and the weaker material with time (bond and material durability) can then be answered. Bond durability can be unknown but material durability can be determined. The durability of the weaker material can be used as a valid standard of comparison against the durability of the bond because of historical knowledge and information are available to design and build field durable materials.

It is necessary that some deterioration take place in at least one of the major components of the pavement structure for the bond durability test to be valid. The test must be continued long enough such that the weaker of the two materials begins to fail, or the bond begins to fail or both fail in the laboratory environment. For the purposes of deriving a standard of comparison, even materials that are sufficiently durable in the field can be made to deteriorate and even fail in the laboratory under accelerated rates and levels of environmental exposure.

The exposure tests can be calibrated by determining the durability of the weaker of the two durable materials (AC or PCC). For each exposure condition, the calibration is represented by two numbers: the remaining percentage of quality and the number of corresponding cycles of exposure. These two numbers will only be applicable for the particular exposure parameters of the particular environmental test.

In other words, the F&T, the W&D, and the H&C test will all have their own set of numbers that represent their calibration. The calibration data can then be used against the unknown bond durability as a standard of comparison. Once the test is calibrated with a durable material, then there is no need to use the separate materials as a comparison since calibration values have been established.

By testing the bond of the composite materials under identical parameters of exposure—size, shape, temperature range, and number of cycles—as that of the individual materials, it can be determined if the bond will endure longer than, the same as, or shorter than (not as well as) the set of numbers determined for the calibration.

5.3. BOND EVALUATION TECHNOLOGIES

Ultrasonic nondestructive testing (NDT) is the standard method for evaluating disbonds in heterogeneous or homogeneous materials and composites or non-composite materials. Ultrasonic waves reflect from the interfaces between materials based on changes in acoustic impedances of the materials. Acoustic impedance is a physical property of all materials and is defined as the product of the ultrasonic velocity and density of the material. If a disbond exists at the interface in a UTW composite and ultrasonic waves are introduced into the structure from the concrete side, the waves reflect from the air or water gap rather than the HMA because the gap has a much lower impedance than the HMA.

No literature was found where the bond between a layer of concrete and a layer of asphalt had been studied, but successful delamination and crack measurements have been performed in concrete by ERDC.

Ultrasonic through-transmission measurements have been made in large concrete structures to detect cracks in a structure [35]. The ultrasonic energy is forced to take an alternative path around the crack as the change in acoustic impedance of a crack blocks the energy from traveling across the crack. The increase in arrival time above that of a straight path, and the fact that the velocity of concrete lies in a narrow range permits the crack to be located.

NDT is normally used to make comparative measurements as opposed to absolute measurements. When used on the surface of pavement that may have various degrees of disbonding or delaminations, NDT can be used to rank all the locations as to the relative degree of degradation. For example, if used on a field apron, taxiway, etc. it can detect, locate, and index the area of the disbonding. NDT is used to test for quality control, quality assurance, and flaw detection in materials and structures.

5.3.1. BENEFITS OF NDT

There are many benefits of periodic NDT material and bond measurements to evaluate the UTW as opposed to destructive testing or FE analysis. Destructive testing requires many specimens, as the specimen is lost for further use once it is tested. As such, another specimen must be tested next time. That presents another problem in that if the first specimen had X cycles of exposure then one must start exposure from the beginning on the next specimen or a series of specimens must be started simultaneously. NDT permits the same specimen to be tested repeatedly. Therefore, the use of NDT requires fewer specimens to be tested and it requires less time for the project; thus, NDT is less expensive than destructive testing.

FE analysis, on the other hand, depends on the input information being correct. Some of the properties that are needed in the analysis are missing—bond strength, for example. Physical tests would be needed in order to calibrate the FE model. Once sufficient knowledge has been gained about all the physical conditions, then future predictions could be carried out with analytical models. Currently, not enough is known about bond strength of PCC/AC for various milling patterns to calibrate the model.

NDT also does not limit the size of the specimen. NDT permits improved statistics, as a large area can be tested and NDT permits the initiation of deterioration to be tracked. For this research a large specimen size of 34 inches by 34 inches (864 mm by 864 mm) was used; this size was set due to limitation on the dimension of the USUMS water bath.

5.3.2. REVIEW OF NDT METHODS FOR BOND ASSESSMENT

NDT methods available to the research team in addition to the USUMS included:

- USUMS
- An impact-echo system referred to in the literature as the 'DOKter' developed by National Institute of Standards and Technology (NIST) personnel
- The James V-meter for ultrasonic through-transmission measurements
- An ultrasonic pulse echo system called the SUPERSCANNER, developed by ERDC to detect delaminations in bridge decks

The impact-echo technique provides a pulse echo bond signal at one location on the specimen whereas the V-meter provides a through-transmission signal at one point. ERDC received a patent in 1999 on the SUPERSCANNER, which was developed to detect delaminations in concrete bridge decks.[36] The SUPERSCANNER operates in the pulse echo mode. It is common for concrete bridge decks to delaminate into two layers at the depth of the reinforcement. Because the physics of ultrasonic behavior is similar for detecting separations in PCC and detecting separations between PCC and AC, the SUPERSCANNER technology was selected for this investigation. The SUPERSCANNER can provide a series of pulse echo bond signals along the location of a straight line on the specimen. The USUMS can provide either a configuration of through-transmission or pulse echo bond signals over a large area of the specimen. Thousands of measurements of either type configuration can be made with the USUMS system. The USUMS permits uniformly spaced measurements, significant statistics, and rapid measurements. Transducers of many varieties can be used with the USUMS having different properties: frequency, focal length, damping, etc.

The benefits of using the USUMS system include capability to provide a series of pulse echo or through transmissions over a large area allowing uniformly spaced rapid measurements. Initial evaluation of the USUMS showed that though it was the most rapid method, not all the available in-house transducers were capable of a satisfactory signal to noise ratio (S/N). A transmitting transducer with sufficient S/N to penetrate the 7-inch (178-mm) thick UTW specimens was designed and assembled. The transmitting transducer permitted sufficient ultrasonic penetration (S/N of 100X at receiver) of the highly attenuative composite material, which permitted use of the USUMS.

The USUMS proved to be invaluable for obtaining through transmissions and amplitude measurements, which were uniformly spaced, significant in number for proper statistics, and rapid. The measurement system permitted thousands of measurements to be made over 90 percent of the large surface area (images are distorted by boundaries of specimen), yielding high spatial resolution. By combining thousands of A-scan signals into one image, this permitted a visual determination that no disbonds existed in the specimens.

The SUPERSCANNER and impact-echo systems were not used in the testing because they were limited in their speed of operation.

5.4. APPROACH TO LABORATORY INVESTIGATION

The method of testing all the variables (temperature [both frozen and thawed] and moisture) at once cannot isolate the cause of the deterioration in the materials or bond or both.

5.4.1. TESTING CONCEPT

During the experimental investigation, all environmental variables were to be controlled except the one of interest, and its effect on the material and bond durability was studied. This approach allowed isolating the variable that had the greatest affect in breaking down the bond or materials. Tests would then enable ranking of the influence of the temperature, moisture, or freeze and thaw conditions on bond deterioration. The project scope did not request data on which environmental variable causes the greatest deterioration; it only requested data on the long-term durability of the bond.

Mechanical loads can accelerate the degradation of the materials or the bond, but an external load is not necessary to cause degradation. In fact, applying an external load simultaneously with the environmental variable could blur the result in that, at the end of the tests, it will not be known what fraction of the degradation was caused by the environmental factors and what fraction was caused by mechanical loads. It is known that any specimen, if cycled enough under any environmental load, will fail due to fatigue. No external mechanical loads were used during laboratory investigation.

5.4.2. SYSTEM TESTS

System tests were defined as tests on the large 3-feet by 3-feet samples such that the composite section could be tested as a system. Small-scale tests permit the specimens or panels to be studied as a function of size and geometry as well as material. Only large-scale tests would be a function of boundary conditions. Thermal changes in UTW may cause sufficient shear stresses to develop at the interface such that it is not sufficient to evaluate the bond with material tests, but material durability can be studied with a small-scale test. Note, however, that if the bond failed in a material test in less number of cycles than some material deterioration in either of the two materials, then it is evident that the specimen will not survive in a system test. Therefore, a material test may be informative but not always sufficient. It is not necessary to test a large section or even a full panel of UTW for a material test. A material test is independent of size, shape, and external loads on the boundaries.

5.5. METHOD TO DETERMINE BOND DURABILITY

The following procedure was developed to determine the durability of the bond relative to the durability of the weaker of the two materials.

5.5.1. PROVISION OF DURABLE MATERIALS FOR TEST SITE CONSTRUCTION

The first step of the procedure verified that durable materials (AC and PCC) were used in the construction of the test site. The test site provided durable AC pavement that had gone through about 7 years of field aging and some traffic loading. As described earlier, a durable PCC mix was placed on the milled AC, and test specimens were obtained by sawing panels from the test site after 28 days of curing. For the purposes of this investigation, it was necessary that both materials be durable, as the durability of the HMA and the PCC was used as the standard for comparison against the durability of the bond.

5.5.2. VERIFICATION OF SAMPLE FLATNESS

The 3-feet by 3-feet samples were tested for flatness (shape of the surface of the PCC) before initiation of exposure testing. This measurement was made to ensure that the sample had not warped or curled during the curing process. Although the absence of flatness (due to curling and warping) does not necessarily mean that a disbond has taken place, it might signal the onset of stress conditions that could lead to disbonding. Flatness measurements were performed on the surface of the PCC layer of each 3-feet x 3-feet specimen before they were subjected to environmental exposure to verify that the specimen had not curled or warped during curing. Lack of flatness in a specimen could introduce a built-in stress between the PCC and HMA, which could then accelerate deterioration when additional stress is introduced during environmental exposure.

To evaluate specimen flatness, the specimen was immersed into the water tank and a high frequency ultrasonic transducer (10 MHz) was scanned over the specimen surface using pulse echo testing. Figure 5.1 illustrates the transducer scanning the sample surface.

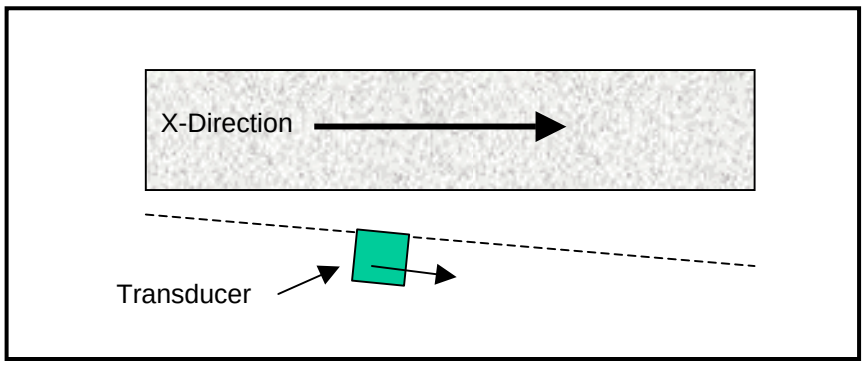

Figure 5.1. Illustration of transducer movement not parallel to the specimen's surface.

5.6. LABORATORY SIMULATION OF FIELD EXPOSURE CONDITIONS

To simulate field exposure conditions (F&T, W&D, H&C), environmental exposure stations were assembled at ERDC.

5.6.1. F&T EXPOSURE STATION

ERDC has conducted freeze-thaw measurements on PCC specimen for over 40 years. The specimen tank used to evaluate the large UTW specimens is shown in Figure 5.2. The glycol fluid in the system is continually circulated from the cold reservoir to the specimen tank and back to the reservoir so that the fluid remains uniformly cold. The refrigeration coils of the system are located in the cold reservoir. Since the circulation of the glycol fluid occurs primarily by gravity from the specimen tank to the sump tank, it is necessary that the level of the specimen tank be higher than the level of the sump tank. As the fluid level rises in the specimen tank, the excess flows into a sump tank by gravity. Electric probes in the sump tank sense the level of the fluid when the tank is full and turns on the sump pump, which moves the fluid into the cold reservoir, and the process of recirculation continues as the fluid flows from the reservoir to the specimen tank by gravity.

Figure 5.2. New F&T exposure tank (with three large and three small UTW samples).

The specimens were placed in stainless steel containers filled with water and the containers placed in the large specimen tank containing the ethylene glycol according to the procedure of ASTM C 666. The specimens were laid horizontally in the containers; the PCC surface was on the bottom so that freezing and thawing proceeded primarily from the surface of the PCC as it occurs in the field. With the specimens upside down relative to the field environment, there was less opportunity for the specimens to receive unintended stress from handling during lifting and transporting, as PCC has a higher strength than AC and can resist the forces of handling better than AC.

ASTM C666, the standard for F&T equipment, requires a 2-hour cycle time using a fixed mechanical timer, which triggers numerous switches as it rotates. The switches control relays, which in turn energize (open or close) the pumps and valves. The large size of the UTW specimens required a longer freeze and thaw time than the small standard-size ASTM C 666 specimens. An electrical alteration was made to the mechanical control; an external computer-based control system was introduced into the power circuit of the timer to permit a variable timer cycle. The external controller worked by disconnecting AC power to the mechanical timer after critical switching operations take place so that the system remains in either the freeze or thaw cycle long enough for the temperatures to reach the correct values dictated by ASTM C 666. A typical temperature-time cycle is shown in Figure 5.3, while Figure 5.4 shows a series of temperature cycles.

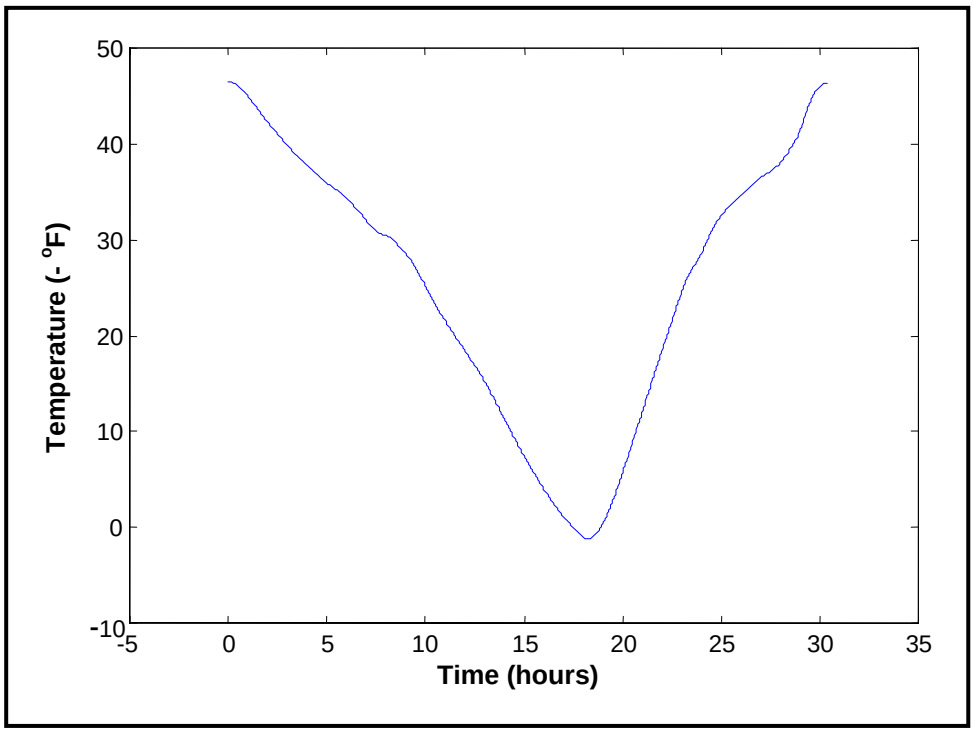

Figure 5.3. Typical temperature-time plot during one F&T cycle of UTW specimen.

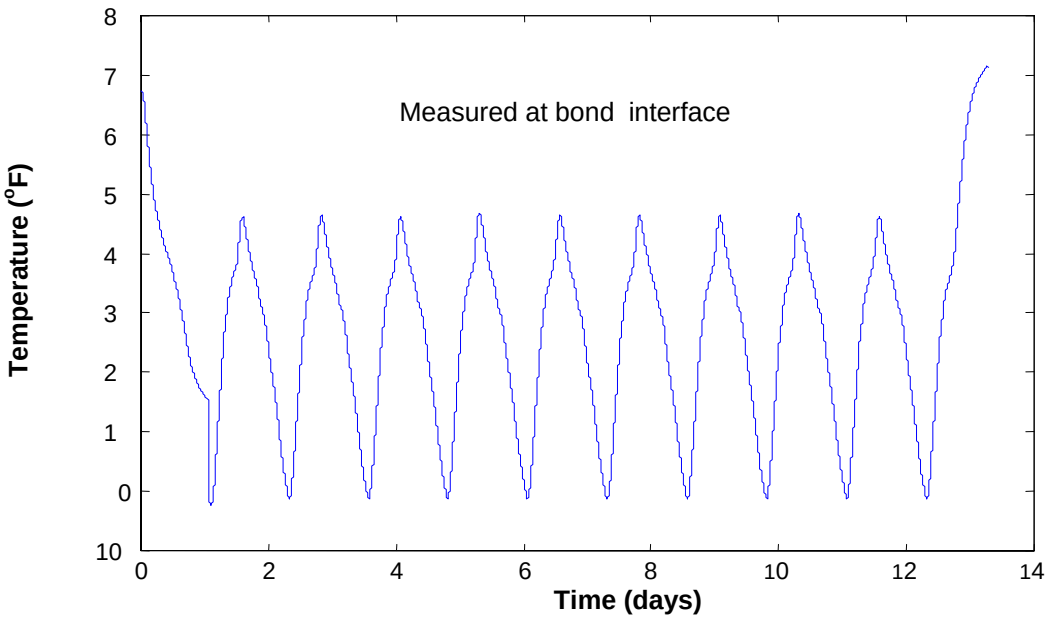

Figure 5.4. Typical temperature-time plot for specimens subjected to F/T exposure.

Interrupting the timer power supply on the existing F&T apparatus permitted the freezing and thawing cycles to be longer than the standard 1-hour each. The computer-controlled timer permitted the specimen tank to be filled with thawing fluid (ethylene glycol) and permitted the fluid to be drained from the tank at the end of the thaw cycle automatically. At the end of the freeze cycle the system automatically fills the specimen tank with warm fluid from the thaw-fluid reservoir when the temperature in the center of the specimens reaches 0^{o}F. After the thaw temperature in the center of the specimen reaches 40^{o}F, the warm fluid is drained out and cold fluid pumped into the specimen tank from the cold-fluid reservoir as the conditions are continually repeated in F&T cycles that follow.

When it was time for the specimens to be tested using the USUMS, the F&T system was stopped at the end of the thaw cycle. The specimen was allowed to warm to room temperature for a period of 24 hours at which time it was placed in the immersion tank (also at room temperature). This precaution was necessary as different temperature gradients in different parts of the specimen can cause misleading ultrasonic velocities leading to a false indication of a disbond in the ultrasonic image.

Five thermal inputs control the glycol bath and specimen temperatures. The control system reads temperature information from three thermocouples in the specimens with the sensing tips located at the PCC/AC bond interface. Figure 5.5 shows a thermocouple that goes to the center of the specimen (at the bond interface). To install these thermocouples, small holes were drilled to the depth of the bond interface and thermocouples inserted and filled with epoxy. The two remaining thermocouples are located in the ethylene glycol bath to monitor the inlet and outlet temperatures to and from the specimen tank.

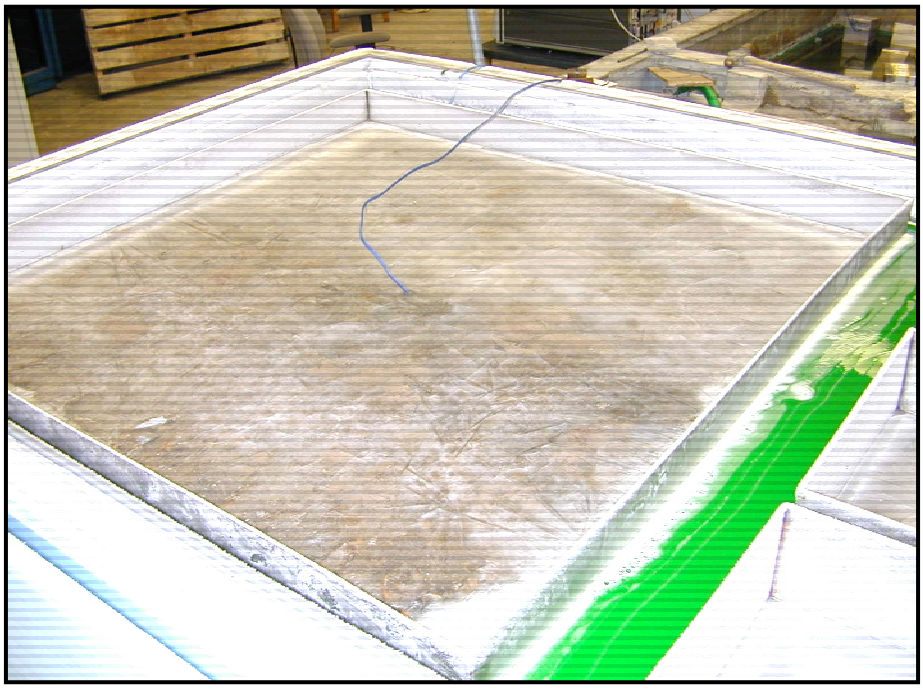

Figure 5.5. Thermocouple were installed in the middle of specimen at the interface.

The temperature control system determines the current status (freeze or thaw) of the F&T system and holds the system in that state until the average temperature from the specimen-implanted thermocouples is either 0^{o}F (frozen) or 40^{o}F (thawed). When either of these two criteria is met, the mechanical timer is released (i.e., re-energized with AC power) so that the system can proceed to the next appropriate cycle in Figure 5.6 shows the monitoring screen of the computer's control software. Text located on the left side of the screen indicates status (freeze or thaw cycle), time spent in either cycle, or whether the timer is being held in the thaw cycle. The five temperature scales display the inlet and outlet temperatures of the glycol as well as the temperature of the three specimen-embedded sensors. The inlet and outlet temperatures are averaged to generate a fluid temperature reading and the three specimen temperatures are averaged to generate an average specimen temperature reading. These readings are plotted on the display screen and stored on the computer's hard drive as permanent record of temperature data.

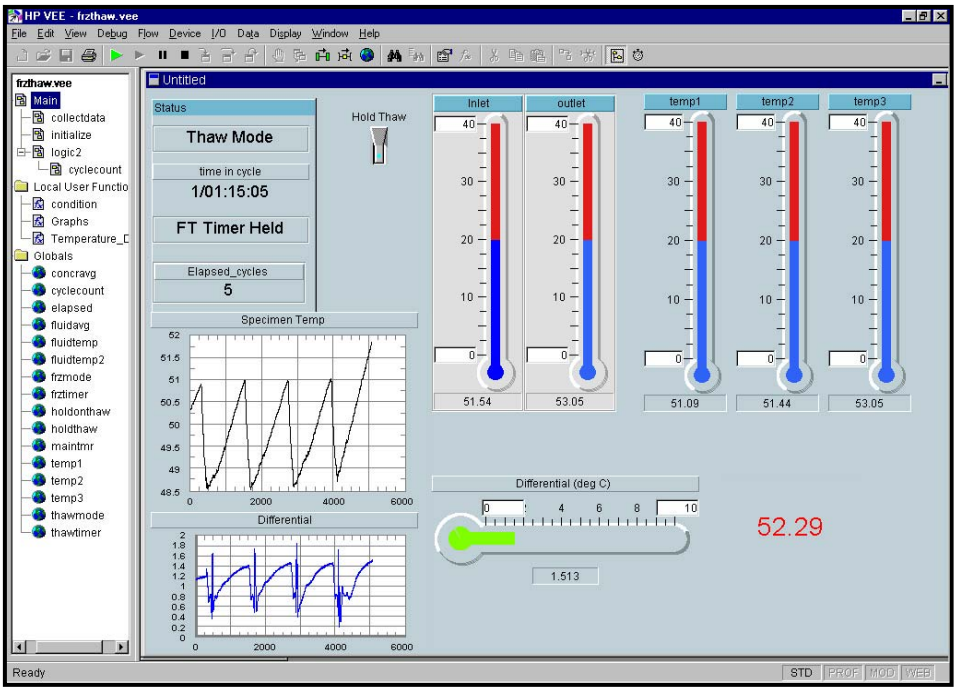

Figure 5.6. Control system screen displaying various F&T parameters.

5.6.2. W&D EXPOSURE STATION

The W&D test was designed to determine the influence of the moisture fluctuations on the UTW specimens; the temperature was held constant during this test. Heat accelerates the drying process in air and increases the rate of deterioration in air or water; thus, the temperature of the W&D exposure was held constant at 150^{o}F. The humidity in the W&D exposure room was maintained at 30 percent. This low humidity caused the water in the specimen tank and the storage reservoir to evaporate rapidly and necessitated that the reservoir be refilled with additional water about every 3 days. The W&D exposure set up is shown in Figure 5.7 (conceptual drawing); Figure 5.8 shows UTW specimens undergoing W&D exposure.

The humidity at the center of the specimen was not monitored; thus, the humidity at the end of the dry or the wet cycle is not known. Water was pumped back into the storage reservoir automatically at the end of the 12-hour wet cycle and pumped back into the specimen tank after the 12- hour drying cycle. The specimens were placed in the exposure tank with the concrete layer on the bottom.

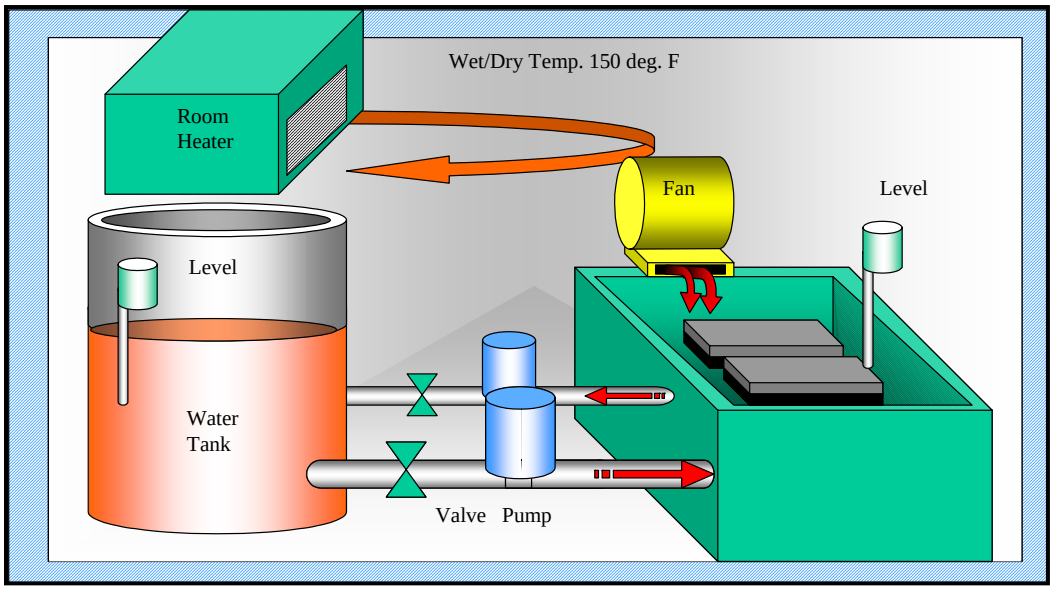

Figure 5.7. Conceptual drawing of the W&D exposure station.

Figure 5.8. UTW specimens undergoing W&D exposure in the W&D tank.

5.6.3. H&C EXPOSURE STATION

The H&C exposure station was designed to study the influence of temperature variations on UTW bond performance. The moisture level during H&C exposures was to be held constant; thus, the test was designed for constant water immersion. The design involved using the same two reservoirs, pumps, pipes, new tank, and timing systems of the modified F&T exposure station and the electronic (computer) control for the timer for the H&C exposure station. The only difference from the F&T test would be the values of the temperatures for the two parts of the H&C cycles. An illustration of the system is shown in Figure 5.9.

F&T and H&C exposure tests use common equipment with different temperature control setting; thus, the tests could not be run concurrently. After completion of the F&T tests, the temperature parameters were to be adjusted to conform to the requirements for the H&C exposure tests. During the high temperature cycle, the UTW specimen was to be immersed in water at 150^{o}F and at 50^{o}F during the low temperature cycle.

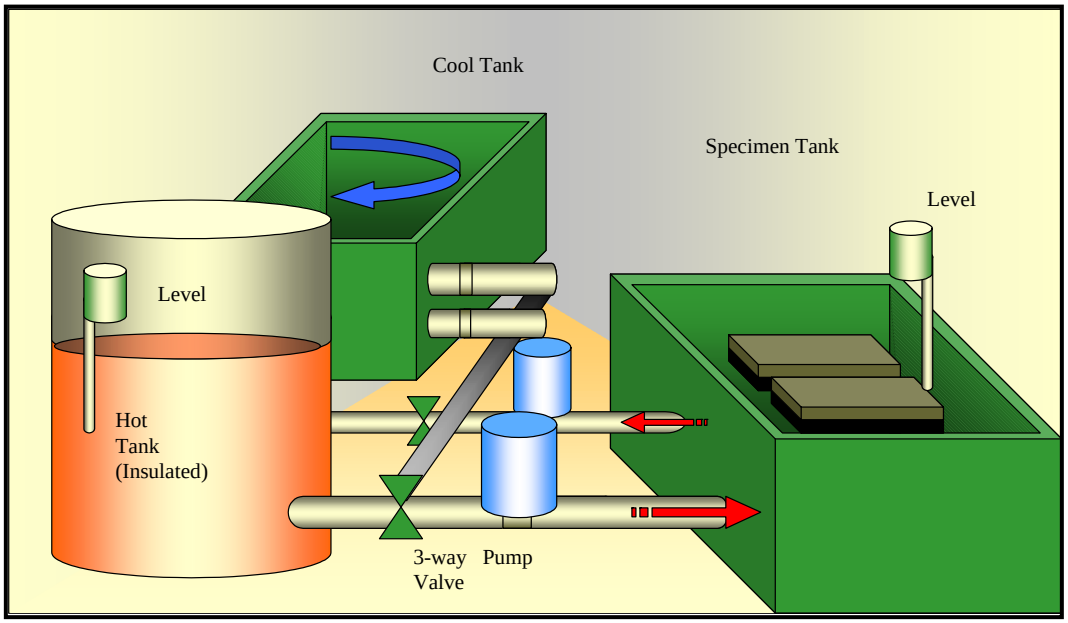

Figure 5.9. Conceptual drawing of the H&C exposure station.

For the H&C tests, an additional heater element with thermostat was added to the reservoir that contains the warmer fluid of the original F&T equipment. The two separate fluid reservoirs of the original F&T system contained the hot and cool fluid modified for use for the H&C test. The test was designed for the refrigeration system of the original F&T system to maintain the center of the specimens at 50^{o}F. At the end of the cool cycle, the circulation of the glycol between the specimen tank and the cool reservoir is stopped and the specimen tank drained of the cool water. Then hot fluid is pumped into the specimen tank and the

glycol fluid is circulated between the specimen tank and the hot reservoir. Electric heater elements maintain the temperature of the specimens at 150°F for the hot cycle. Again, the specimens are installed upside down so that the exposure more closely simulates the exposure that occurs in the field (PCC on bottom, AC on top).

5.7. EXPOSURE STATION SEVERITY

The time required to induce deterioration of UTW specimens could not be predicted beforehand, as the three exposures are not standard procedures. However, for the evaluation process to be successful, deterioration of one of the three UTW components (PCC, AC, or bond) was essential. This is further complicated by a lack of history on the required level of severity to initiate deterioration in specimens this size for any of the three exposure stations.

It is important that the specimens not be fatigued too slowly or too rapidly. If the accelerated test is too slow and does not create sufficient fatigue in the specimens, it may not be possible to get either bond or material deterioration in the time frame of the investigation. If the accelerated test fatigues the specimens too rapidly and the bond and the two materials deteriorate too rapidly, it may not be possible to get sufficient data before failure. In addition, deterioration is more accurately measured in the earlier stages as highly deteriorated specimens can create excess noise in the measurement equipment.

5.8. HANDLING TEST SPECIMENS

It was essential that the test specimens only receive stress from environmental exposures and no stress from other sources. The test specimens were carefully moved from the test site to the laboratory using a flatbed truck. A method was developed to protect the specimens in laboratory against damage when handling.

A 2-ton crane, shown in Figure 5.10, was used to remove specimens from the exposure tanks. Then, a metal cart with solid rubber wheels was used to transport specimens from the exposure room to the ultrasonic testing room and back. A permanently installed 10-ton capacity crane was used for lifting the specimens from the metal cart and positioning in the immersion tank.

A metal frame, shown in Figure 5.11, was used to further safeguard the specimen during testing. The frame had four main parts to surround the specimen: a bottom part, a top part, and two end pieces.

Figure 5.10. A 2-ton capacity crane was used to handle specimens in exposure stations.

Figure 5.11. Frame used to handle specimen during transport in the laboratory.

Once the specimen and lower frame were removed from the stainless steel containers in the specimen tank (at the time for testing), the end pieces and top portion of the frame were attached to the lower part with rods. Rubber stops were placed between the frame and the specimen for added protection. The long metal rods permitted the frame to be easily removed once the specimen was lowered into the measurement tank and reinstalled when the measurement was over. The rods permitted a quick release of the frame in the ultrasonic immersion tank so the fixture can be laid to the side for unobstructed ultrasonic testing of the specimen.

Specimen handling including the following steps:

- Removing specimen from exposure tank and placing it on a metal cart with the largest surface area lying in a horizontal plane,
- Attaching upper half of frame to lower half of frame
- Transporting specimen on cart to ultrasonic testing location
- Rotating specimen 90 degrees with 10-ton room crane such that the largest surface area lies in a vertical plane and then raising specimen above immersion tank
- Lowering specimen into immersion tank and positioning specimen precisely in tank
- Detaching metal frame from specimen by removing easy-release rod
- Determining presence of bonding/disbonding with ultrasonic testing
- Removing specimen from immersion tank after testing
- Reversing process until specimen is back into the respective exposure tank.

This page intentionally left blank.

6. LABORATORY TESTING AND DATA COLLECTION

6.1. OPTIMIZATION OF USUMS

To determine the sensitivity of the USUMS to detect a disbond, the system was tested by detecting an artificial disbond introduced into test site specimens. Installing a foam board with a rigid backing, as shown in Figure 6.1 simulated an artificial disbond between AC and PCC layers (note that the two colors on the foam board are not significant). Styrofoam is an excellent material for simulating a disbond because it has an acoustic-impedance close to that of air (a disbond).

This model permitted a known case to be studied with ultrasonic through-transmission signals. The differences in characteristics between the signals of the bonded and disbonded parts of the specimen could be analyzed. The model provided a ceiling on the maximum resolution possible under ideal conditions. After the concrete overlay had cured, the artificial disbond was first detected at the test site with resonant frequency testing energy introduced into the concrete surface by impacts with a small hammer. Later, the disbond was detected in the laboratory with ultrasonic immersion testing.

The image from the foam board artificial disbond is shown Figure 6.2. The darker area represents the area of the disbond. The incorporation of the disbonds into the specimens showed that the USUMS gave an obvious distinction between the bonded and unbonded areas and revealed a ceiling on the maximum resolution that could be expected with the USUMS system.

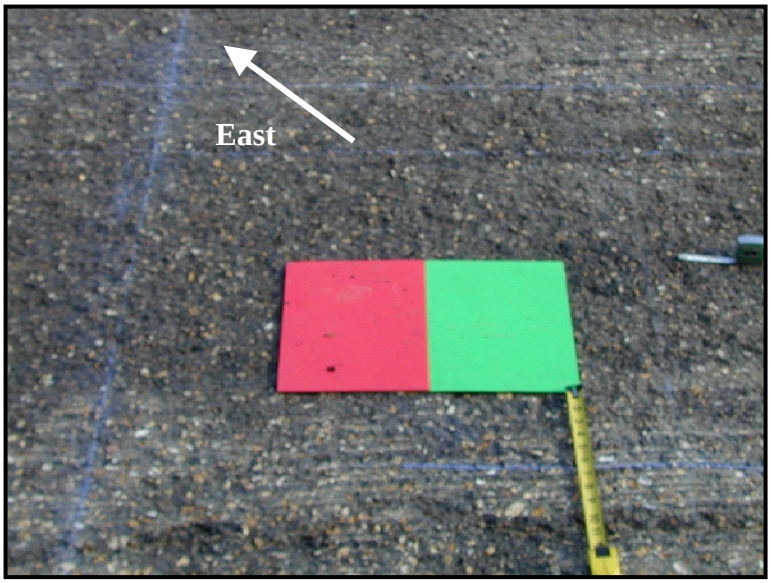

Figure 6.1. Foam board was used to create an artificial disbond to evaluate the USUMS.

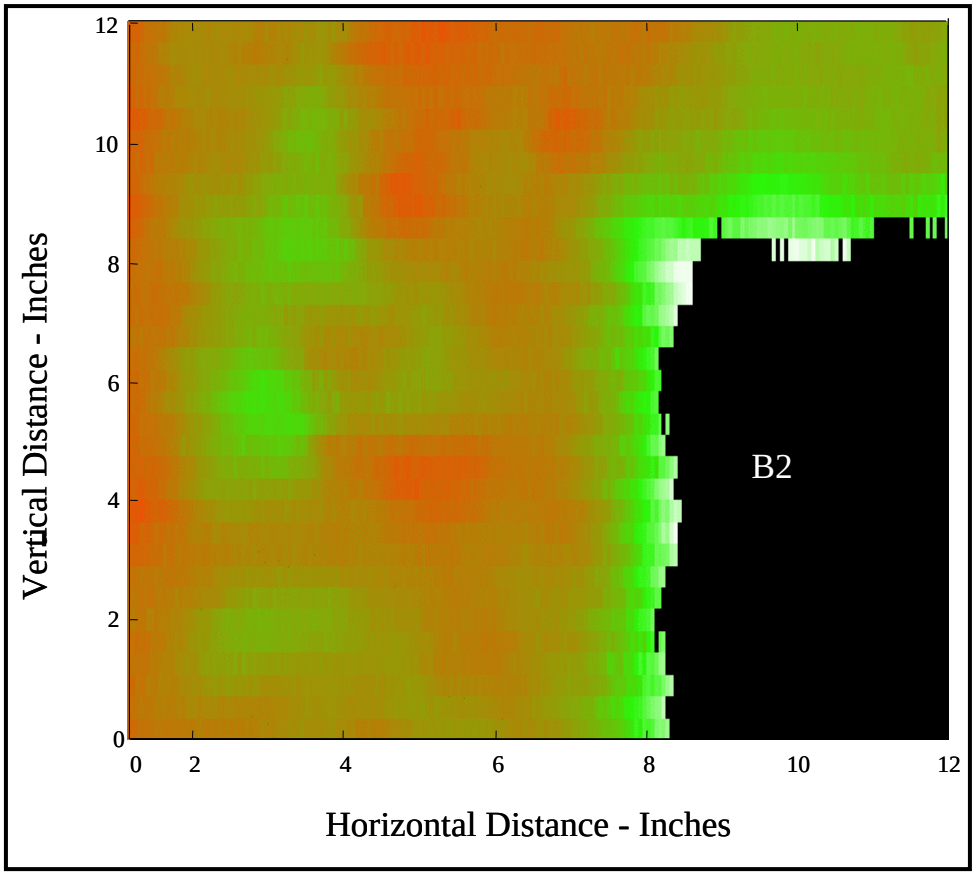

Figure 6.2. Image from artificial disbond.

6.2. VERIFICATION OF INITIAL SPECIMEN SOUNDNESS

To determine the initial soundness of the UTW specimens after curing, tests were made with the V-meter. These tests verified that the ultrasonic velocities measured for AC and PCC were in the range for sound materials. During the V-meter tests, the ultrasonic velocity for AC averaged 12,000 ft/sec (3,658 m/sec), while the ultrasonic velocity for PCC averaged 15,000 ft/sec (4,572 m/sec). These measurements were made in a transverse direction to the thickness.

All the specimens were evaluated prior to subjecting them to the environmental exposure tests, and no disbonds were found using the USUMS. There was no location on the UTW specimen that the transmitter could not get a through transmission. The measurements indicated that the full area was bonded.

6.3. VERIFICATION OF SPECIMEN FLATNESS

All UTW specimens were checked for flatness before subjecting to environmental exposures. To verify specimen flatness, the specimen was immersed into the water tank and a high frequency ultrasonic transducer (10 MHz) was scanned over the 34-inch (864-mm) square surface of the PCC overlay in a pulse echo configuration. Bowing of the PCC surface was determined by measuring the time of arrival of the ultrasonic echo from the surface. Because the ultrasonic velocity in water is constant, the time of arrival is directly related to the separation distance between the plane of the transducer movement and the plane of the concrete surface. Distance measurements were made to the nearest 0.001 in.

The bowing measurements were not entirely straightforward. It was not possible to place the concrete specimen in the testing tank such that the concrete surface is in an exact plane with the plane of the transducer movement. Because the separation distances between the transducer and concrete planes can vary even for a specimen with a flat surface, a mathematical algorithm was developed that compensated for the two planes being nonparallel.

6.4. BOND SHEAR STRENGTH TESTS

The bond between AC and PCC, prior to exposure, was shown to be of standard strength. This was verified by making shear strength measurements made on cores drilled from the test specimens.

Composite cores of 6-in (152-mm) diameter and approximately 7-in (178-mm) length were drilled from the larger 34-in.-square-area specimens sawn from the test site. The cores were drilled from the specimens after the specimens had been removed from the test site prior to any environmental exposure.

Shear strength measurements were made on the cores to determine the integrity of the bond. These tests were performed to determine the average bond strength of the composite specimens as taken from the site prior to any environmental exposure. These strength numbers were to be compared to strengths of other UTW specimens documented in the literature from other projects. The shear rig is shown in Figure 6.3. An example of a core in which a shear strength test was made is shown in Figure 6.4.

Wu and Sheehan [37] report that 100-psi (689 kPa) is an adequate value for shear strength of bonded composite pavement. Tests conducted on four cores cut from the specimens resulted in bond strength values of 75, 93, 106, and 118 psi (517, 641, 731, and 814 kPa), indicating that the bond shear strength was similar to that as reported by Wu and Sheehan. The PCC surface of the sheared interface was usually covered with clumps of AC after testing, as shown in Figure 6.4.

Figure 6.3. Shear rig for testing PCC/AC bond strength.

Figure 6.4. Shear test on PCC/AC bond.

6.5. DURABILITY OF AC AND PCC

The durability of AC and PCC used in laboratory investigation is essential for reliable results on bond performance, as the less durable of the two materials is used as the deterioration reference. ASTM C 666 test method was used to determine the relative durability of the PCC and AC materials. AC and PCC prisms were cut from the test specimens (in dimensions meeting test requirements, 3.5 x 4.5 x 16 inches [89 x 114 x 406 mm]) and subjected to F&T exposure. Ten prisms of AC and 10 prisms of PCC were subjected to different number of exposure cycles. Some of the AC and PCC prisms after testing are shown in Figure 6.5.

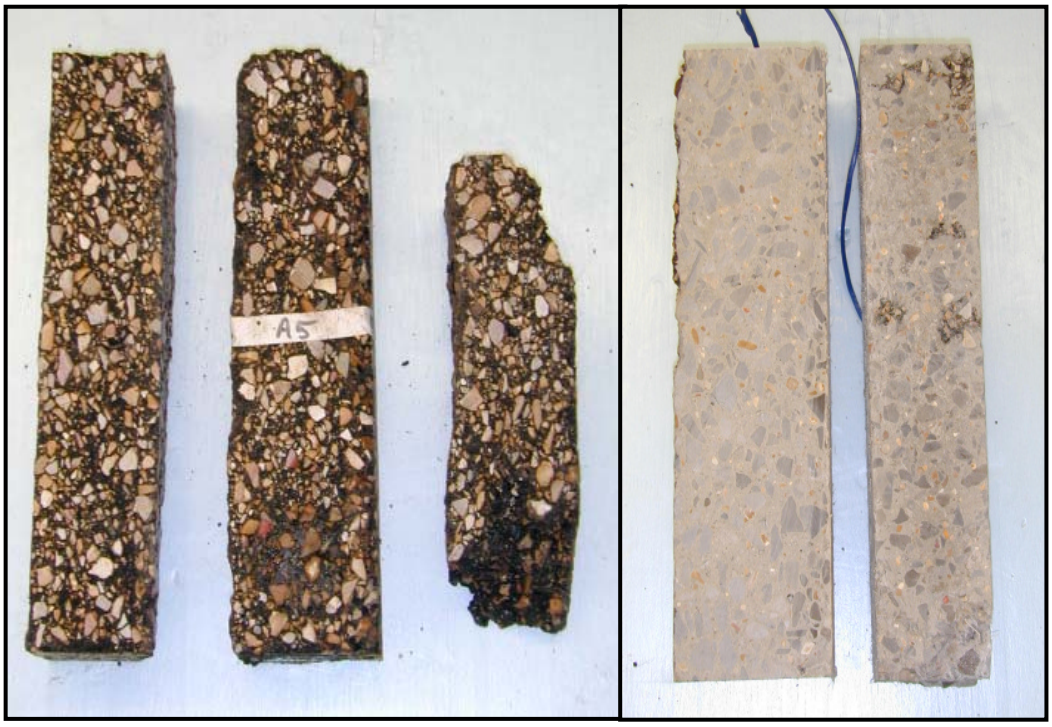

Figure 6.5. AC and PCC prisms were deteriorated using F&T exposures.

This deterioration was engineered to determine which of the two materials would serve as a standard of comparison to determine the durability of the bond. The two materials were exposed and tested as individual materials rather than as a composite.

The ultrasonic pulse velocity [38] of each prism was measured according to ASTM C 597, "Standard Test Method for Pulse Velocity Through Concrete," to determine its level of deterioration. Ultrasonic pulse velocity measurements in the dry condition (not underwater) were used to determine which of the two materials had the durability of lesser durability. Table 6.1 shows of rankings of concrete quality as a function of pulse velocity following deterioration due to the F&T tests. Figure 6.6 shows remaining pulse velocities for AC prisms.

Table 6.1. Suggested pulse velocity ratings for concrete.

Ultrasonic Pulse Velocity (ft/sec)	Percentage Drop in Velocity (versus 15,000 ft/sec)	Quality of Concrete
> 15,000	0	Excellent
12,000 - 15,000	0 – 20	Good
10,000 - 12,000	20 – 33	Questionable
7,000 - 10,000	33 – 53	Poor
< 7,000	>53	Very Poor

Note: 1 ft/sec = 0.3048 m/sec

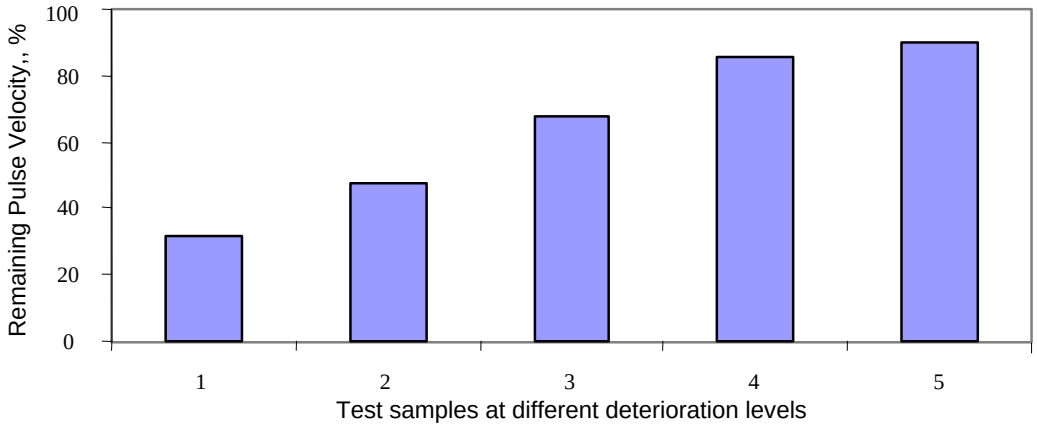

Figure 6.6. Remaining pulse velocity of different AC prisms subjected to F&T exposures.

6.6. FREEZE-THAW EXPOSURE TEST PROGRAM AND TEST RESULTS

Following tests to ensure the large specimens were not warped/curled, and after initial base-line measurements to determine that bond existed between the PCC and AC across the entire specimen, the F&T tests were initiated. The F&T exposure station was described earlier. Figure 5.2 showed the F&T tank with the 34-inch by 34-inch specimens submerged (note that 3 smaller specimens are also being tested in the tank). Figure 5.4 showed the tank frozen with ice surrounding the test specimens. Figure 5.3 showed the temperature cycle for a 24-hour period and Figure 5.4 showed the temperature cycles over several days. Figure 5.6 showed the controls and readings associated with the F&T exposure cycling.

6.6.1. BOND TESTS ON F&T SPECIMENS

USUMS tests were made in a water immersion tank and an attenuation and velocity image constructed from the many signals recorded to represent the area of bond/disbond. Figure 6.7 shows a specimen being put into the scanning tank. Through-transmission measurements require a transmitter and receiver on opposite sides of the specimen as illustrated in Figure 6.8. Figure 6.9 gives an overall view of the scanning equipment and Figure 6.10 shows a specimen being scanned.

Figure 6.7. Winch for lowering and removing UTW specimen into scanning tank.

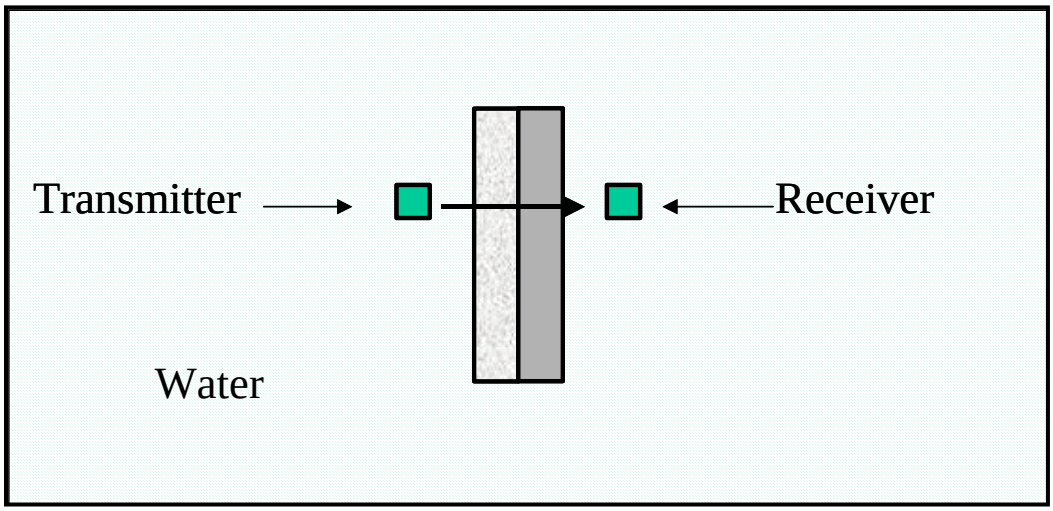

Figure 6.8. Method of measurement for bond evaluation.

Figure 6.9. USUMS for imaging anomalies in large PCC specimens.

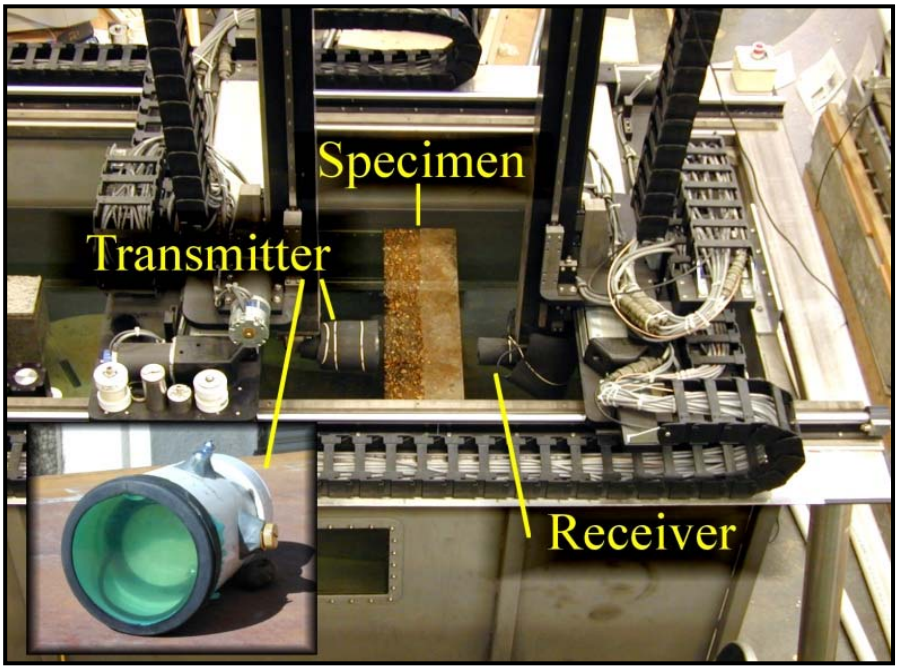

Figure 6.10. View of UTW specimen in ultrasonic immersion tTank.

Two different types of images were obtained with through-transmission measurements: one of the velocities through the material and one of the attenuation of the signals through the material. The velocity is calculated from measurements of time-of-arrival (TOA) data of the signal. The attenuation (signal strength) is calculated from measurements of voltage amplitude of the signal. Zero attenuation (signal strength) indicates a disbond; as long as UPV signal is passing through the thickness of the sample, there is no disbond (irrespective of signal strength which could decline due to material deterioration).

An initial image of velocity and attenuation were obtained on all specimens before subjecting the specimens to any environmental exposure. Figure 6.11 shows the velocity image on specimen D2 at zero F&T cycles; measured attenuations did not indicate a disbond as shown in Figure 6.12. Presence of a signal indicated that there was no air (disbond) between the AC and PCC and that signals were getting through.

Figure 6.11 through Figure 6.33 show scan results at various stages of F&T exposure testing. The interpretation of these scans indicated no change in the bond condition up to this point. A disbond developed between the layers of AC (at the lift interface) on Specimen C9 at 64 cycles. This failure is shown in Figure 6.34.

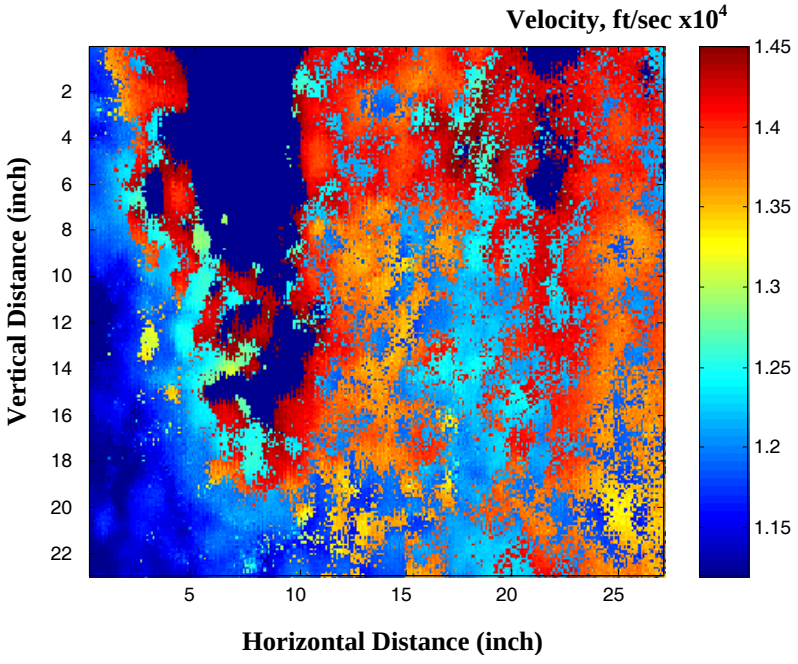

Figure 6.11. Velocity image on Specimen D2 at zero F&T cycles.

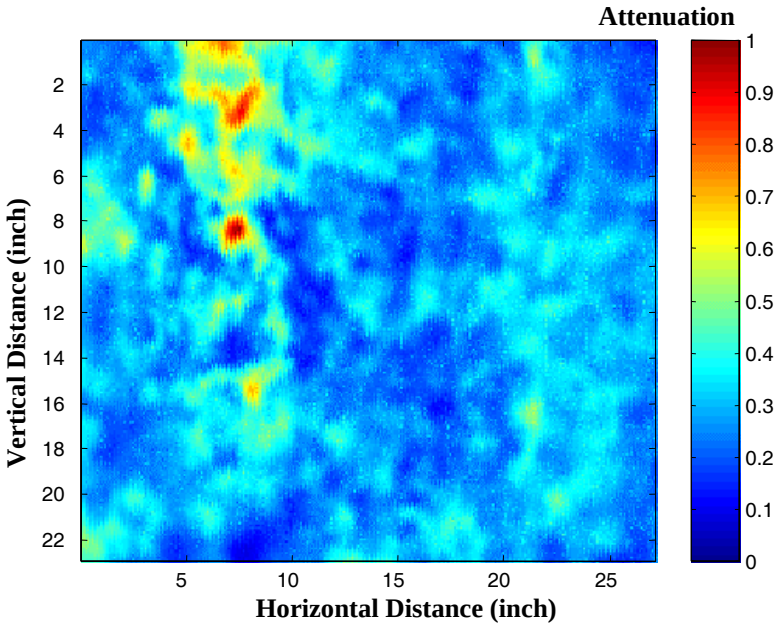

Figure 6.12. Attenuation image on Specimen D2 at zero F&T cycles (no disbond).

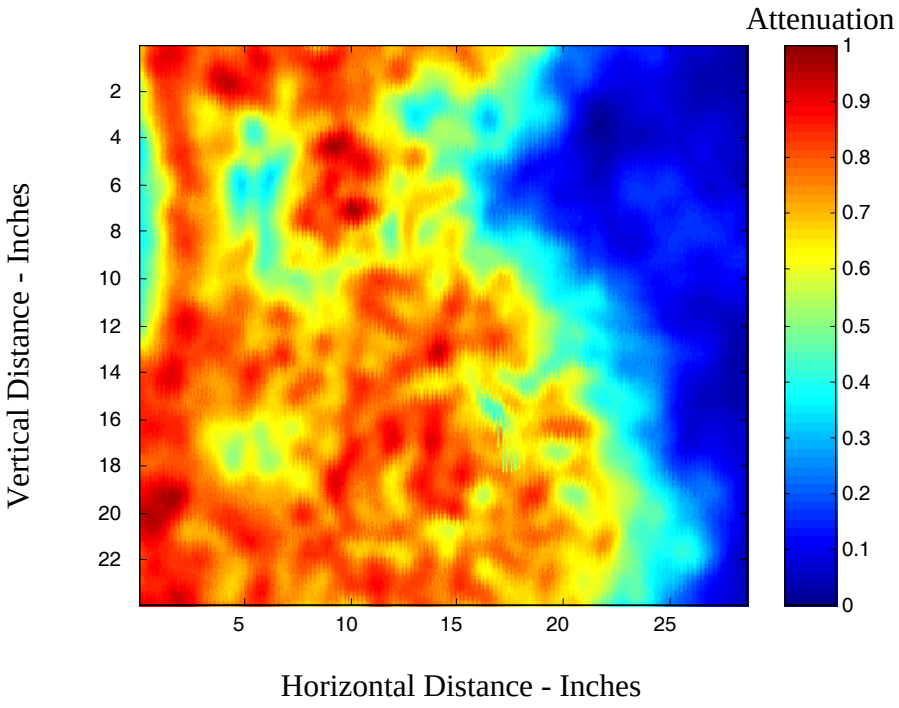

Figure 6.13. Attenuation image on F&T specimen D2 at 25 cycles.

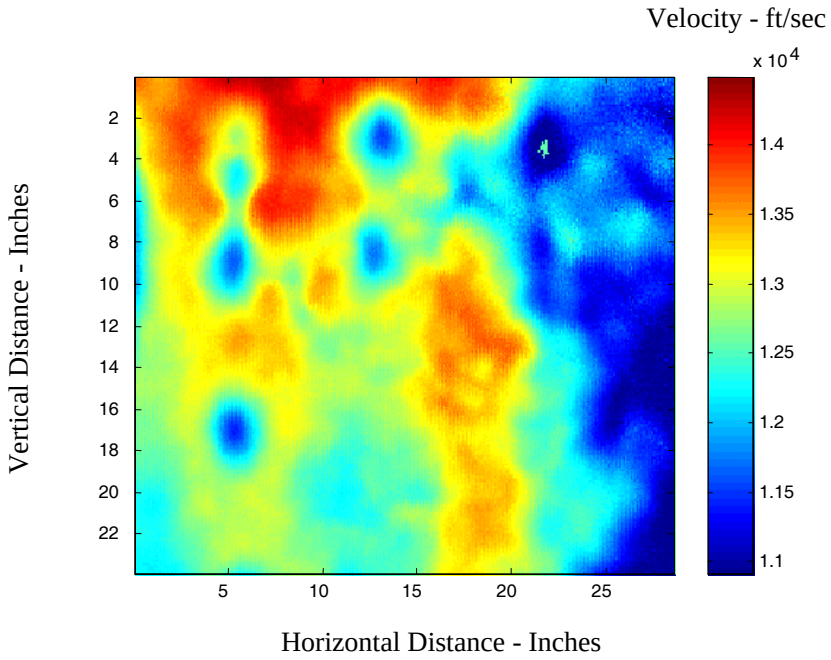

Figure 6.14. Velocity image on F&T specimen D2 at 25 cycles.

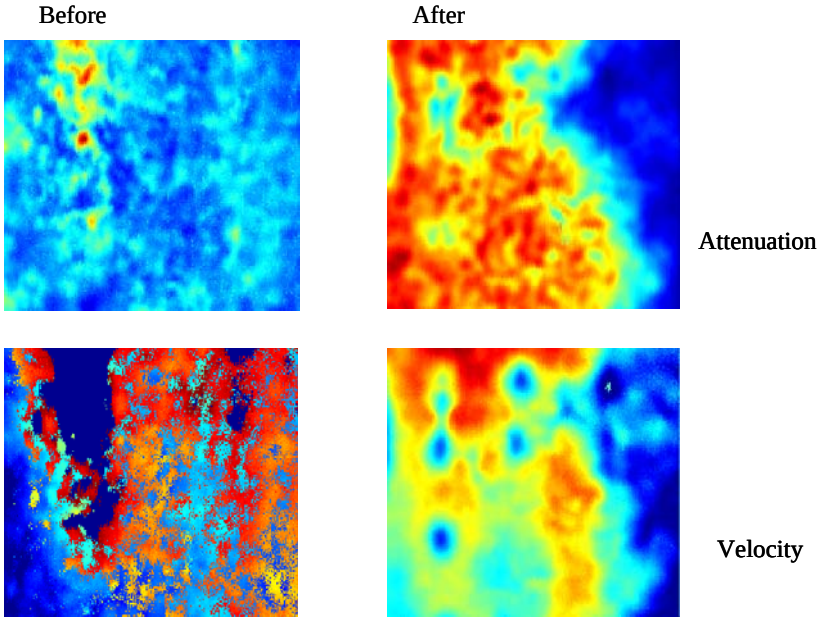

Figure 6.15. Attenuation and velocity images on F&T specimen D2 at 0 and 25 cycles.

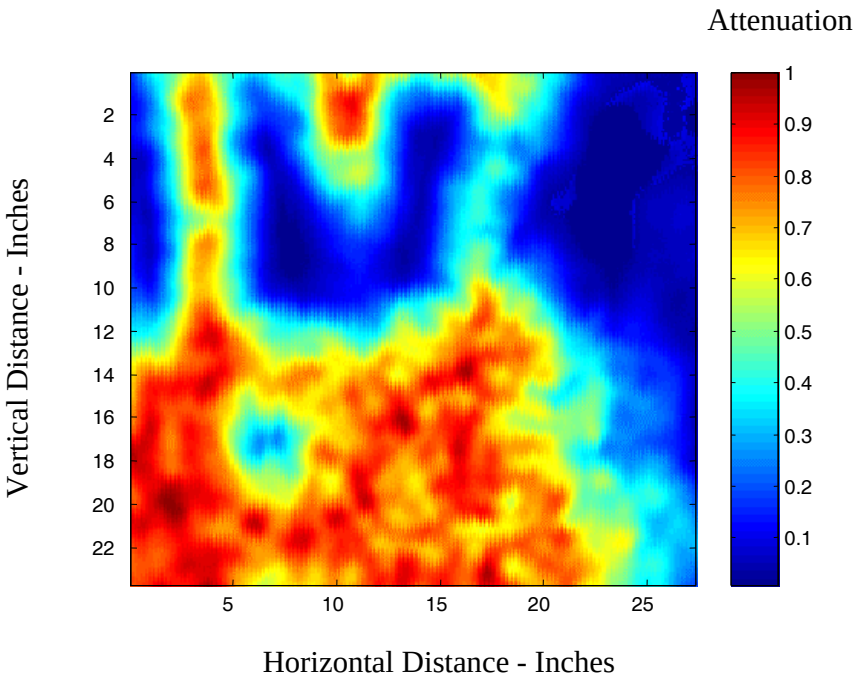

Figure 6.16. 37. Attenuation image on F&T specimen D2 at 50 cycles.

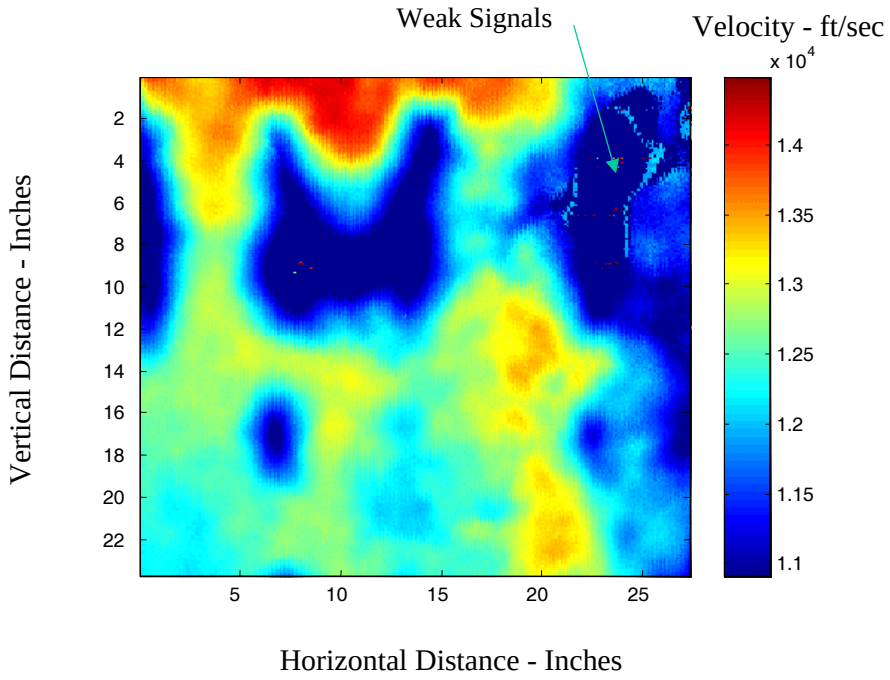

Figure 6.17. Velocity image on F&T specimen D2 at 50 cycles.

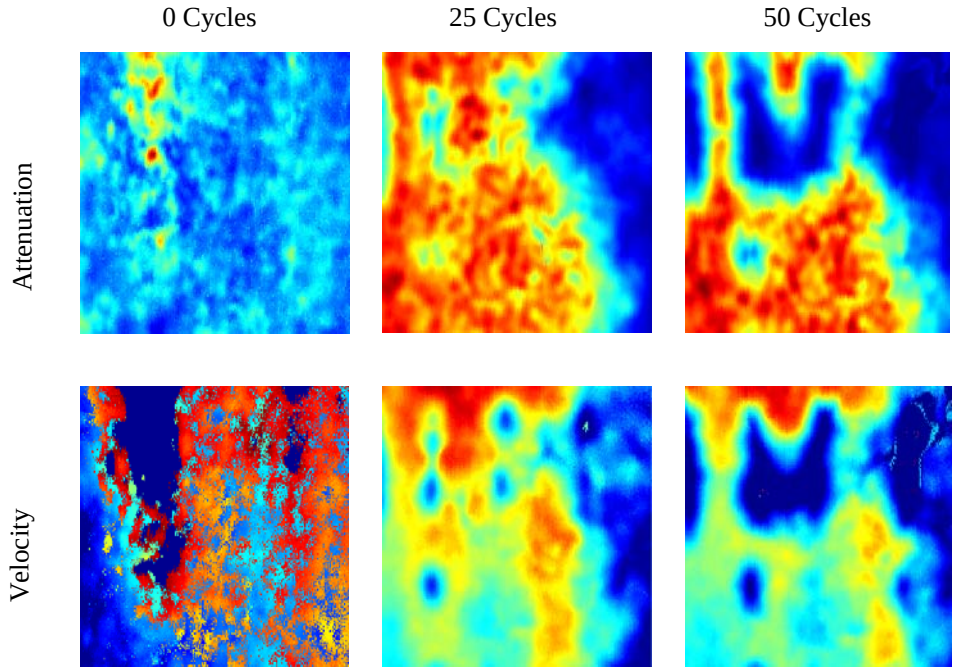

Figure 6.18. Attenuation and velocity image on F&T specimen D2 at 0, 25, and 50 cycles.

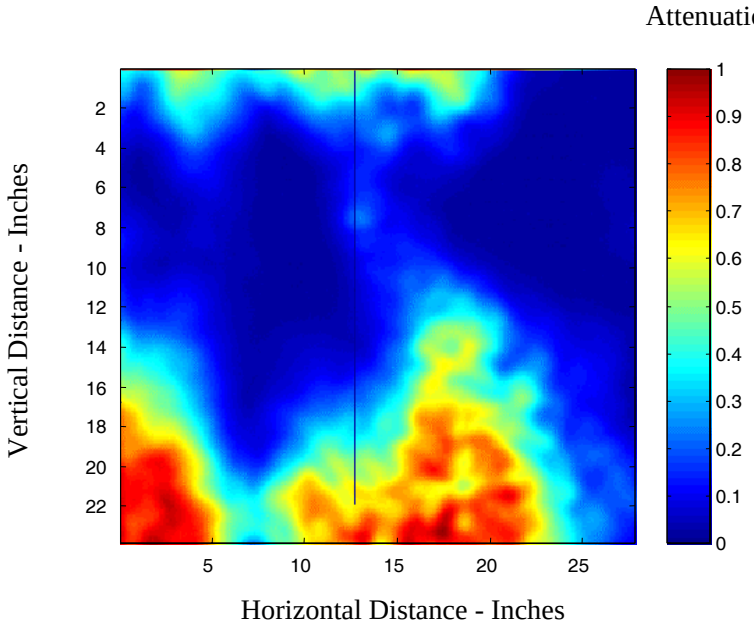

Figure 6.19. Attenuation image of F&T specimen D2 at 86 cycles.

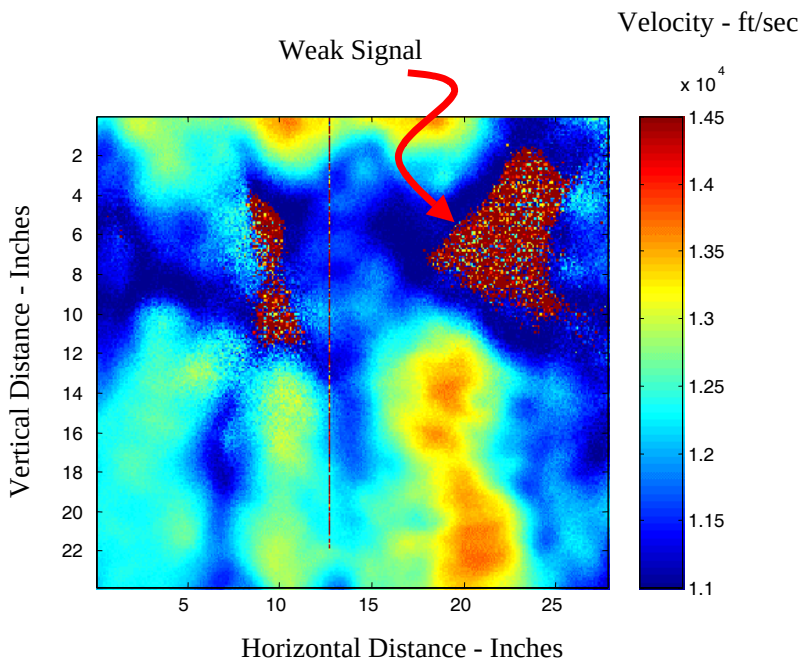

Figure 6.20. Velocity image of F&T specimen D2 at 86 cycles.

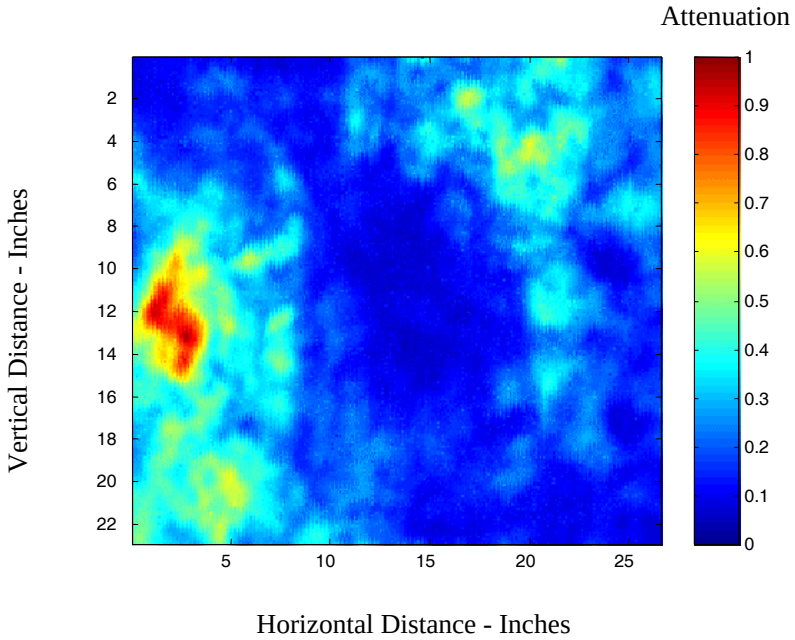

Figure 6.21. Attenuation image on F&T specimen D3 at 0 cycles.

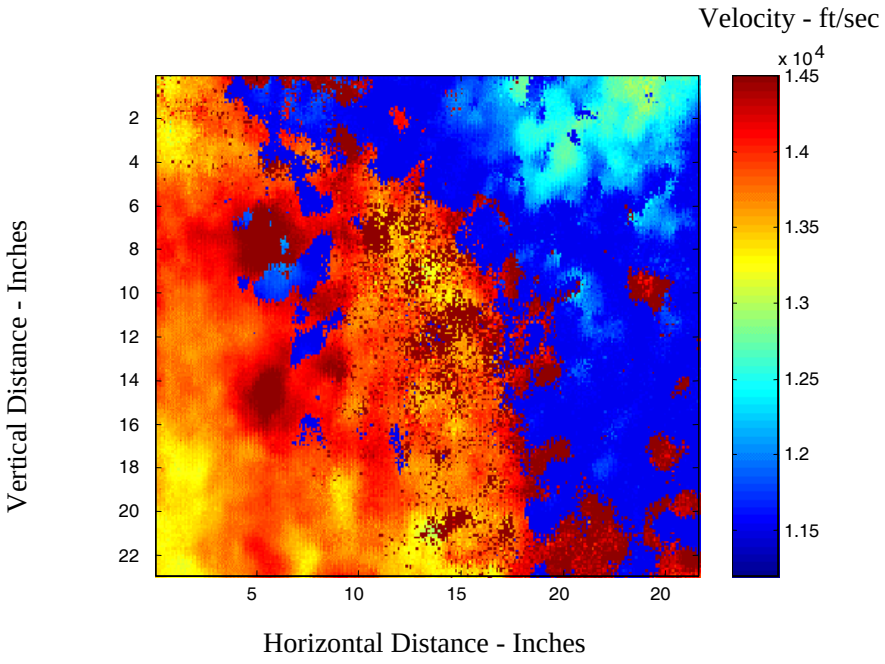

Figure 6.22. Velocity image on F&T specimen D3 at 0 cycles.

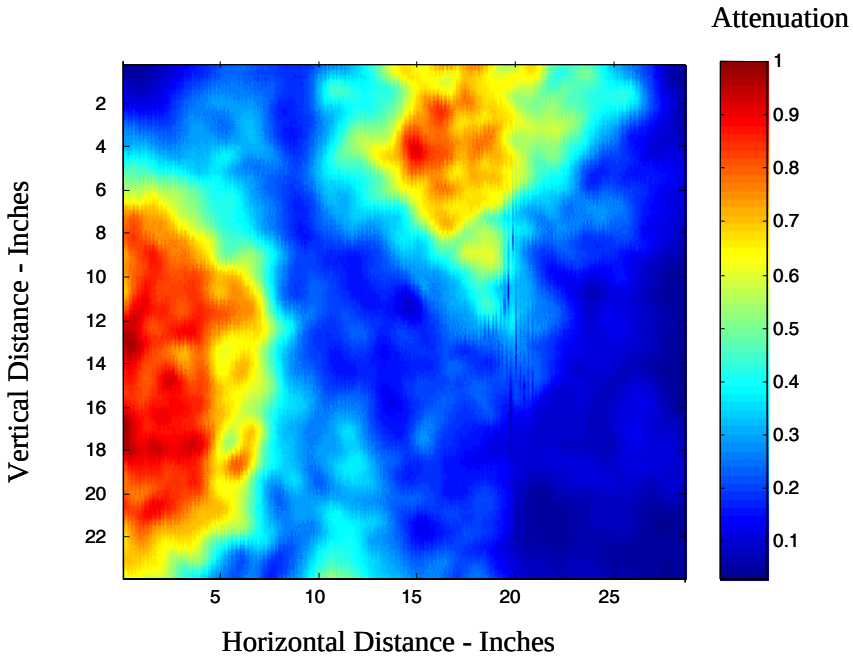

Figure 6.23. Attenuation image on F&T specimen D3 at 25 cycles.

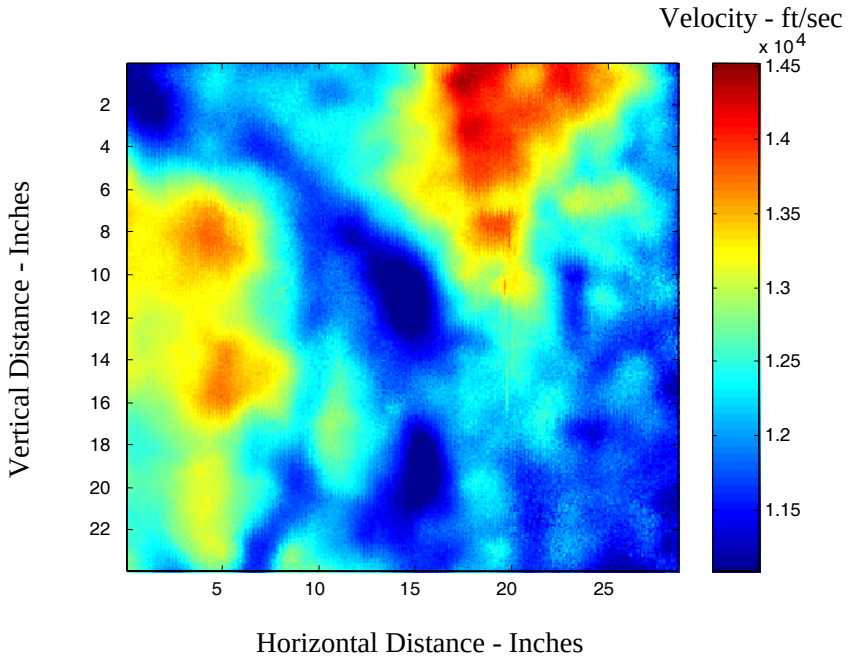

Figure 6.24. Velocity image on F&T specimen D3 at 25 cycles.

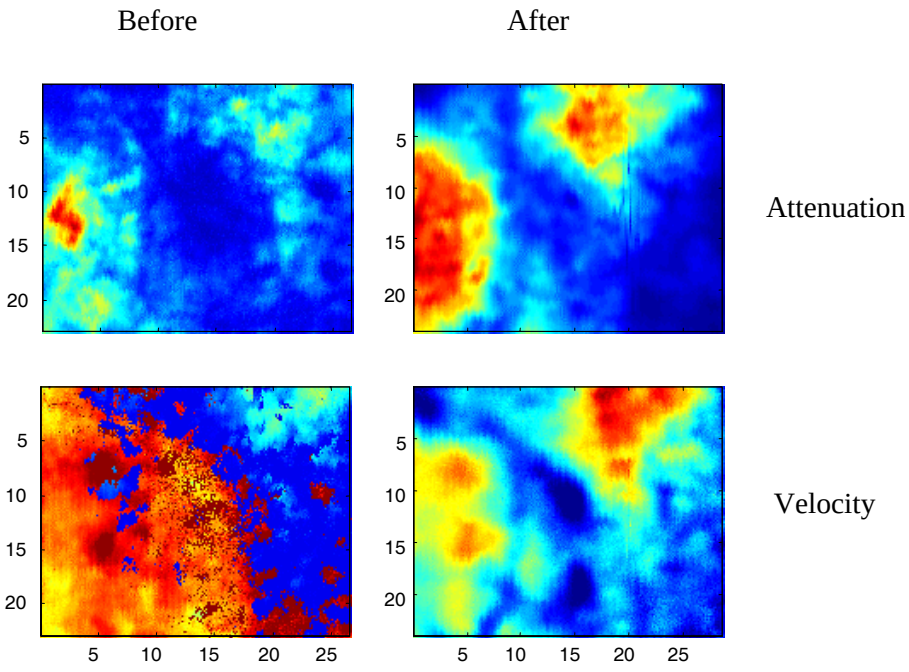

Figure 6.25. Attenuation and velocity image on F&T specimen D3 at 0 and 25 cycles.

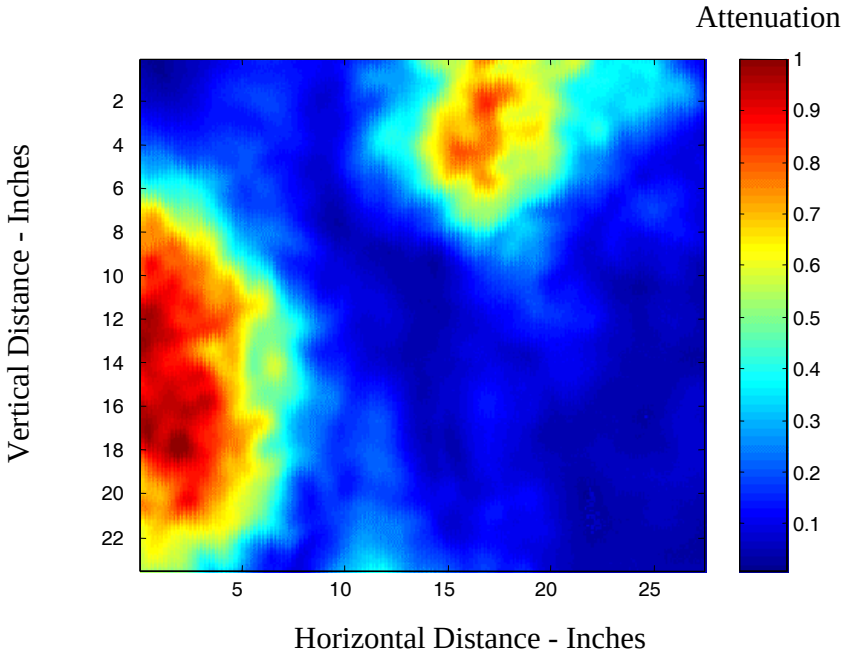

Figure 6.26. Attenuation image on F&T specimen D3 at 50 cycles.

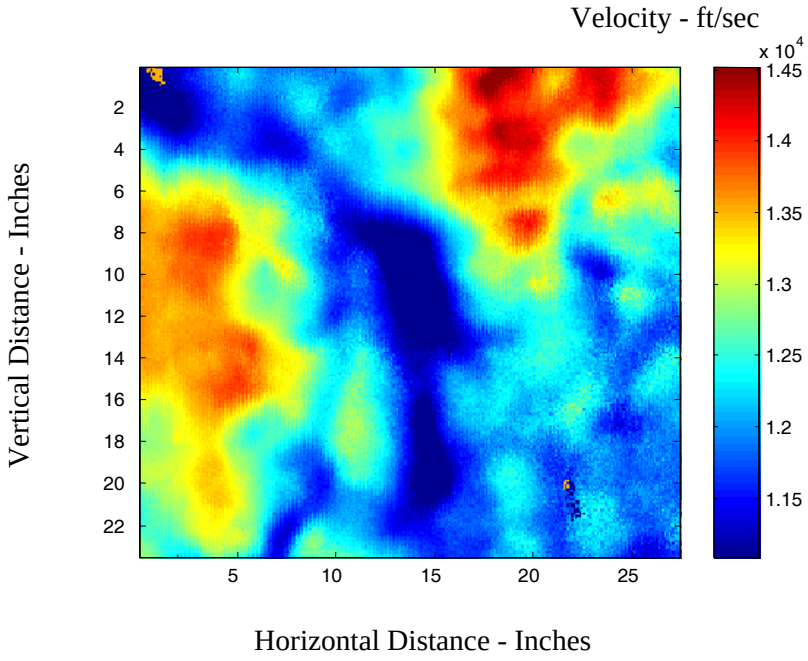

Figure 6.27. Velocity image on F&T specimen D3 at 50 cycles.

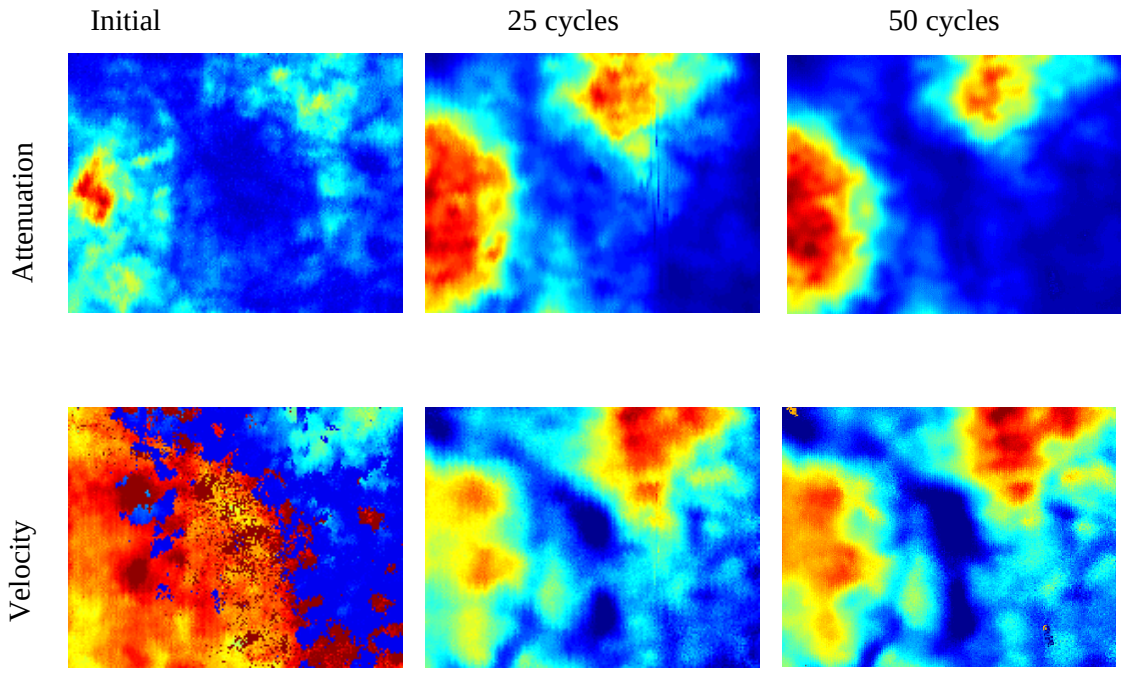

Figure 6.28. Attenuation and velocity images on F&T specimen D3 at 0, 25, and 50 cycles.

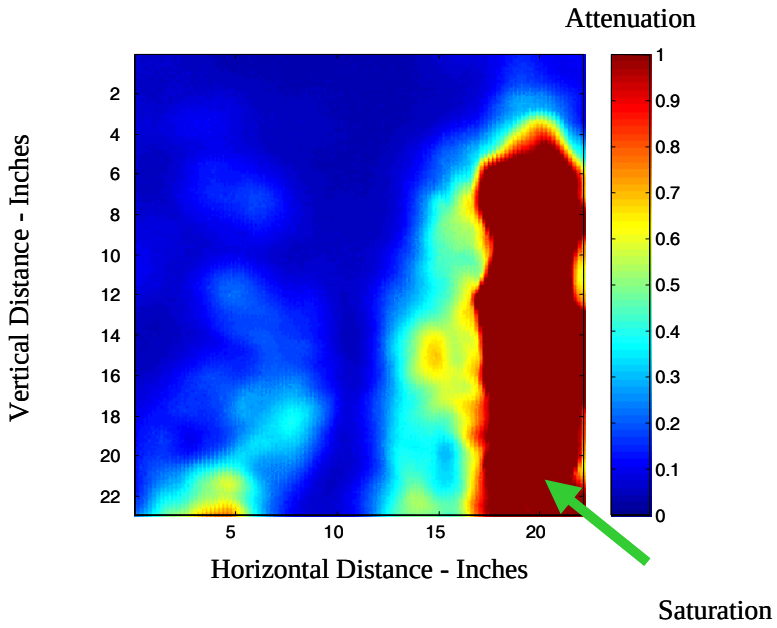

Figure 6.29. Attenuation image on F&T specimen C9 at 14 cycles.

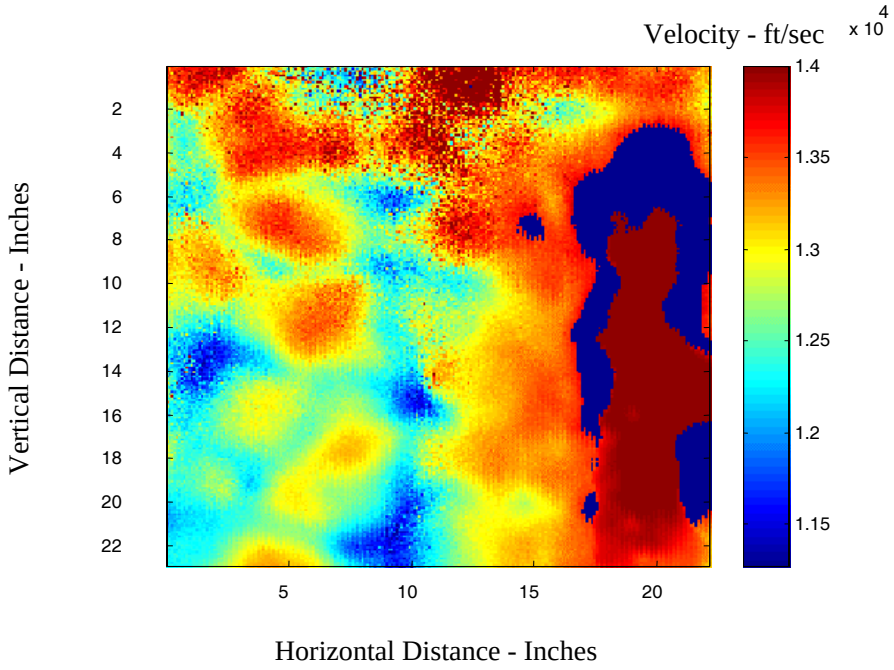

Figure 6.30. Velocity image on F&T specimen C9 at 14 cycles.

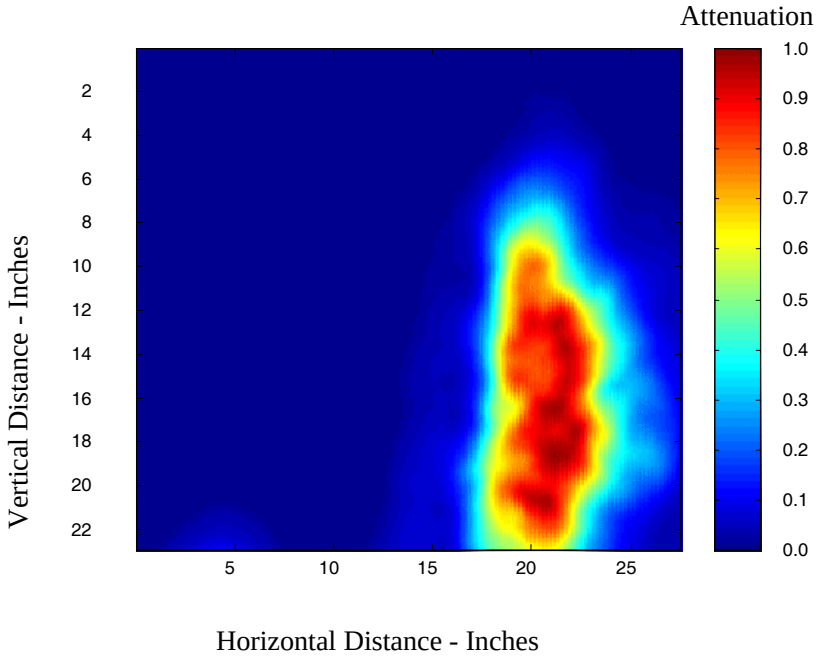

Figure 6.31. Attenuation image on F&T specimen C9 at 39 cycles.

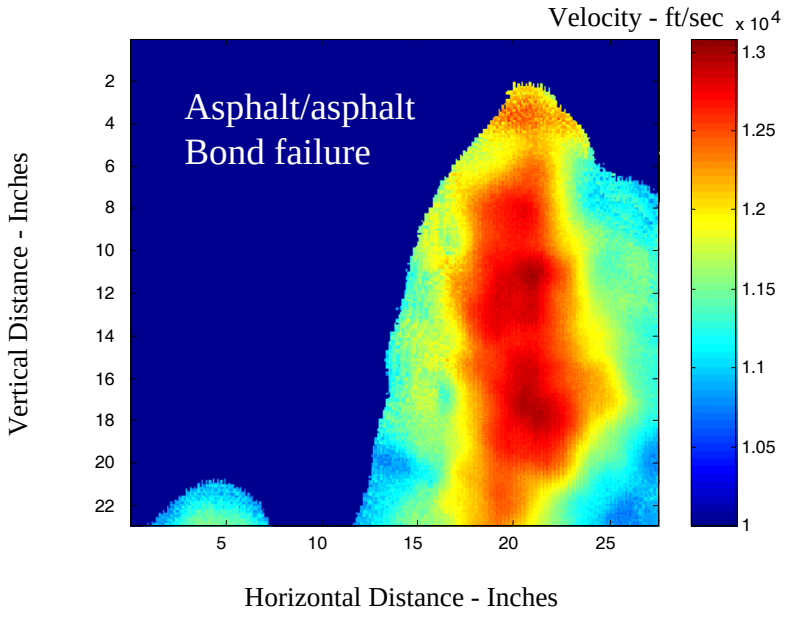

Figure 6.32. Velocity image on F&T specimen C9 at 39 cycles.

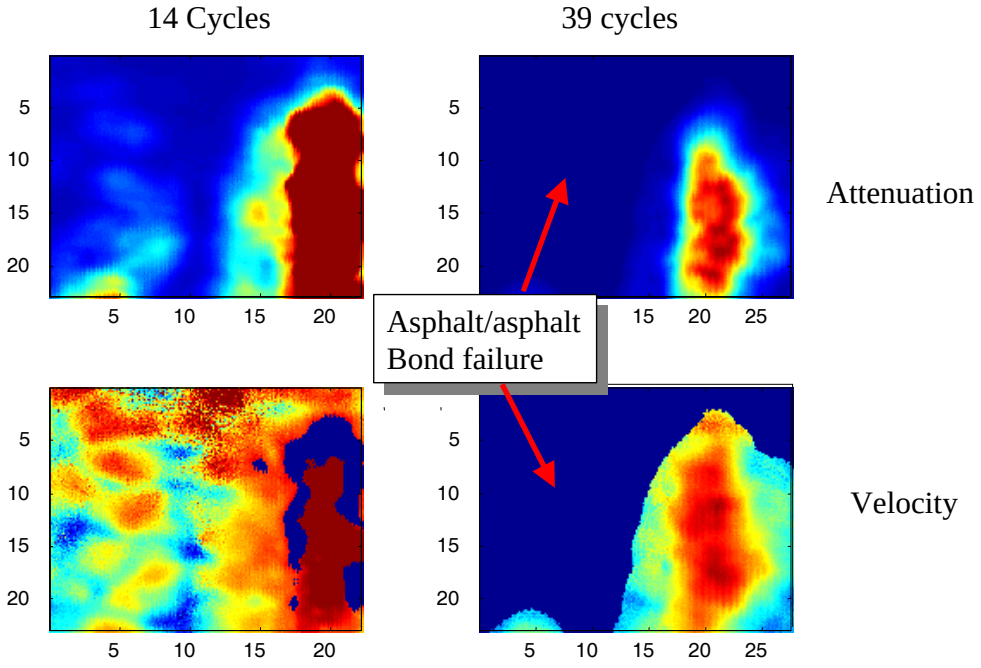

Figure 6.33. Attenuation and velocity images on F&T specimen C9 at 14 and 39 cycles showing delamination between two layers of asphalt.

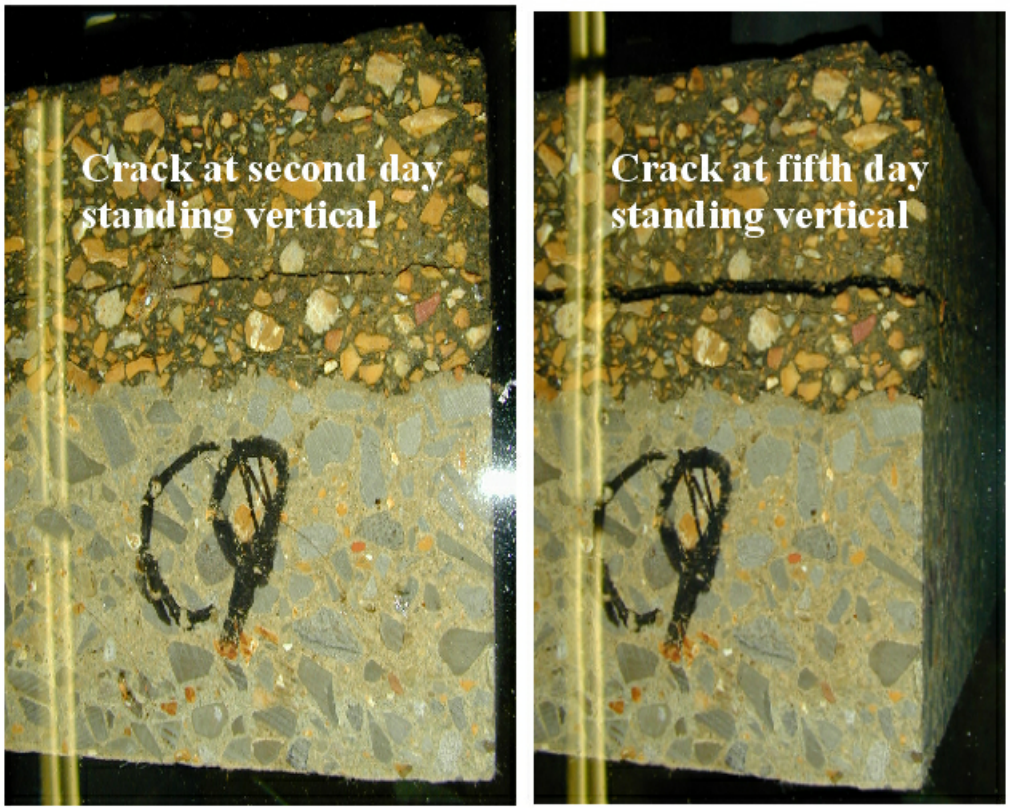

Figure 6.34. Delamination between asphalt layers on F&T specimen C9 at 64 cycles.

6.6.2. VELOCITY AND ATTENUATION SCANS

Figure 6.35 and Figure 6.36 show the attenuation and velocity images for specimen D2 at 86 F&T cycles, respectively.

No disbonds were detected between the PCC and AC for any specimen in either the F&T test or the W&D test; thus, no attempt is made to describe every image since no disbond occurred between the AC and PCC. C9 is the only specimen that had a disbond but it was an AC-to-AC disbond (the AC was comprised of two lifts) rather than a PCC-to-AC disbond. A dark violet color of the image represents the area of disbond as shown in Figure 6.37.

Since the complete range of colors from red to violet can be spread over any range of velocities or attenuations, it is difficult to interpret images unless someone is trained to read them. However, the red color represents the higher velocity while the violet color represents the lowest velocity. Generally, a disbond will be recognized by a complete loss of signal. That is, the signal level is below the level of noise and cannot be detected. A gap containing air will transmit less energy across the disbond than a gap filled with water.

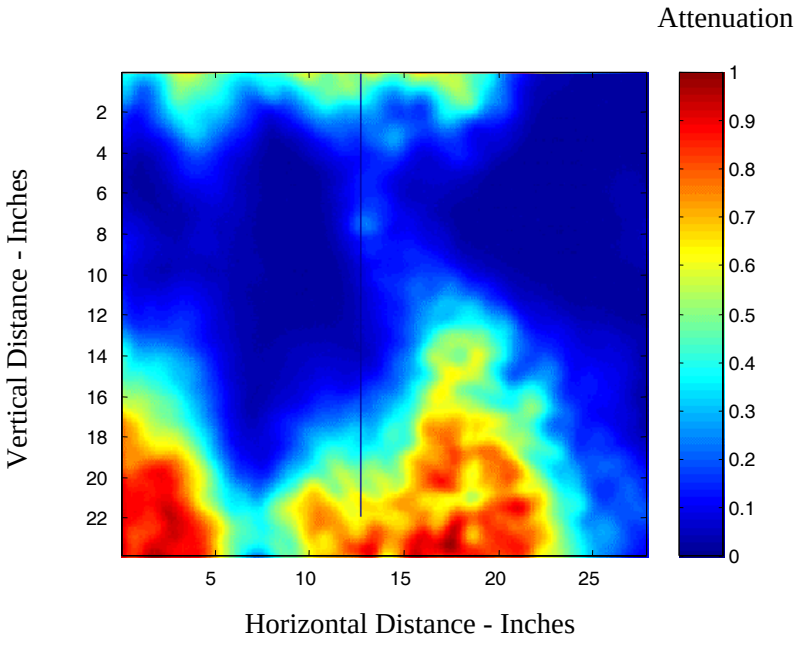

Figure 6.35. Attenuation image of specimen D2 at 86 F&T cycles.

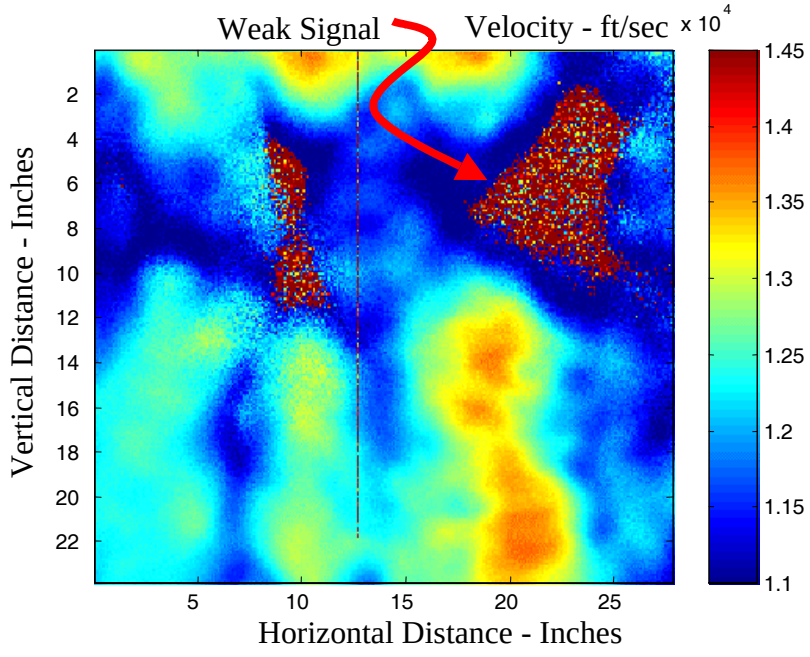

Figure 6.36. Velocity image of specimen D2 at 86 F&T cycles.

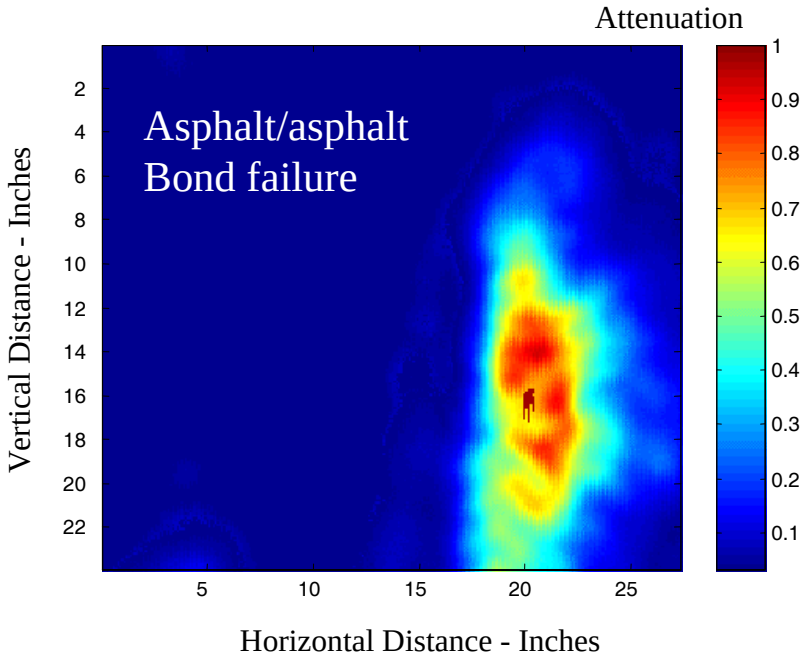

Figure 6.37. Attenuation image on F&T specimen C9 at 64 F&T cycles.

The F&T exposure tests were stopped at 105 F&T cycles; it was not possible to get images of these specimens for that number of cycles. The concrete material has deteriorated to such an extent that it was not possible for the ultrasonic energy from the USUMS transducer to penetrate the thickness of the PCC/AC specimens. In addition, the W&D exposure specimens were taken to 200 cycles. No images were made of these either because the USUMS system had experienced a breakdown. However, V-meter readings made through the thickness of the specimens verified that no disbonds had occurred either in the F&T or W&D specimens.

6.6.3. THICKNESS-VELOCITY RESULTS

Table 6.2 gives statistics (minimum, maximum, mean, and standard deviation) for the data collected from the thickness-velocity scans. The statistics were used as an aid to determine whether material deterioration and/or bond deterioration was occurring. The statistics are based on a large number of measurements as a complete scan of a specimen consist of about 14,400 readings. All 14,400 individual signals, or A-scans, were used in the calculation of the mean and standard deviation (STD).

Table 6.2. Statistics on velocity scans on F&T exposure specimens.

Specimen Identification	Number of Cycles	Velocity (ft/sec)			
		Mean	Min	Max	Standard Deviation
D2	0	12789	11200	14500	974
D2	25	12655	10910	14480	428
D2	50	12089	9723	14200	--
D2	86	12086	10736	15039	--
D3	0	13008	11200	14500	916
D3	25	12416	11085	14517	581
D3	50	12467	10195	14656	694
C9	14	12940	11270	14000	253

The standard deviation results were inconclusive, while other statistics indicated that deterioration was taking place. For example, velocity images taken for cycle numbers 0, 25, 50, and 86 of F&T specimen D2 indicated that some deterioration was taking place. The image for F&T specimen D2 for zero cycles had a speckled look (see Figure 6.38). It was later determined, after the specimen had been restored to the specimen tank, that the pulser was misadjusted and was introducing two closely spaced excitation pulses to the ultrasonic transmitting transducer instead of one. The two pulses were separated by a short time, causing errors with the TOA measurements. This double excitation pulse caused the velocity calculations from adjacent areas on the specimen to jump from one discrete value to another discrete value with a jump greater than what would be normal between two adjacent areas of the specimen. This caused the standard deviation statistics for specimen D2 for zero cycles to be higher than the true condition.

The standard deviation measured 974 ft/sec, as shown in Table 6.2, which was higher than what later measurements showed. Since the TOA data were jumping between larger discrete values than was normal, it created highly dispersed data. For the 25^{th} cycle, the standard deviation of 428 ft/sec was probably correct. Then the standard deviation was incorrect again on the 50^{th} and 86^{th} cycles because of a region in the specimen that produced weak signals. The region is shown in the upper right hand portion of the image in Figure 6.39.

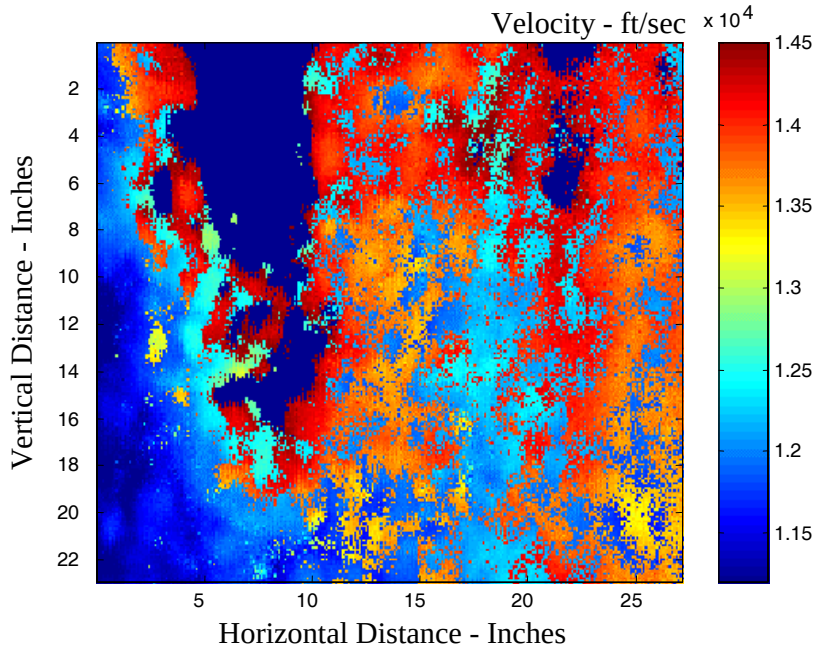

Figure 6.38. Velocity image on F&T specimen D2 at zero F&T cycles.

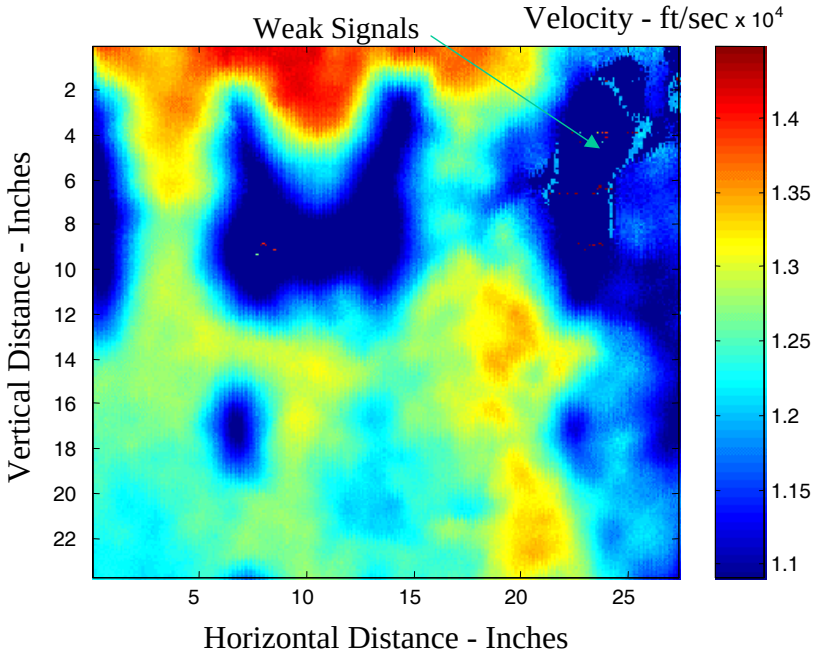

Figure 6.39. Velocity image on F&T specimen D2 at 50 cycles.

6.6.4. MEAN VELOCITY RESULTS

The region of weak signals, shown in Figure 6.39, caused the calculation of the mean velocity to be higher than the true mean velocity since the peaks could not be detected and, consequently, there were no velocity values for that section of the specimen. As there were no velocities calculated for the weak signals, a velocity equal to the lowest velocity measured for the specimen was assigned to each signal to reduce the errors in the statistical calculation. Of course, this causes the calculation of the mean velocity to be higher than the true value. The other option was not to include any of the weak signals in the statistical calculations, but this option would also have created a mean velocity higher than the true condition.

Since the true mean velocity would have been lower than the mean velocity calculated from the assigned velocities, the mean velocity was weighted toward the high side. It was not possible to calculate the true mean velocity since the dynamic range of the data fell outside the dynamic range of the measurement system. The true mean velocity was dropping since the dynamic range of the data was falling below the dynamic range of the measurement equipment.

The calculated mean velocity of F&T specimen D2 dropped from 12,789 ft/sec to 12,086 ft/sec, or 5.5 percent, after 86 cycles of exposure using the calculated values. The percentage drop in velocity was conservative because it consisted of numerous assigned velocities equal to the lowest value detectable. The point to be made is that deterioration was taking place in the materials of F&T specimen D2.

The velocity of F&T specimen D3 also dropped, at a minimum, from 13,008 ft/sec to 12,467 ft/sec, or 4.2 percent, after 50 cycles of F&T exposure. After 105 F&T exposure cycles, the deterioration in specimen D2 prevented penetration by the transducers of the USUMS.

Thickness-velocity measurements made in the air (dry condition) using the V-meter verified that the mean velocity of specimen D3 actually fell by a large percentage, although it could not be measured with the USUMS. The V-meter determined that the mean velocity of specimen D3 dropped to a value of 10,600 ft/sec. That represents a drop of velocity of 18.5 percent, which corresponds to significant deterioration in the specimen. In addition, it is possible that the thickness-velocity measurements did not register a larger drop in value for both F&T specimens D2 and D3 because the specimens were becoming increasingly saturated with moisture and the mean velocity was on the rise (velocities are somewhat higher in moist concrete than in dry concrete). The air voids in the PCC and AC become filled with water permitting the ultrasonic wave to take a shorter and faster path through the PCC/AC yielding a higher velocity for the composite specimen.

Since the USUMS was not capable of penetrating the deteriorated concrete, it was not possible to measure the scatter (standard deviation). The scatter should have been greater at this stage than earlier cycles.

6.7. W&D EXPOSURE TESTING AND RESULTS

Figure 6.40 through Figure 6.52 present USUMS scan data on specimens D6 and D12 as they were subjected to the W&D exposure tests. There was no measurable change in the mean velocity and standard deviation of W&D specimens D6 and D12. After 200 cycles of W&D exposure, V-meter velocity readings through the thickness of specimen D6 revealed that the velocity was still high, at a mean velocity of 12,398 ft/sec (3,779 m/sec). The initial thickness-velocity was measured to be 13,560 ft/sec (4,133 m/sec) as shown in Table 6.3. That represented an 8.6 percent drop in mean velocity, which indicated that some deterioration of the materials was beginning to occur. However, no signals were blocked or missing, indicating no apparent disbonding.

Table 6.3. Statistics on velocity scans on W&D exposure specimens.

Specimen Identification	Number of Cycles	Velocity (ft/sec)			
		Mean	Min	Max	Standard Deviation
D6	0	13560	11896	15290	392
D6	60	13549	12550	14670	253
D12	0	12538	11016	13900	330
D12	90	12554	10700	14000	274
D12	175	12560	11100	13885	270

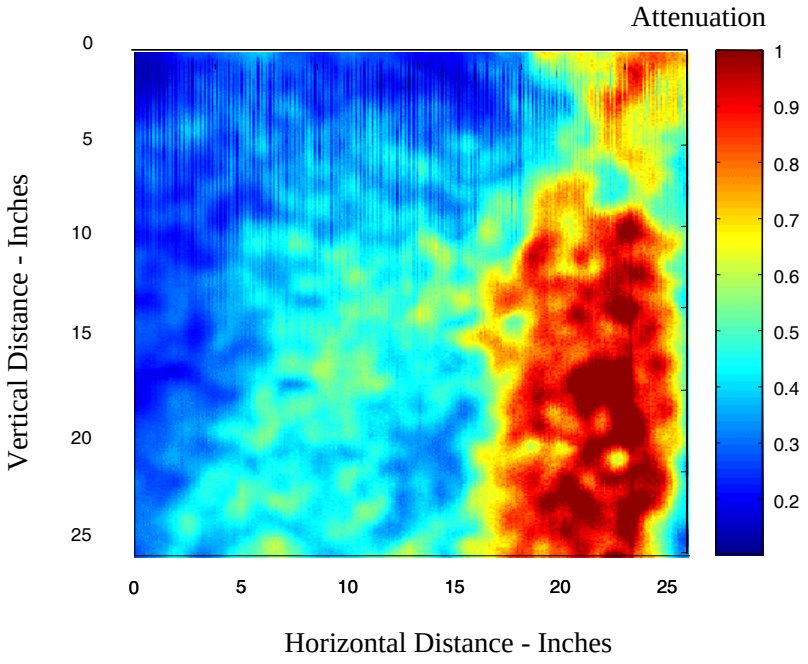

Figure 6.40. Attenuation image on W&D specimen D6 at 0 cycles.

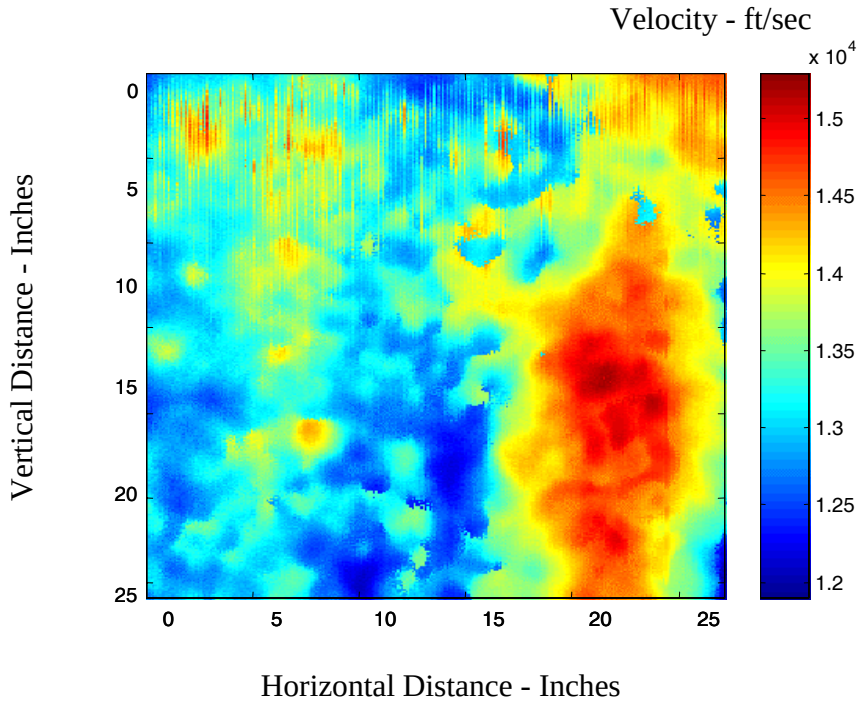

Figure 6.41. Velocity image on W&D specimen D6 at 0 cycles.

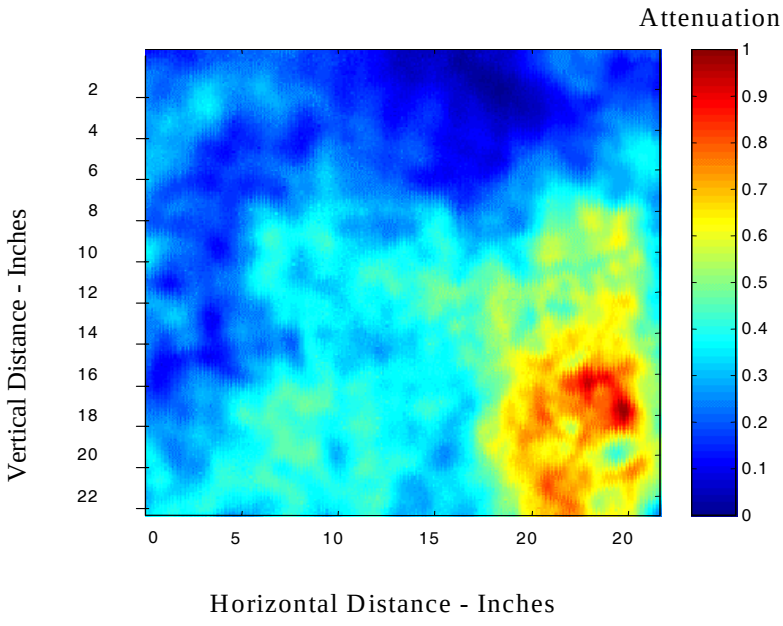

Figure 6.42. Attenuation image on W&D specimen D6 at 60 cycles.

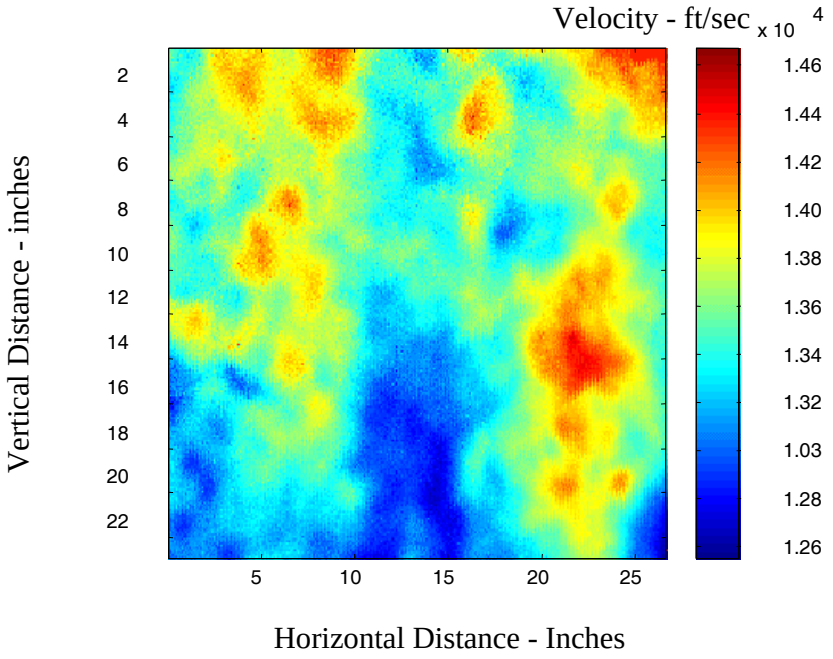

Figure 6.43. Velocity image on W&D specimen D6 at 60 cycles.

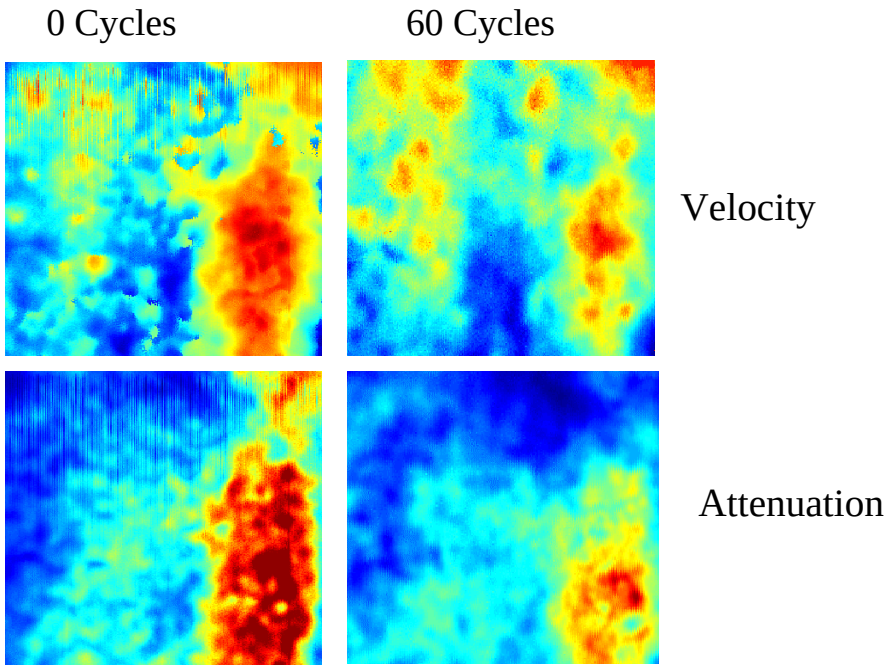

Figure 6.44. Attenuation and velocity image on W&D specimen D6 at 0 and 60 cycles.

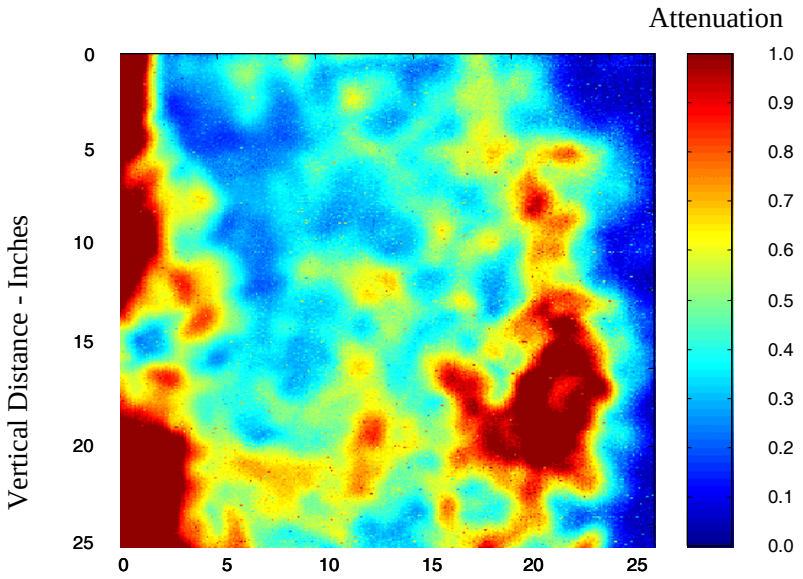

Figure 6.45. Attenuation image on W&D specimen D12 at 0 cycles.

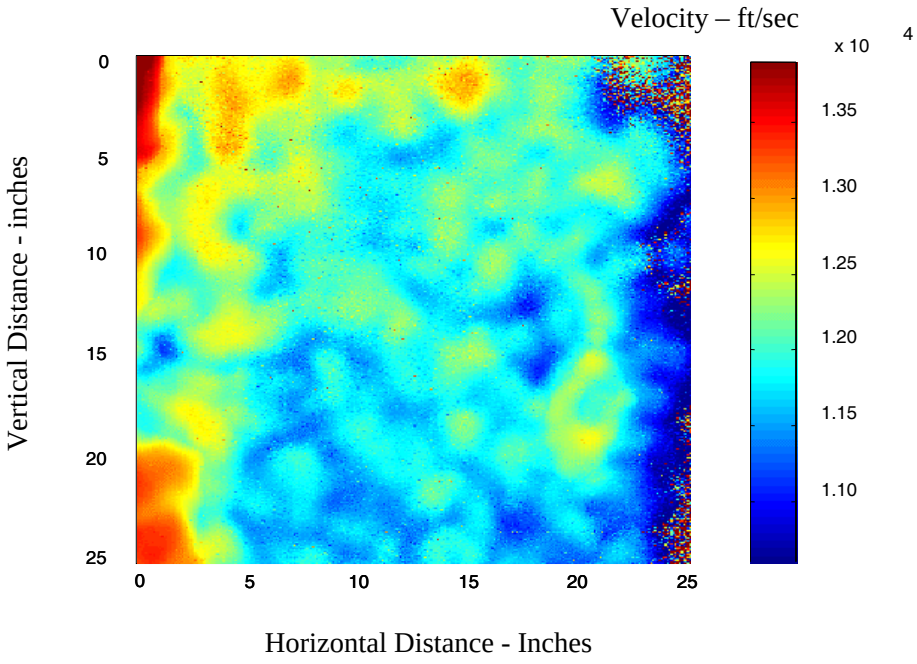

Figure 6.46. Velocity image on W&D specimen D12 at 0 cycles.

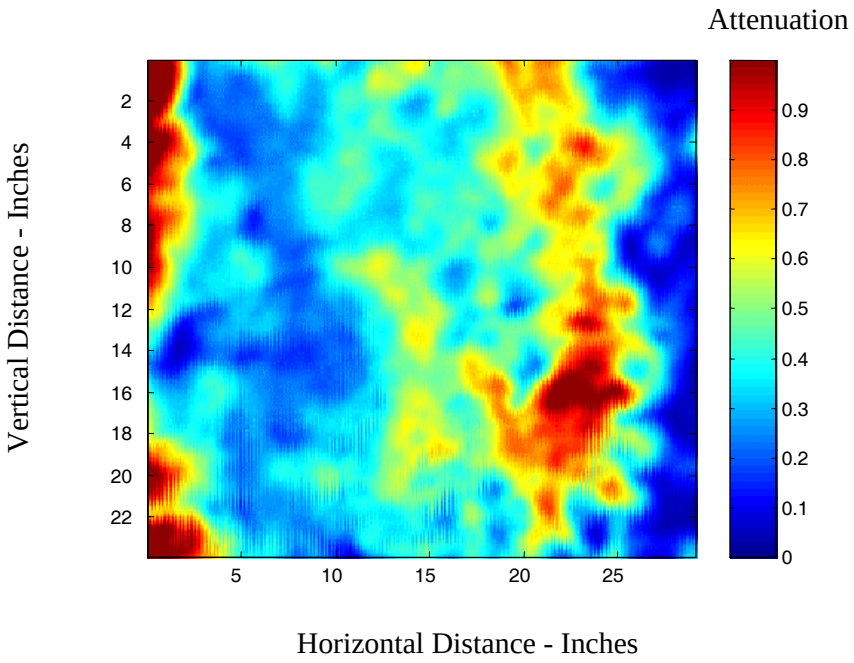

Figure 6.47. Attenuation image on W&D specimen D12 at 90 cycles.

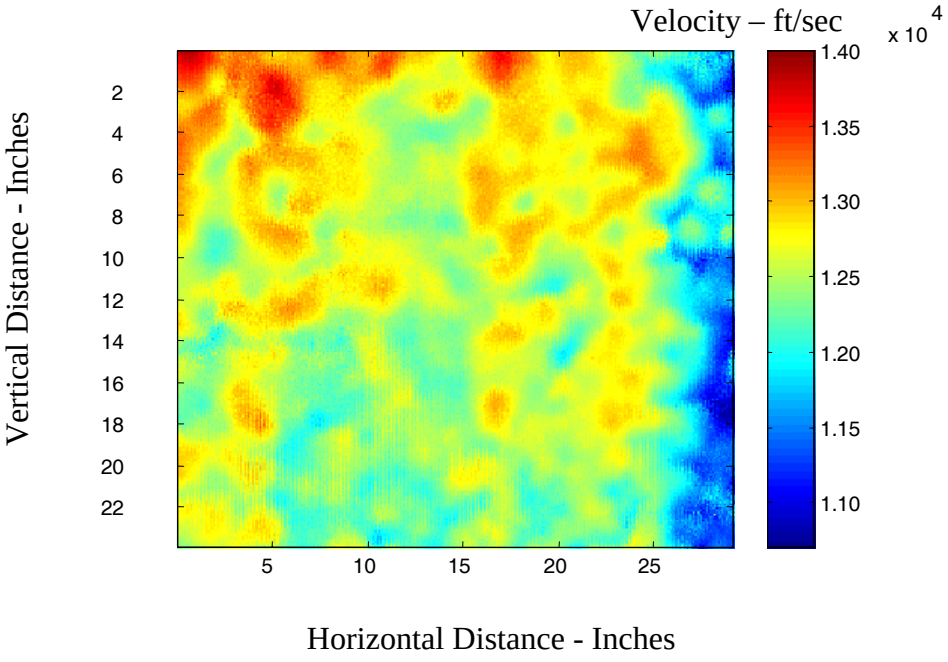

Figure 6.48. Velocity image on W&D specimen D12 at 90 cycles.

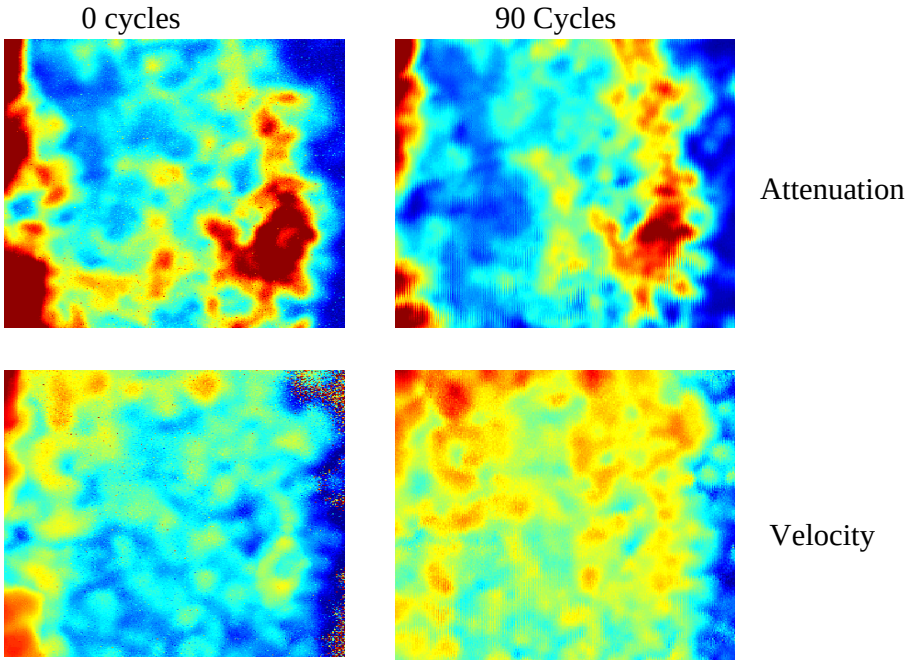

Figure 6.49. Attenuation and velocity images on W&D specimen D12 at 0 and 90 cycles.

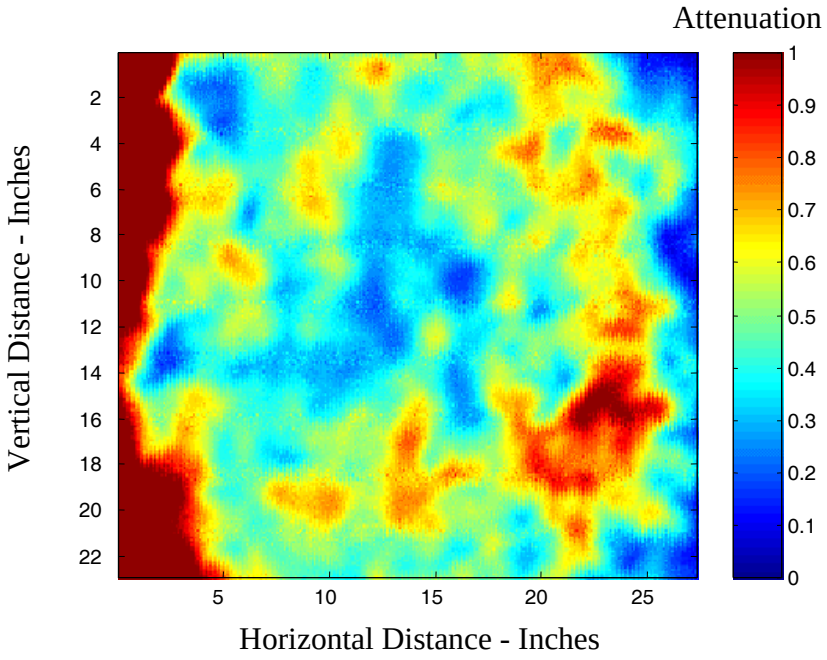

Figure 6.50. Attenuation image on W&D specimen D12 at 175 cycles.

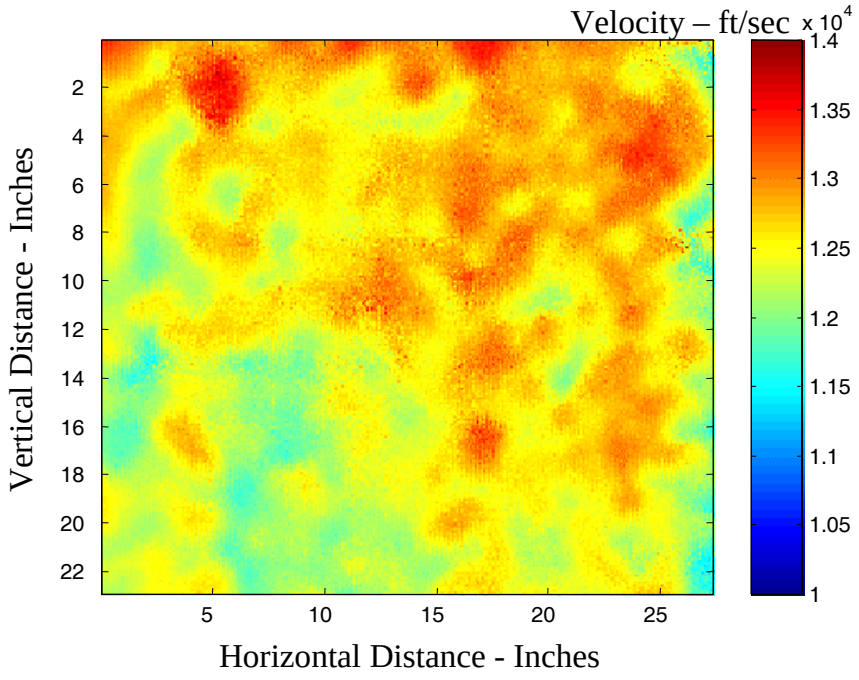

Figure 6.51. Velocity image on W&D specimen D12 at 175 cycles.

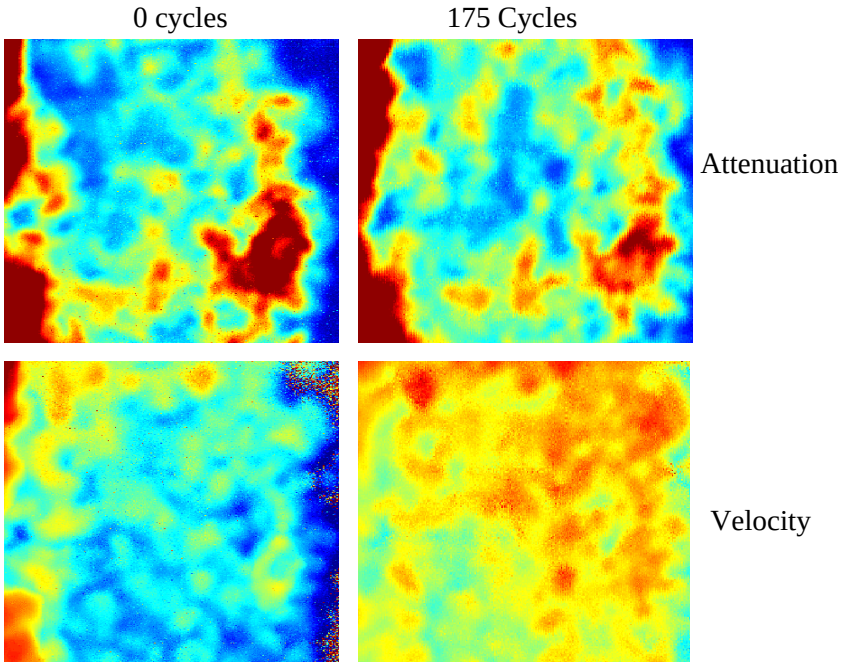

Figure 6.52. Attenuation and velocity images on W&D specimen D12 at 0 and 175 cycles.

6.8. DISCUSSION OF MEASUREMENT TO DETERMINE BOND INTEGRITY

Deterioration in the materials causes weak signals to arrive at the receiving transducer. Disbonds create weaker and missing signals. Weak signals and missing signals cause the calculation of the statistical parameters for the mean, maximum, and minimum velocity and for the STD for velocity scans to contain some error. This is because the data fall outside the dynamic range of the measurement equipment. When the dynamic range of the data is less than or equal to the dynamic range of the measurement system and the range of voltages for both coincide, the statistics are accurate.

Dynamic range in a system or device is the ratio of the specified maximum level of a parameter (power, current, voltage, or frequency) to the minimum detectable value of that parameter. Dynamic range is usually expressed in dB or in terms of a simple ratio. Voltage is the parameter of interest for this discussion.

Measurement systems vary in the size of their dynamic ranges; however, the dynamic range is constant for a given system. For example, a measurement system has a dynamic range of 20 decibels (10X) would be able to handle a data range from 1 to 10 times a given minimum voltage. Usually, the minimum value is the level of noise and no signals can be detected below that level. This means that if the measurement scale of the system is set to handle a maximum voltage of 100 millivolts, the minimum voltage it can detect is 10 millivolts for a dynamic range of 10X. Alternatively, if the system is scaled to handle a voltage of 10 volts, then the minimum voltage of detection is 1 volt. As long as the dynamic range of the data (ratio of highest voltage to lowest voltage) is no greater than 10X, then a dynamic range of 10X for the measurement equipment will measure the data correctly when the two ranges coincide for the lowest and highest voltage.

The digitizer of the measurement system can also affect the capability of the system to detect peaks in addition to the dynamic range of the system when the signal amplitude is low. In fact, it may limit the detection of signals even when the dynamic range of the data coincides with or falls within the dynamic range of the measurement system. The USUMS digitizer has a capacity of 8 bits, and it can uniformly divide the dynamic range of the measurement system into 2^8, or 256, pieces.

6.8.1. ANALYSIS OF VELOCITY DATA

6.8.1.1. Detection of Material Deterioration

Velocities will lie in a narrow range of values before any deterioration occurs in the specimen. That is, the data initially have a narrow dynamic range. In that situation, the dynamic range of the data will easily fall within the dynamic range of the measurement system and all signals can be detected. A lower velocity implies deterioration has occurred. The USUMS has been scaled to measure data whose amplitudes vary from 1 volt to 10 volts; the maximum voltage is equal to 10 times (10X) the minimum voltage. The amplitude of the

measurement scale is maintained constant during a complete scan of a specimen. If the PCC/AC specimen remains bonded and the materials have not experienced deterioration, then all signal amplitudes fall within that same dynamic range of 1 volt to 10 volts. Figure 6.53(a) illustrates the two conditions for all signals to be detected.

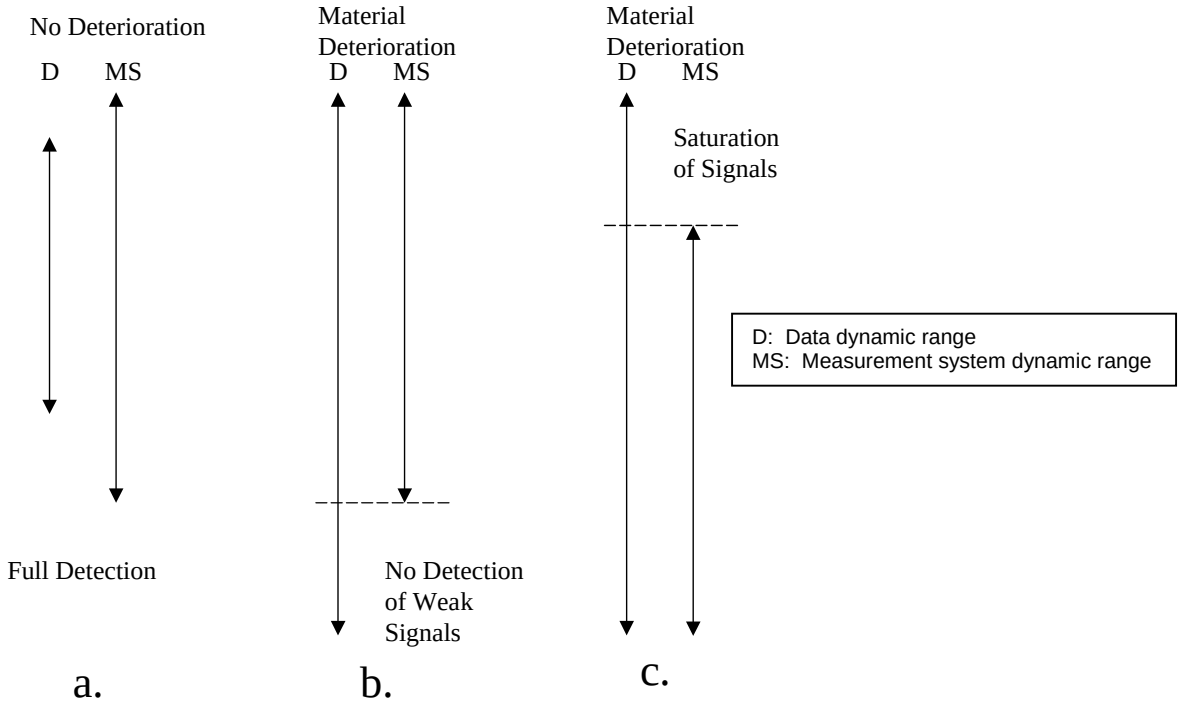

Figure 6.53. Relationship of data and measurement system dynamic ranges for material.

The dynamic range of the data must fall within the dynamic range of the measurement system for full detection. In addition, the maximum voltage of the data must be equal to or less than the maximum detectable voltage of the measurement system, and the minimum voltage from the data must be equal to or greater than the minimum voltage detectable from the measurement system.

As an example, assume that material deterioration occurs and suddenly the weaker signals from the data in the deteriorated area (that once had a voltage above 1 volt) now fall below 1 volt. The data now have a larger dynamic range than the measurement equipment as shown in Figure 6.53(b). The system can no longer detect the peaks, and some of the signals now have a voltage below the detectable range of the measurement system.

The measurement system can be rescaled to accept a lower voltage range; the scale can be made more sensitive for weak signals by increasing the gain of the receiving amplifier and/or increasing the pulser voltage for the transmitter. Increasing the sensitivity of the scale gives the weak signals sufficient amplitude for the automatic detection system to detect the weak

signals and to record the time of arrival (TOA), as shown in Figure 6.53(c). Increasing sensitivity of the scale does not change the dynamic range of 10X for the measurement system but it does shift the measurement scale to a range that permits the voltages of the weak signals to be detected and measured. Any data with signal peaks that fall above 0.1 volt (100 millivolts) and below 1 volt can be detected; the maximum voltage is still 10 times (10X) the minimum voltage of 0.1 volt. Now the amplitude peaks from weaker signals that arrive from the deteriorated area can be detected. However, improving the detection of the signals from the area of material deterioration results in a trade-off as the signals on the higher side are now saturated.

The dynamic range of the signals in the low-quality areas and high-quality areas could have been increased to a ratio of greater than 10X. Since the amplifier of the measurement system saturates at 1 volt (maximum value that amplifier is able to output), there could be hundreds of signals from the higher quality area that would fall in the range of 1 volt to 10 volts, but they would all get converted to 1 volt. Now the image would be distorted in the portion of the image from the signals that come from the higher quality area of the specimen because all signals would be displayed as a voltage value of 1 volt, which, of course, yields only one color in the image. No variation in color would be seen in the higher quality area. Increasing the sensitivity of the measurement scale would permit detection from signals in the deteriorated area but would distort the information from the higher quality area.

6.8.1.2. Detection of Bond Deterioration

Signals from disbonded areas are blocked from transmission across the air/water gap, resulting in the absence of signals for the receiver to detect. F&T specimen C9 that had experienced a disbond between two layers of asphalt illustrated this phenomenon. The specimen experienced a disbond sometime later than the 14^{th} cycle of F&T exposure. Figure 6.54 shows that approximately 50 percent or more of the interface between the 2 layers of asphalt in specimen C9 had disbonded by the 39^{th} cycle; Figure 6.55 shows the area of disbond had increased to 75 percent at 64 cycles.

The ultrasonic through-transmission signals in the disbonded portion of the specimen were highly attenuated by the disbond gap to very low levels of amplitude. In most locations, the area of contact was so small that the amplitudes were below the noise level. However, for weak signals that do not fall below the noise level, as is the case when the materials began to deteriorate, the signal exists but their voltage amplitudes are below the scale of the measurement system chosen.

Because of the low amplitude signals, the automatic detection system of the USUMS could not detect the peaks hidden in the noise. Generally, material deterioration only creates weak signals, while a disbond creates either weaker signals or missing signals or both. Therefore, a velocity could be not recorded for the location of these particular ultrasonic shots through the specimen.

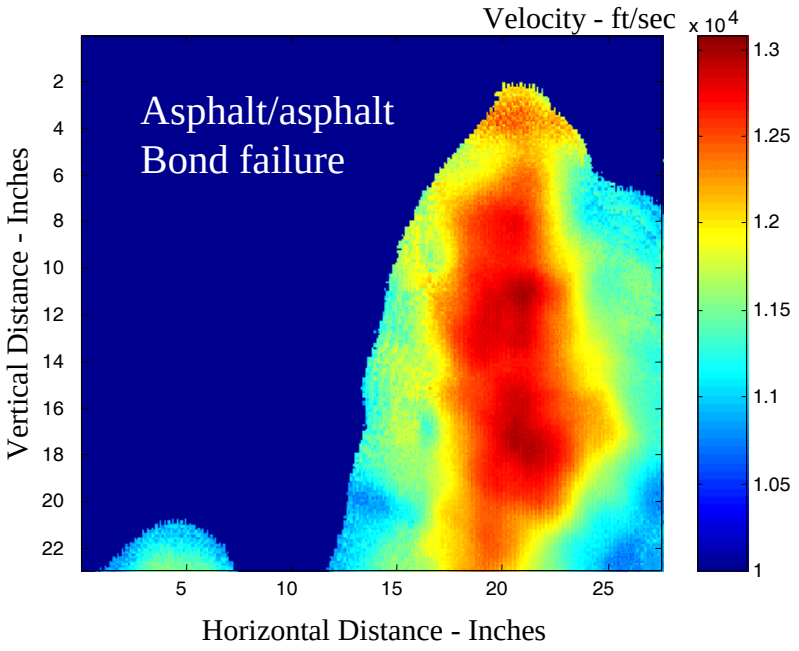

Figure 6.54. Velocity image on F&T specimen C9 after 39 cycles of F&T exposure.

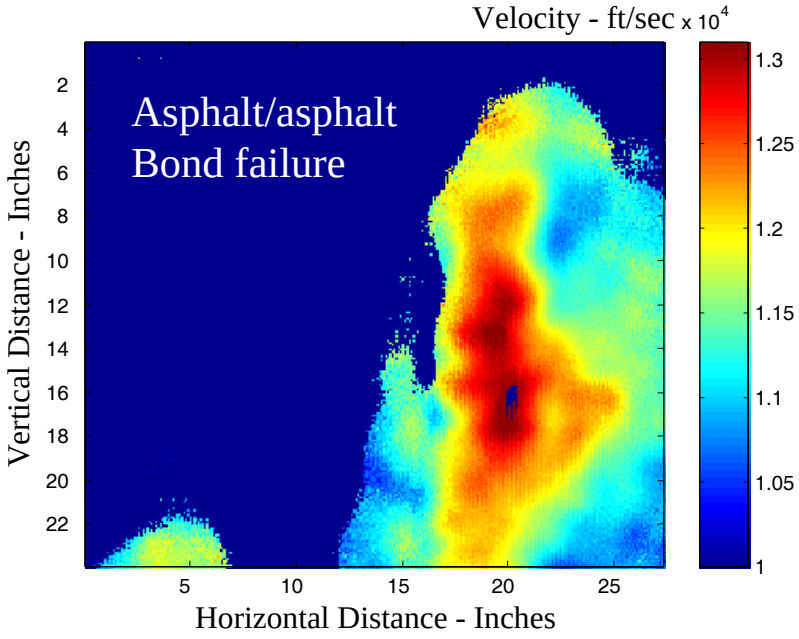

Figure 6.55. Relationship of data and measurement system dynamic ranges for bond.

A disbond can cause a relative reduction in accuracy as compared to measurements from material deterioration. Figure 6.56(a) illustrates the initial measurement when it was possible to detect all signals. There were no velocities recorded for the disbonded area because the signals were too far below the level of the noise to be detected as illustrated in Figure 6.56(b). This is because the amplitude peaks of the signals from the disbonded area fall below the noise level of the measurement system and no TOAs are recorded for that signal.

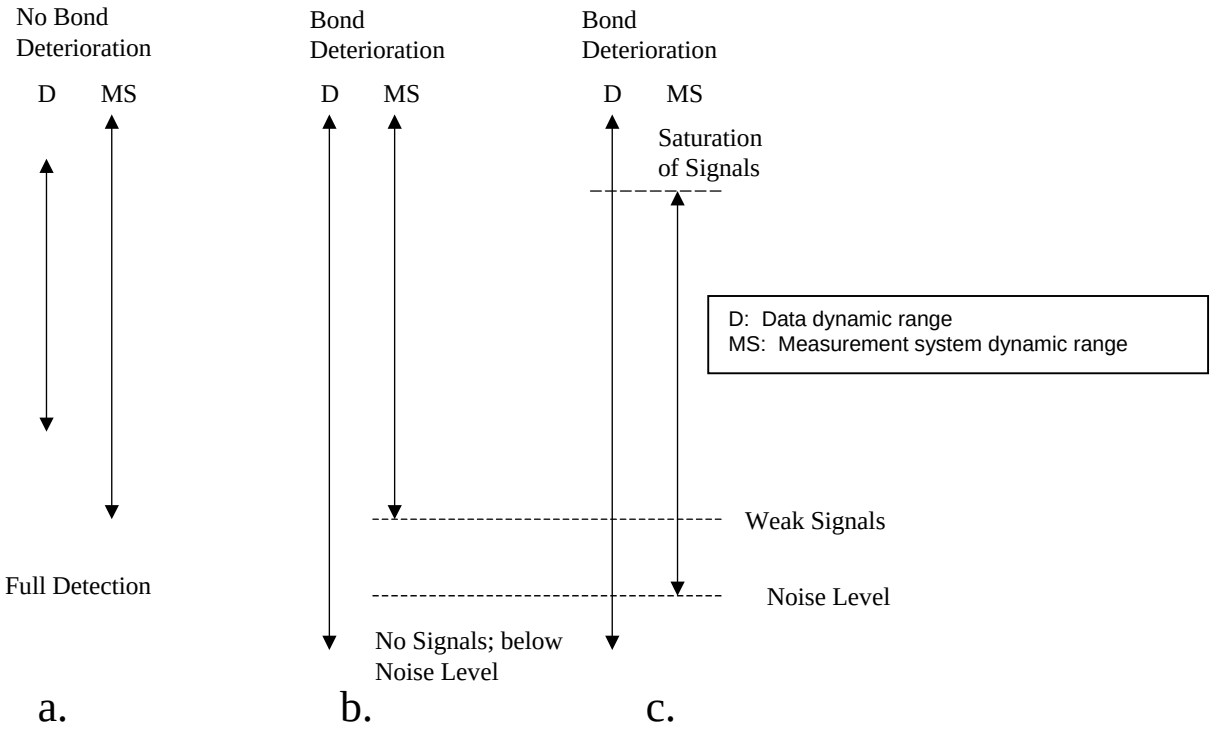

Figure 6.56. Relationship of data and measurement system dynamic ranges for bond assessment.

6.8.2. ANALYSIS OF ATTENUATION DATA

6.8.2.1. Factors Influencing Attenuation of Signals

The USUMS also measures amplitude (source of attenuation data) as well as TOA (source of velocity data). Both velocity and attenuation were measured during this laboratory investigation. Some of the variables that affect signal attenuation are:

- Air content of water in scanning tank
- Degree of moisture saturation of specimen
- Entrapped air on surface of specimen

- Level of pulser power
- Amplifier gain
- Water temperature
- Degree of material deterioration of the specimen
- Degree of bond deterioration of the specimen

The velocity of the signal is affected primarily by deterioration in the AC and PCC of the specimen. A change in pulse power or amplifier gain can influence the amplitude of the signal without altering the velocity of the materials. Since the amplitudes used to determine the value of attenuation are affected by many factors in addition to material and bond deterioration, the signal amplitudes for attenuation images are normalized each time a specimen is scanned. The maximum amplitude of voltage is always converted to a value of 1, and the remaining amplitudes for all signals in a complete specimen scan are scaled between 0 and 1.

Assume that if the highest amplitude for all 14,400 signals in a specimen scan is 9 volts and the lowest amplitude is 2 volts; the lowest value of 2 volts is displayed as a value of 0 and the highest value of 9 volts is given a value of 1. All voltages in between the maximum and minimum are given proportional values. If in a later scan on the same specimen, the maximum amplitude drops from 9 to 7 volts and the minimum amplitude drops from 2 to 1 volt, then those data are also displayed from 0 to 1.

By contrast, the scaling of the velocity display is kept constant for velocity scans between cycles of exposure while the amplitude is rescaled each time for attenuation scans between cycles. Absolute values of velocities are calculated from the variation in TOA data, while relative values of attenuation are calculated from the variation in amplitude.

6.8.2.2. Statistical Data

Most of the statistics for attenuation data are meaningless between cycles of exposure. The statistical parameter of “maximum amplitude” is always converted to a value of 1 and does not vary between specimen scans. The “minimum amplitude” is always converted to a value of 0 and does not vary between specimen scans. The “mean amplitude” is always calculated on data that lies between 0 and 1 and would not be expected to change significantly between scans.

Obviously, it would not be instructive to compare the statistics of normalized attenuation data across successive images, as it is with velocity data. Why do we rescale all amplitude values and not velocity data? The short answer is that the attenuation data are a function of many variables while velocity data are not. Signal coupling between the transducers and the PCC/AC has a significant effect on the amplitude of the signal for dry measurements but is stable with immersion measurements. While an immersion measurement provides more consistent signal coupling than dry measurements for a given scan, there are still other sources of variations of signal amplitude from one location on the specimen to another location.

6.9. COMPARISON OF ATTENUATION AND VELOCITY DATA

The measurement of absolute values of attenuation can be misleading for interpreting deterioration in the materials. It is more instructive to compare relative values of attenuation from one image to another. However, absolute values of velocity are instructive because they are primarily a function of bond and material deterioration.

Although the amplitude of the signal peak can vary by a large amount (± 50 percent or more), the TOA will not be altered nor the resulting velocity. The factors that influence the amplitude of the signals for a particular specimen will affect each signal in the same manner; thus, relative differences between bonded and unbonded areas should show up clearly in the image. For example, amplifier gain and pulser voltage is maintained constant during a scan and does not affect the amplitude for that scan. It can cause problems across scans should one of the parameters be changed unless the data are normalized.

The data for the velocities were not normalized since velocity strongly corresponds to changes in deterioration in the materials and/or bond. This permits the velocity data to be comparable across later images; velocity is determined using TOA values on a velocity scan and the data are presented in absolute units (feet per second). The statistics on velocity scans on F&T and W&D exposure specimens were shown in Table 6.2 and Table 6.3.

6.10. MATERIAL DURABILITY TESTS ON UTW SPECIMENS

Ultrasonic through-transmission measurements were made through the 34-inch direction in AC and PCC. It was assumed that any deterioration in either of the two materials would be uniformly distributed throughout the specimens. These tests were done to obtain separate transverse-velocity measurements on AC and PCC layers of the UTW specimens to determine their durability (percent remaining velocity versus number of cycles). (Note that the thickness-velocity measurements through the thickness of the composite using the USUMS were an average velocity of the AC and PCC and do not provide separate velocities of each material. The direction of the USUMS velocity measurement is perpendicular to the measurements discussed in this section.)

It was reasoned that by making transverse-velocity measurements through the composite materials, separate velocity values could be determined for each material because the change in acoustic impedance at the PCC/AC bond interface would tend to channel the energy in that particular material. In other words, when the transducers were placed on the ends of the PCC layer, the energy would only travel in the concrete and not in the AC, and when placed on the ends of the AC layer, the energy would travel only in the AC layer.

The measurements verified that AC and PCC materials were in fact durable; the PCC material had a pulse velocity of about 15,000 ft/sec (4,572 m/sec), and the AC material had a pulse velocity of about 12,000 ft/sec (3,658 m/sec). This corresponded to separate velocitie measurements of the materials determined earlier on prism samples of AC and PCC. If the

energy had been crossing over from the AC to the PCC when the transducers were placed on the ends of the asphalt layer, it would have given a higher velocity than 12,000 ft/sec (3,658 m/sec). These material tests permitted the detection of the onset of deterioration and tracking the progression of deterioration in the specimens.

Prior to and during the early part of the testing, it was assumed that the two materials would deteriorate uniformly over their volume. However, it was discovered late in the investigation, at the 105th exposure cycle of the F&T specimens, that the surface of the concrete layer was much more deteriorated than the interior concrete. Although only a 5-percent drop in velocity was seen in the transverse-velocity measurements, it was obvious that the velocity of the concrete on the surface had dropped by a much larger percentage. It was highly deteriorated for a depth of an inch or more. When the surface was scraped by hand with a metal tool, the material fell apart easily. By using a small jackhammer-type device the PCC could be penetrated to a depth of 2 inches with a few impacts from the hammer. Deteriorated PCC surface is shown in Figure 6.57and scraping of PCC surface using the small jackhammer is shown in Figure 6.58. Figure 6.59 shows the surface of the scrapped PCC.

Figure 6.57. Close-up of PCC surface before scrapping with a jackhammer.

It was expected that the ultrasonic pulse velocity (UPV) readings would give an indication of the degree of deterioration of each of the two materials. However, this hypothesis did not hold true during the course of exposure testing and the PCC, in particular, deteriorated non-uniformly in a direction perpendicular to the plane of the surface.

A large temperature gradient can be a significant cause of deterioration in materials such as PCC and apparently, because the gradient was highest near the surface of the concrete in the thickness direction, the concrete deteriorated more there than near the bond interface. A surface measurement with the V-meter on F&T specimen D2 revealed a velocity of 7,400 ft/sec (2,256 m/sec). A velocity less in 10,000 ft/sec (3,048 m/sec) indicates PCC in poor condition.

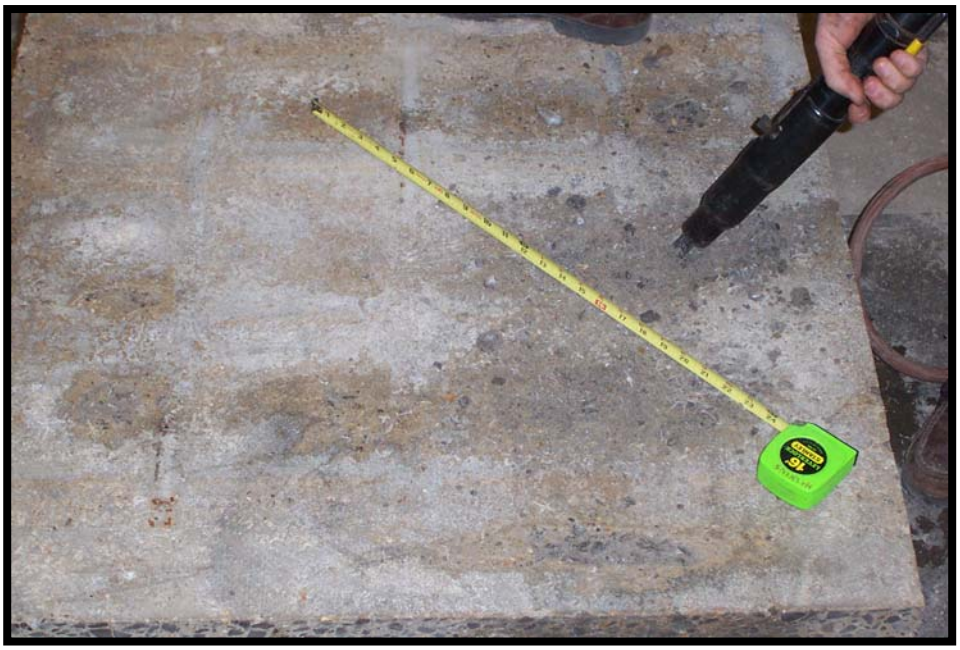

Figure 6.58. Severely deteriorated PCC surface was easily scrapped using a jackhammer.

Figure 6.59. PCC surface after cleaning with small jackhammer.

Since the temperature difference between the center of the PCC and the fluid temperature at either end of the PCC/AC specimen were spread over a distance of at least 17 inches (432 mm), the surface likely had no significant temperature gradients in either the X or Y directions—i.e., lying in any plane parallel with the concrete surface. In the thickness direction, the temperature difference between the fluid and the center of the specimen is spread over a distance of 3.5 to 4.0 inches (89 to 100 mm) and therefore the temperature gradients are high. The temperature gradient was high (55^{o}F) perpendicular to the plane of the large concrete surface. The glycol was –15^{o}F when the bond temperature was 40^{o}F at the beginning of the freeze cycle. This created deterioration to a depth of 1 inch (25 mm) or so beneath the PCC surface. Figure 6.60 shows that the depths closest to the surface experiences the greatest temperature gradient and therefore the greatest deterioration.

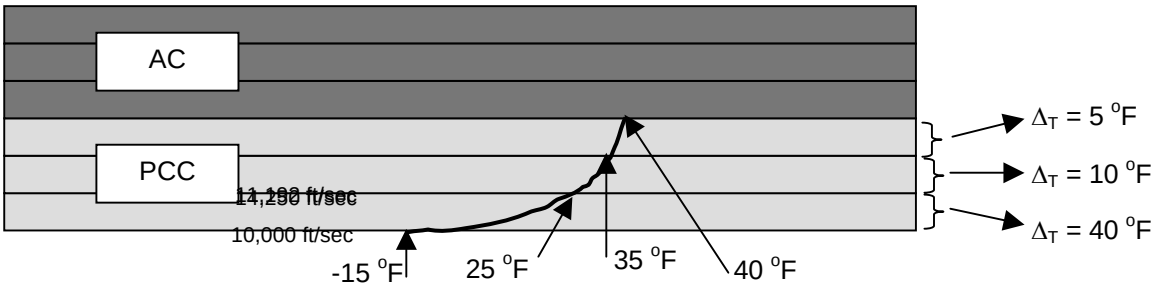

Figure 6.60. Hypothetical temperature gradient in the UTW specimen.

The V-meter was used to measure and record the time of arrival of the first pulse to arrive at the receiver. The V-meter operates in the through-transmission mode—i.e., two transducers are placed on opposite ends of the PCC layer rather than both on the same side, as is the case with the pulse echo mode. The V-meter measured a high transverse velocity in the PCC of F&T specimen D2, 14,250 ft/sec (4,343 m/sec), which meant that the signal was traveling a path other than through the upper 1-inch (25 mm) layer of concrete, which, as mentioned, had a low velocity of about 7,400 ft/sec (2,256 m/sec). This meant that the high velocity signal was traveling in sound PCC and obviously, that sound PCC was closer to the bond interface than to the surface. Later tests made in the dry with the V-meter through the thickness of the UTW specimen revealed that the average velocity of the PCC and AC was much lower than what the transverse measurements indicated. This tended to confirm that there was high velocity material located away from the surface of the PCC.

Although it was not possible to calculate the separate transverse-velocities of the AC and PCC (actually the PCC layer did not have one fixed transverse velocity), some reasonable assumptions can be made. If the AC and PCC deteriorated to the same degree percentage wise, then the average velocity of the PCC would be about 11,778 ft/sec (3,590 m/sec) and the AC would be 9422 ft/sec (2,872 m/sec) as shown in Figure 6.60. Since the transverse measurements in the concrete layer yielded about 14,250 ft/sec (4,343 m/sec) and this represented a layer of the concrete with the least deterioration (fastest velocity), then that concrete layer was closer to the bond than to the surface.

Although the initial deterioration measurements on the materials were difficult to interpret, it was determined by the 105th F&T cycle that the PCC had experienced much more deterioration than previously estimated. By that time, it was not possible to make USUMS measurements through the thickness of the composite specimens. The S/N of the individual signals had dropped from 100 to almost zero. This was due to significant deterioration in either or both of the AC and PCC layers.

Although the S/N was too low for underwater transducers of the USUMS to penetrate the thickness of F&T specimen D2, the V-meter transducers, which are designed for dry measurements, had a much higher S/N and could still penetrate the thickness. (No V-meter measurements were made through the thickness of specimen D2 as the surface concrete had been removed with a jackhammer device.) V-meter measurements made in the dry through the thickness of the F&T specimen D3 composite revealed that the average thickness-velocity of the composite was around 10,600 ft/sec (3,231 m/sec) and that no disbond existed at the interface between the materials.

6.11. LABORATORY VERSUS FIELD DURABILITY

There are no historic data for the new environmental tests—based on the particular parameters of exposure and the size and shape of the specimens—for either of the two materials. There are no known relationships between the laboratory durability and field durability. ASTM C 666, a widely used standardized test procedure for PCC durability, states that if the specimen endures 300 cycles of laboratory exposure and has 60 percent or

more remaining Dynamic E from an initial value of 100 percent, then it is passes the test as a field durable PCC. If the specimen falls below 60 percent remaining Dynamic E in less than 300 cycles then it fails the test and is not considered a field durable PCC. The test is stopped when the first of the two numbers reaches its threshold value; i.e., the number of cycles reaches 300, or the Dynamic E falls below 60 percent.

Each environmental exposure factor has its own rate and level of exposure and, hence, relationship of laboratory durability to field durability for new tests. Each environmental test simply provides a pair of numbers (percentage remaining NDT quality after X cycles) that represents the laboratory durability of the two durable materials for the particular test and test conditions.

For this work it was assumed that if the percentage remaining bonded area is greater than the percentage remaining NDT material quality of the least durable material in the laboratory for the same number of cycles, then the bond will hold up better than the materials in the field. Vice versa, if the specimen has less percentage remaining bonded area than the percentage remaining NDT quality of the material in the laboratory for the same number of cycles, then the bond will not hold up as well as the material in the field.

This page intentionally left blank.

7. CONCLUSIONS AND RECOMENDATIONS

7.1. PROJECT SUMMARY

The reported research included both field and laboratory investigations to determine if the bond between AC and PCC in UTW overlays (4 inches [100 mm] or less) placed on milled, aged asphalt had long-term durability when subjected to environmental exposure. The following activities were accomplished to meet the project objective:

- Compiled and reviewed information on UTW airport and select highway projects
- Formulated laboratory testing plan based on analysis of field visits
- Developed laboratory test program to evaluate bond deterioration
- Constructed test section to obtain samples for laboratory evaluation
- Conducted laboratory tests using simulated environment exposure conditions

The field investigation conducted performance evaluation of UTW pavements in the U.S. and documented construction practices for UTW. Construction of a UTW test section followed typical construction methods. The test section was used to obtain full size (34-inch by 34-inch by 7-inch) UTW panels for F&T and W&D exposure tests in the laboratory.

The approach taken to evaluate the performance of the bond between AC and PCC was to assume that the UTW pavement cannot be field durable if either the AC or PCC materials fail or if the bond between the two materials fails. Both the materials and the bond must have a common durability if the UTW as a whole is to perform satisfactorily. The durability of the individual PCC and AC materials subjected to environmental exposures is the standard against which the durability of the bond is compared. If the bond is more durable than the either of the two materials when subjected to environmental exposure, then the bond is sufficiently field durable.

7.2. CONCLUSIONS

The field investigation indicated that:

a. UTW provided good performance except in areas where a disbond existed and/or where the pavement was subjected to concentrated, heavy wheel loads (conclusion derived from vehicle parking lot evaluations).
b. The UTW apron at the Spirit of St. Louis Airport was experiencing significant cracking along the path used by fuel trucks. Also, this apron had significant cracking in slabs containing tie-downs.
c. Poor quality in the existing AC pavement can cause problems during construction of the UTW, and may result in failures of the UTW as demonstrated on the apron pavement at the SNH airport. These failures highlight the need for proper evaluation of the existing AC before UTW is selected as the rehabilitation choice.

The F&T tests were determined to be most severe exposure, while the W&D test was relatively less severe. Approximately 200 12-hour W&D exposure cycles were able to cause measurable deterioration in the AC and PCC materials. The W&D exposure test could be made more severe by using a salt (sodium sulfate or magnesium sulfate as described by ASTM C 88) solution instead of water to increase the rate of deterioration of the bond and the two materials. Using a salt solution should not represent a deviation from field conditions, as salts are generally present in rainwater and in the run off water from soil.

The laboratory investigation demonstrated excellent bond retention characteristics between the UTW and underlying AC when subjected to F&T and W&D exposure. No disbonding occurred even though *both* composite materials experienced significant deterioration.

The laboratory investigation indicated that a UTW pavement, constructed using durable materials and AC surface properly milled and cleaned prior to PCC placement, should have a bond between the PCC and AC that is at least as durable as the PCC and AC materials themselves. This essentially means that if a UTW pavement is constructed using proper construction techniques, bond failure due to environmental factors should not be a concern.

A reference number of cycles was determined for the F&T exposure test; the UTW bond should be able to endure 135 30-hour cycles of exposure to pass a durability test when all exposure parameters match the parameters described in this investigation. For the W&D exposure, the bond should be able to endure 200 12-hour cycles.

Site investigations indicated distresses in the form of corner breaks and cracks where heavy loads operated.

Laboratory shear tests showed failure in surface of AC; this is potential failure location and will be of concern when the quality of AC is not adequate – need test to determine if AC is suitable.

This investigation did not consider the methodologies used for design of the UTW at the sites, nor was any evaluation made of the condition of the old AC material or structural support of the existing AC pavement structure.

7.3. RECOMMENDATIONS

Field investigations indicated that the degree of bond between AC and PCC depends upon whether the AC surface was milled or broom cleaned. Samples used in this research effort had only one milling pattern and depth. Future research studies could be conducted to determine the effect of milling pattern and texture depth on UTW bond performance. Furthermore, other techniques that could facilitate bond between AC and PCC and different cleaning techniques should be investigated.

Research should be devoted to identifying the suitability of an existing AC pavement to qualify as a viable candidate for UTW construction. Two issues of concern are:

a. Need method to evaluate structural support of existing AC pavement and an analysis method to determine if suitable candidate for UTW.
b. Need method to evaluate the quality of existing AC to determine its suitability for UTW construction, further deterioration of the AC after placement of the UTW can reduce the effectiveness of the UTW and cause early failure.

This page intentionally left blank.

8. REFERENCES

1 Mack, J.W., Hawbaker, L.D., and Cole, L.W. (1998). "Ultra-thin whitetopping (UTW): The state-of-the-practice for thin concrete overlays of asphalt." *77th Annual Meeting Preprint CD-ROM*, Transportation Research Board, Washington, D.C.

2 Cole, L.W., and Mack, J.W. (1999). "Thin bonded concrete overlays of asphalt pavement: The U.S. experience with ultra-thin whitetopping." http://www.pavement.com/techserv/usutw2.html (April 8, 2002).

3 Wu, C.L., Tayabji, S., and Sherwood, J. (2001). "Repair of ultra-thin whitetopping pavements." *80th Annual Meeting Preprint CD-ROM*, Transportation Research Board, Washington, D.C.

4 Armaghani, J. M., and Tu., D. (1999). "Rehabilitation of Ellaville Weigh Station with ultra-thin whitetopping." *Transportation Research Record 1654*, TRB, National Research Council, Washington, D.C.

5 Saeed, A., and Hall, Jr., J.W. (2001). "Non-destructive pavement evaluation and design of ultra-thin whitetopping at a general aviation airport in Tennessee." *Proc.*, Second International Conference on Maintenance and Rehabilitation of Pavements and Technological Control (CD-ROM), Auburn University, Alabama.

6 Saeed, A., Hammons, M. I., and Hall, Jr., J.W. (2001). "Design, construction, and performance monitoring of ultra-thin whitetopping at a general aviation airport." *Proc.*, 2001 ASCE Airfield Pavement Specialty Conference, American Society of Civil Engineers, Chicago, Illinois.

7 *Engineering News Record*, (2000). McGraw Hill, New York, New York. May 29.

8 Kuo, S.S., Armaghani, J.M., and Scherling, D., (1999). "Accelerated pavement performance testing of ultra-thin fiber reinforced concrete overlay, recycled concrete aggregate, and patching material." *Conference Presentations, 1999 International Conference on Accelerated Pavement Testing CD-ROM*, Reno, Nevada.

9 Cole, L.W., Sherwood, J., and Qi, X. (1999). "Accelerated pavement testing of ultra thin whitetopping." *Conference Presentations, 1999 International Conference on Accelerated Pavement Testing CD-ROM*, Reno, Nevada.

10 Vandenbossche, J.M., and Rettner, D.L., (1999). "One-year performance summary of whitetopping test sections at the Mn/ROAD test facility." *Conference Presentations, 1999 International Conference on Accelerated Pavement Testing CD-ROM*, Reno, Nevada.

11 Cable, J. K., and Hart, J. (1998). "Evaluation of bond between ultra-thin PCC and asphalt concrete." *Crossroads 2000 Proceedings*, Iowa State University, Ames, Iowa.

12 Risser R.J., LaHue, S.P., Voigt, G.F., and Mack, J.W., (1993). "Ultra-thin concrete overlays on existing asphalt pavement." *Proceedings of the Fifth International Conference on Concrete Pavement Design and Rehabilitation*, Volume 2, Purdue University, West Lafayette, Indiana.

13 Crawley, A.B., and Pepper, J.M. (1999). "Application of fiber reinforced concrete for ultra-thin whitetopping on I-20 in Mississippi." *78th Annual Meeting Preprint CD-ROM*, Transportation Research Board, Washington, D.C.

14 Speakman, J. and Scott, N.H. (1996). "Ultra-thin, fiber-reinforced concrete overlays for urban intersections." In *Transportation Research Record 1532*, TRB, National Research Council, Washington, D.C.

15 Dumitru, N.I., and Hussain, M. (2002). "Construction and performance of ultra-thin whitetopping in Kansas." *81st Annual Meeting Preprint CD-ROM*, Transportation Research Board, Washington, D.C.

16 Grove, J.D., Cable, J., and Heyer, M. (1996). "Iowa ultra thin whitetopping research at two years of age." Iowa Department of Transportation, Ames, Iowa.

17 Cable, J.K., and Chia, T.L. (2000). "Ultrathin Portland cement concrete overlay extended evaluation." Iowa Department of Transportation, Ames, Iowa.

18 Cable, J.K., and Streit, N.A., (2002). "Ultrathin Portland cement concrete overlay extended evaluation." Iowa Department of Transportation, Ames, Iowa.

19 Tarr, S.M., Sheehan, M.J., and Okamoto, P.A. (1998). "Guidelines for the thickness design of bonded whitetopping pavement in the State of Colorado." Colorado Department of Transportation, Denver, Colorado.

20 Wu, C.L., Tarr, S.M., Ardani, A., and Sheehan, M.J. (1998). "Instrumentation and testing of ultra-thin whitetopping pavement." *77th Annual Meeting Preprint CD-ROM*, Transportation Research Board, Washington, D.C.

21 CRD Campbell, Inc. (1993). "Engineer's report for ramp rehabilitation at Spirit of St. Louis Airport, Chesterfield, Missouri." CRD Campbell, Inc., St. Louis, Missouri.

22 Armaghani J. M. (1997). "Evaluation of ultra-thin whitetopping in Florida." Presented at the 1997 TRB Conference. TRB, National Research Council, Washington, D.C.

23 Bristol, Childs & Associates, Inc. (1996). "Engineers report for ultra-thin concrete overlay demonstration project at New Smyrna Beach Municipal Airport." Bristol, Childs & Associates, Inc., Coral Gables, Florida.

24 Webster, S.L., Grau, R.H., and Williams, T.P. (1992). "Description and application of dual mass dynamic cone penetrometer," Instruction Report GL-92-3, USAE Waterways Experiment Station, Vicksburg, MS.

25 Webster, S. L., Brown R. W., and Porter, J. R. (1994). "Force projection evaluation using the electric cone penetrometer (ECP) and the dynamic cone penetrometer (DCP)," Technical Report GL-94-17, USAE Waterways Experiment Station, Vicksburg, MS.

26 Saeed, A., Hall, Jr., J.W., and Hammons. M.I. (2000). "Field evaluation results and design recommendations for the Savannah-Hardin County Airport runway rehabilitation." Final Report. ERES Consultants, a division of Applied Research Associates, Inc., 112 Monument Place, Vicksburg, MS 39180.

27 Saeed, A., and Hall, J.W., Jr., (2001). "Whitetopping strain response analysis for the Savannah-Hardin County Airport runway rehabilitation." Final Report. ERES Consultants, a Division of Applied Research Associates, Inc., 112 Monument Place, Vicksburg, MS 39180.

28 Wu, C.L., and Sheehan, M.J. (2002). "Testing and performance evaluation of UTW pavements at the Spirit of St. Louis Airport." *81st Annual Meeting Preprint CD-ROM,* Transportation Research Board, Washington, D.C.

29 Kuo, S.S., Blazek, D.C., and Lewis, N., (1996). "Testing and analysis of ultra-thin fiber reinforced and non-reinforced Portland cement concrete (PCC) over asphaltic layer." Final Report. Florida Department of Transportation – Aviation Office, Tallahassee, Florida.

30 U.S. Department of Transportation (2000). "The U.S. Department of Transportation's Comprehensive Truck Size and Weight Study." U.S.DOT, Washington, D.C.

31 Webb, R.D., and Delatte, N.J. (2000). "Performance of whitetopping overlays." *79th Annual Meeting Preprint CD-ROM,* Transportation Research Board, Washington, D.C.

32 Tarr, S.M., Ardani, A., and Sheehan, M.J. (2000). "Mechanistic design of thin whitetopping pavements in Colorado." *79th Annual Meeting Preprint CD-ROM*, Transportation Research Board, Washington, D.C.

33 Vandenbossche, J.M., and Fagerness, A.J. (2002). "Performance and repair of ultra-thin whitetopping: The Minnesota experience." *81st Annual Meeting Preprint CD-ROM*, Transportation Research Board, Washington, D.C.

34 Rasmussen, R.O., McCullough, B.F., Ruiz, J.M., Mack, J., and Sherwood, J.A. (2002). "Identification of pavement failure mechanism at the FHWA ALF UTW project." *81st Annual Meeting Preprint CD-ROM*, Transportation Research Board, Washington, D.C.

35 Naik, T.R., and Malhotra, V.M. (1991). "The ultrasonic velocity method," in *Handbook on Nondestructive Testing of Concrete*, V.M. Malhotra and N. J. Carino, eds., CRC Press, Inc.

36 Alexander, A.M., Haskins, R.W., Cook, R., Baishya, M., and Kelly, M. (1998). "Technologies for improving the evaluation and repair of concrete bridge decks: ultrasonic pulse echo and polymer injection," WES CPAR Technical Report SL-98-1, U.S. Patent Number 5,814,731.

37 Wu, Chung-Lung and Sheehan, Matthew J., "Testing and performance evaluation of UTW pavements at the Spirit of St. Louis Airport," January 2002 Annual Meeting of the Transportation Research Board, p. 4.

38 "Standard test method for pulse velocity through concrete." CRD-C 51 (ASTM Designation: C 597).